Applied Geochemistry 57 (2015) 236–266

Contents lists available at ScienceDirect

Applied Geochemistry

journal homepage: www.elsevier.com/locate/apgeochem

Review

Characteristics and environmental aspects of slag: A review

Nadine M. Piatak [a,*], Michael B. Parsons [b], Robert R. Seal II [a]

[a] U.S. Geological Survey, 954 National Center, Reston, VA 20176, United States
[b] Geological Survey of Canada, 1 Challenger Drive, Dartmouth, Nova Scotia B2Y 4A2, Canada

ARTICLE INFO

Article history:
Available online 30 April 2014

ABSTRACT

Slag is a waste product from the pyrometallurgical processing of various ores. Based on over 150 published studies, this paper provides an overview of mineralogical and geochemical characteristics of different types of slag and their environmental consequences, particularly from the release of potentially toxic elements to water. This chapter reviews the characteristics of both ferrous (steel and blast furnace Fe) and non-ferrous (Ag, Cu, Ni, Pb, Sn, Zn) slag. Interest in slag has been increasing steadily as large volumes, on the order of hundreds of millions of tonnes, are produced annually worldwide. Research on slag generally focuses on potential environmental issues related to the weathering of slag dumps or on its utility as a construction material or reprocessing for secondary metal recovery. The chemistry and mineralogy of slag depend on the metallurgical processes that create the material and will influence its fate as waste or as a reusable product.

The composition of ferrous slag is dominated by Ca and Si. Steel slag may contain significant Fe, whereas Mg and Al may be significant in Fe slag. Calcium-rich olivine-group silicates, melilite-group silicates that contain Al or Mg, Ca-rich glass, and oxides are the most commonly reported major phases in ferrous slag. Calcite and trace amounts of a variety of sulfides, intermetallic compounds, and pure metals are typically also present. The composition of non-ferrous slag, most commonly from base-metal production, is dominated by Fe and Si with significant but lesser amounts of Al and Ca. Silicates in the olivine, pyroxene, and melilite groups, as well as glass, spinels, and SiO_2 (i.e., quartz and other polymorphs) are commonly found in non-ferrous slag. Sulfides and intermetallic compounds are less abundant than the silicates and oxides. The concentrations of some elements exceed generic USEPA soil screening levels for human contact based on multiple exposure pathways; these elements include Al, Cr, Cu, Fe, Mn, Pb, and Zn based on bulk chemical composition. Each slag type usually contains a specific suite of elements that may be of environmental concern. In general, non-ferrous slag may have a higher potential to negatively impact the environment compared to ferrous slag, and is thus a less attractive material for reuse, based on trace element chemistry, principally for base metals. However, the amount of elements released into the environment is not always consistent with bulk chemical composition. Many types of leaching tests have been used to help predict slag's long-term environmental behavior. Overall, ferrous slags produce an alkaline leachate due to the dissolution of Ca oxides and silicates derived from compounds originally added as fluxing agents, such as lime. Ferrous slag leachate is commonly less metal-rich than leachate from non-ferrous slag generated during base metal extraction; the latter leachate may even be acidic due to the oxidation of sulfides. Because of its characteristics, ferrous slag is commonly used for construction and environmental applications, whereas both non-ferrous and ferrous slag may be reprocessed for secondary metal recovery. Both types of slag have been a source of some environmental contamination. Research into the environmental aspects of slag will continue to be an important topic whether the goal is its reuse, recycling, or remediation.

Contents

* Corresponding author. Tel.: +1 7036486254; fax: +1 7036486252.
E-mail address: npiatak@usgs.gov (N.M. Piatak).

http://dx.doi.org/10.1016/j.apgeochem.2014.04.009
0883-2927/

1. Introduction

Slag examined in this study is defined as the predominantly silicate and oxide by-product derived from smelting metallic ore. The two main types of slag included in this discussion are from the primary production of ferrous ores, from iron and steel manufacturing, and from non-ferrous ores, from the recovery of base metals and some precious metals. Other non-ferrous slags include those generated from phosphate, chromite ($FeCr_2O_4$), and Al ores, among others; however, these slag types are not discussed due to the limited number of environmental studies on these slags. Slag can also be generated during the recycling of raw materials (i.e., Pb scrap recycling, alkaline battery recycling) and during the vitrification of municipal and nuclear waste. These types of slag are not included in this paper, which focuses on mining and ore processing waste.

Scientific interest in slag has been increasing steadily since the early 1990s. The number of slag studies that are referenced in this paper by publication date is shown in Fig. 1 (see Appendices A and B). Research on slag can generally be divided into two categories: reuse and environmental effects. Studies of slag reuse fall into three main areas: the utility of slag as a construction material, metal recovery from slag, and slag use in environmental remediation applications (Appendix B). Many of these studies, most commonly on ferrous slags, characterize and test the geotechnical properties of slag from an engineering and construction perspective. Environmental studies, most commonly on non-ferrous slag, focus on understanding the potential environmental impacts of slag deposited as waste, and concentrate on the geochemical and mineralogical properties of the material.

Large volumes of slag are produced during the process of removing metals from ore and, thus, extensive slag dumps are

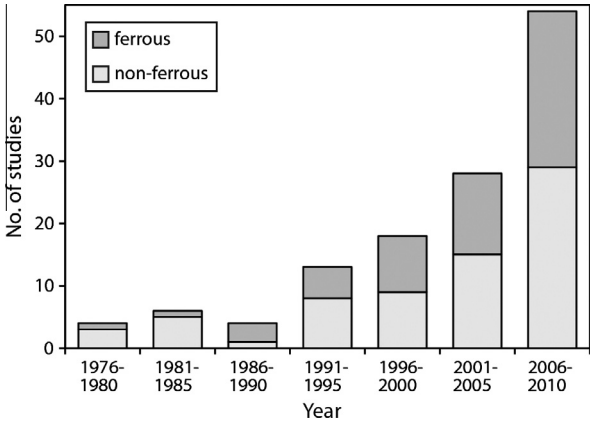

Fig. 1. Number of slag studies published by year between 1975 and 2010 that are included in this review (See Appendices A and B for references).

present at both historical and modern smelting sites. In the past, the lack of environmental regulations and limited scientific understanding of slag's environmental behavior resulted in little public concern regarding slag waste and its reuse. More recent studies indicate that some types of slag do contain high concentrations of potentially toxic elements such as As, Ba, Cd, Cu, Pb, and Zn (Costagliola et al., 2008; Ettler et al., 2009b; Piatak and Seal, 2010). Globally, there is increasing concern over the potential environmental impacts of slag. Slags were and still are widely used as construction materials and are increasingly used in environmental applications. Characterization of the environmental aspects of slag helps to evaluate its potential to release contaminants and its suitability as a potential resource.

This paper is a review of over 150 published studies on slag, and incorporates some new data generated by the authors on steel slag from the Chicago (USA) area. Appendices A and B list the studies included in this review, identify the slag types in each article, as well as the types of data included in this chapter. We first present an overview of the metallurgical processes that create ferrous and non-ferrous slag followed by a discussion of the methods used to characterize slag. The next section is a summary of the chemical and mineralogical characteristics of slag. Next we focus on environmental aspects of slag presenting a comparison of the bulk chemical composition to relevant environmental guidelines, followed by discussions on secondary weathering products that form on slag, on the quantification of their acid-generating and acid-neutralizing potentials, and then on the chemistry of leachates produced when aqueous solutions interact with slag. A few case studies are then highlighted for each slag type to illustrate salient points. The last section focuses on slag as a resource with a discussion of its various uses. Overall, this review paper focuses on characterizing slag and discussing its potential environmental impacts and its role as a valuable resource for reuse and recycling.

2. Metallurgical overview

2.1. Ferrous slag

Ferrous slags are created during the recovery of Fe from natural ores or recycled materials to produce either Fe or steel. Different types of slag are produced in the various furnaces used. Blast furnace slag (i.e., Fe slag) is produced in a blast furnace simultaneously with Fe. Iron oxides are reduced to molten Fe in the furnace by adding a flux such as limestone or dolomite and a fuel and reductant such as coke (Fig. 2). Molten Fe slag can solidify by slow cooling under atmospheric conditions (air cooled), moderate cooling with the use of controlled amounts of water (expanded or foamed), quick cooling in air (pelletized), or quenching with high-volume, high-pressure sprays of water (granulated). The rate and method of cooling affect the properties of the slag, which influence its commercial uses. Air-cooled slags are crystalline and vesicular, expanded slags are a porous crystalline and glassy material, pelletized slags are glassy and crystalline pellets, and granulated slags are vitrified granules (Fig. 3) (Lewis, 1982). The hard and dense nature of the air-cooled slag makes it suitable as a construction aggregate. The strong cementitious properties of granulated slag help increase its long-term strength when added to concrete. Pelletized and expanded slag is commonly used as a lightweight aggregate because of its low density (Van Oss, 2013).

Steel slags are produced when the molten Fe from the blast furnace and scrap steel are combined with alloys to produce a particular type or grade of steel (Fig. 2). The types of primary steel slag are usually categorized based on the type of furnace used in the creation: open hearth, basic oxygen furnace (BOF), and electric arc furnace (EAF). The open hearth process uses waste gases from the molten Fe to generate temperatures reaching 2000 °C, but has now been replaced in most countries by BOFs and EAFs. A BOF uses large amounts of oxygen to oxidize the charge, which is mostly

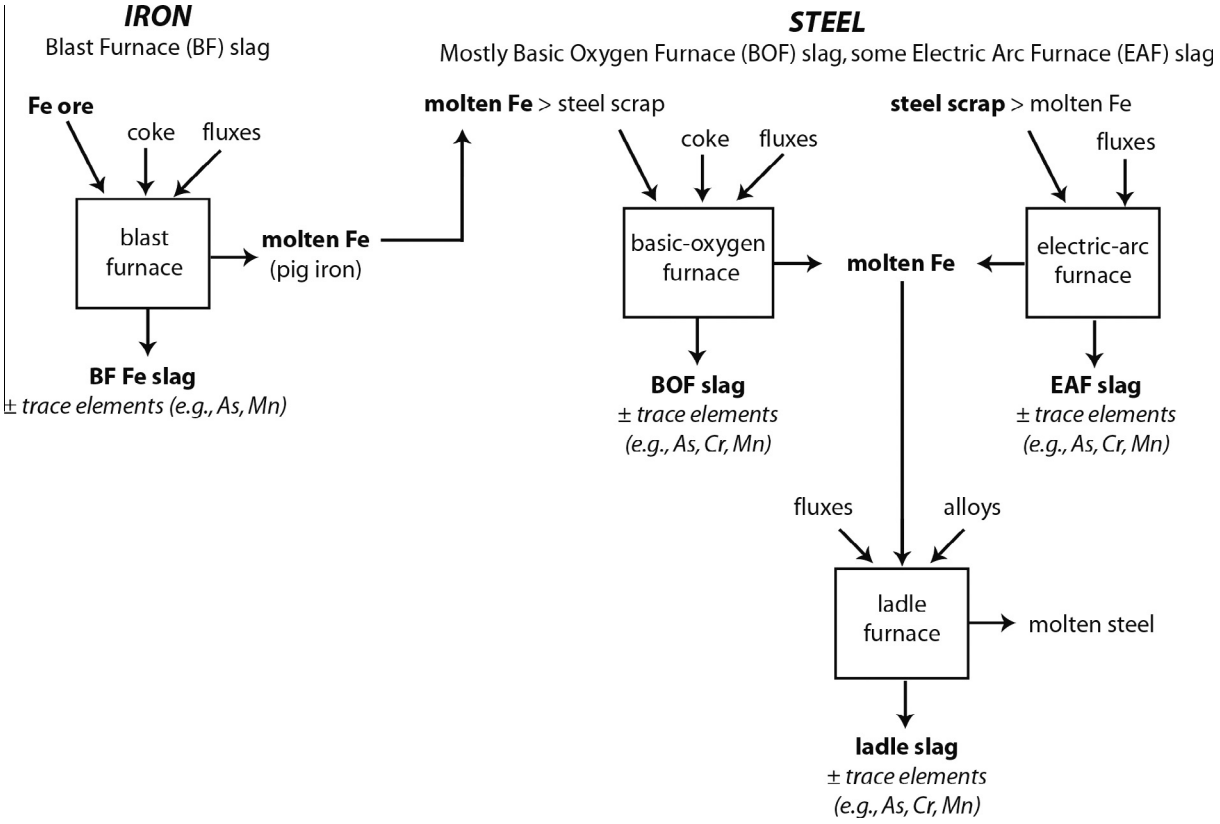

Fig. 2. Schematic of slag generation in a blast furnace operation to produce iron and in a modern steel plant to produce steel (modified from Yildirim & Prezzi, 2011).

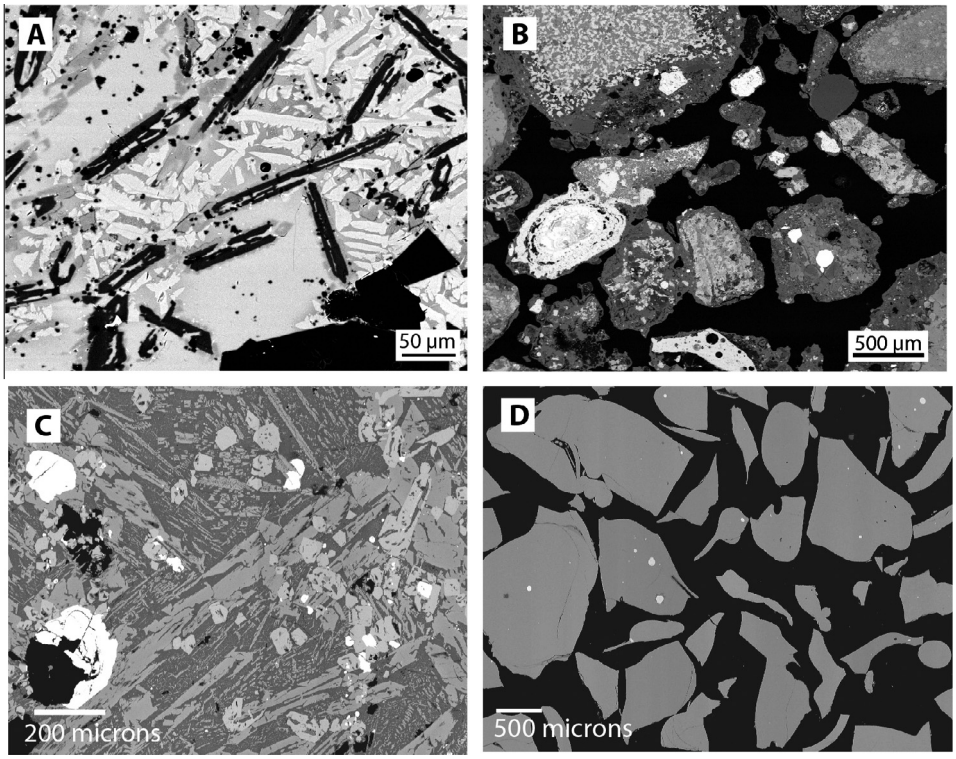

Fig. 3. Backscattered scanning electron photomicrographs of slag. (A) Air-cooled pre-1900 blast furnace iron slag from the Hopewell Furnace National Historic Site in Pennsylvania, USA. Image shows euhedral spinel and skeletal olivine laths within a background of skeletal pyroxene (dark gray), glass (light gray), and subhedral melilite (white) (from Piatak and Seal, 2012a). (B) Pelletized steel slag from Chicago. Image illustrates the heterogenous nature of the pellets that are composed of a wide variety of minerals including: quartz, larnite, melilite, brownmillerite, spinel group, wüstite, brucite, calcite, and Fe metal (from Piatak and Seal, unpublished). (C) Air-cooled Cu slag from the Elizabeth mine, Vermont, USA. Image shows randomly oriented elongate skeletal laths of olivine (dark grey), euhedral spinel (grey), and fine to coarse-sized sulfide blebs (white) set in a glass matrix (from Piatak et al., 2004). (D) Granulated Cu slag from Copper Basin, Tennessee, USA. Image shows sulfide blebs (light grey) set in glass (dark grey) mounted in epoxy resin (black) (from Piatak et al., 2004).

molten Fe with lesser amounts of scrap steel. An EAF uses an electric current to produce the heat necessary to melt recycled steel scrap with lesser amounts of molten Fe from the blast furnace. The temperatures in these furnaces fluctuate but commonly reach approximately 1650 °C (Brandt and Warner, 2009). Steel slags are usually slowly cooled under atmospheric conditions and form crystalline materials. In addition to slag produced in the primary stage of steelmaking, slags are also produced in secondary steel refining operations that adjust C content and remove remaining S, gases or impurities. Molten Fe from the BOF and EAF process may be refined in a ladle furnace with the possible addition of alloys and fluxes to produce different grades of steel. Slag produced in this process is ladle slag (Fig. 2). Steel furnace slags are cooled similarly to iron slags, have similar properties, and are used for similar purposes. However, some steel slags expand and need to be cured in piles before use (Van Oss, 2013).

Van Oss (2013) estimated that 0.25–0.30 tonnes of slag are generated per tonne of crude or pig iron in modern blast furnaces for typical Fe ore grades (60–66% Fe). For steel production, furnaces typically produce 0.2 tonnes of slag per tonne of crude iron, but the slag, up to half of which is metal, is returned to the furnace for further metal recovery. After final processing, the steel slag generated is approximately 10–15% of crude steel output. Based on Fe and steel production data, approximately 260–330 Mt of blast furnace Fe slag and approximately 150–220 Mt of steel slag were produced world-wide in 2011 (Van Oss, 2013).

2.2. Non-ferrous slag

Non-ferrous slags discussed in this chapter are produced during the recovery of non-ferrous metals from natural ores. Fig. 4 illustrates the general process for producing non-ferrous slag for base-metal production from sulfide ores. In general, three critical steps are involved in processing Cu, Ni, and Pb sulfide ores: concentrating, roasting, and smelting (Fig. 4). After mining, ore is generally crushed and ground and concentrated using gravity or, more commonly, flotation methods to separate the ore minerals from gangue. Next, the roasting process oxidizes sulfide minerals and aids in the removal of S, which is emitted as SO_2. During the smelting step, SiO_2, limestone, or iron sources (e.g., ironstone, iron silicates or iron oxides) are added as fluxes and carbon in the form of coke, charcoal, coal, or wood is added as a fuel and reductant. For Cu ores, the matte or molten metal phases are separated from the slag and enter the converter. During conversion, the melt is further desulfurized and other impurities removed by adding oxygen and fluxes (e.g., lime, Fe ore, or basic slag) (FHWA, 1997). The free metal is frequently combined with other elements or compounds to form the desired alloys. Slag is produced during smelting, converting, and some possible additional refining steps. Some is recycled to the smelter because of its high metal content (Fig. 4).

Nickel ore, which is commonly associated with Cu sulfide ore, may be processed with the Cu ores during concentrating, roasting and smelting. However, the combined Cu and Ni matte is roasted and then reduced with carbon or leached with acid to separate the Cu and Ni; additional refining further purifies the metals (Rosenqvist, 2004). Lead sulfide concentrates are roasted and then reduced in a blast furnace with a carbon fuel source and Ca and Fe compounds as fluxes (Cottrell, 1995). Next, additional impurities are removed in a reverberatory furnace by selective oxidations and then silver can be separated by the Parkes process (Cottrell, 1995). Non-ferrous ores can also be processed by leaching (hydrometallurgy) and/or reduction (electrometallurgy) methods such as

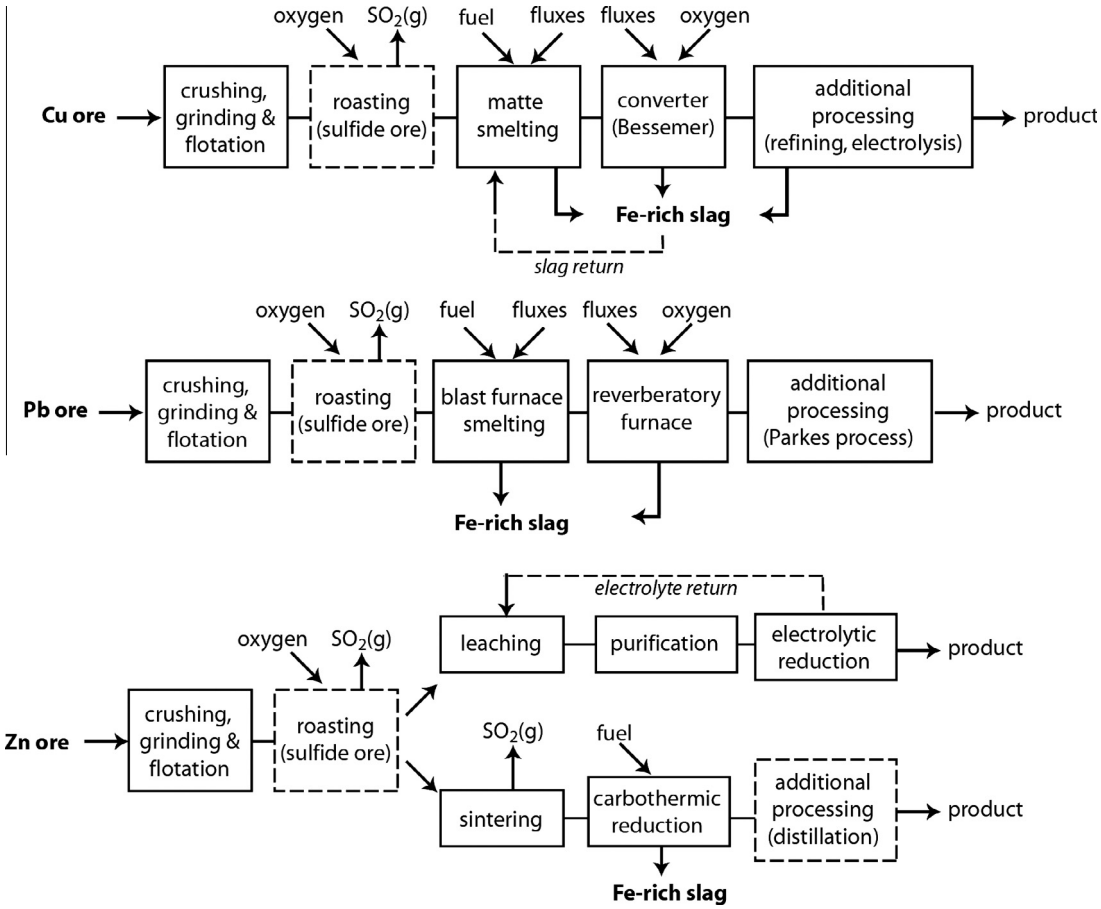

Fig. 4. General flow diagrams for processing non-ferrous ores and slag production. Not all metallugical processes used to recover base metals are represented. Modified from Cottrell (1995), FHWA (1997), and Rosenqvist (2004).

shown in Fig. 4 for Zn ores; slag is generated during reduction by carbon (i.e., carbothermic reduction).

Sulfide ores are predominantly processed by pyrometallurgical techniques, resulting in a slag. However, not all base metals are extracted from sulfide ores. For example, Cu can be extracted from oxides and carbonate ores, Pb from carbonate or sulfate ores, Zn from oxide, carbonate, or silicate ores, and Ni from oxide, silicate, or carbonate ores. The optimal recovery methods for some of these ores may or may not involve pyrometallurgy. Most of the studies reviewed here are from the pyrometallurgical processing of sulfide ores. An example of a study on slag that was produced from a non-sulfide ore is that associated with the extraction of Ni from laterite ores discussed in Kierczak et al. (2009). Precious metals such as Ag or Au may also be extracted from base-metal ore. For the purposes of this review, base-metal slag includes some slags produced during the recovery of precious metals as well. There are several other types of slag generated from processing natural ores such as phosphate, chromite, and Al slag that are not included in this review.

The types of furnaces used to smelt non-ferrous ore include blast, reverberatory, electric arc, or oxygen flash furnaces. An oxygen flash furnace injects compressed oxygenated air to promote combustion of the furnace charge. In contrast to furnaces where the fuel and materials are mixed in a single chamber, a reverberatory furnace typically separates the material being processed from the hot gases, but not from the combustion gases. Copper, Ni, Pb, and Sn ores are commonly smelted in reverberatory furnaces. Blast furnaces have been used to smelt Cu, Pb, Sn, and Zn ores, and oxygen flash furnaces to process Cu ore. In addition to blast furnaces, Zn ores are commonly processed in a retort where Zn reduction and distillation take place simultaneously. In this type of furnace, the fuel and all of the products of combustion are isolated from each other. Non-ferrous slags are commonly removed from the furnace and cooled slowly under atmospheric conditions creating a crystalline porous material (Fig. 3C). These slags are less commonly quenched forming a glassy product (Fig. 3D).

Furnace temperatures vary for non-ferrous smelters based on the type of furnace, processing methods, and composition of the ore; temperatures may reach up to 1400 °C (Cottrell, 1995). Although modern smelter operations have specific optimal furnace temperatures, historical furnaces likely had less rigorous temperature controls. A few studies report inferred temperatures for historical furnaces that smelted different types of ore and include the following: Sáez et al. (2003) proposed a furnace temperature of approximately 1200 °C for the smelting of Cu-sulfide, Cu-carbonate, and Cu-oxide ores in Spain during the 21st century B.C.; Manasse et al. (2001) reported slightly over 1100 °C for smelting Cu-sulfide ores in Italy during the 13th century or before; Kierczak and Pietranik (2011) stated a furnace temperature of approximately 1200 °C for 14th to 16th century Cu slag from Poland; and Lottermoser (2002) suggested temperatures likely over 1000 °C for late-1800 to mid-1900 furnaces that generated base-metal slag from a variety of ores in Australia.

The amount of slag produced in comparison to the amount of metal produced varies based on the commodity. Sobanska et al. (2000) estimated that 0.6 tons of slag were generated per ton of Pb for a smelter in France. In contrast, approximately 2.2 tonnes of slag are generated for every tonne of Cu produced according to Gorai et al. (2003) for a worldwide estimate.

3. Methods used to characterize slag

3.1. Empirical

3.1.1. Bulk chemistry

Characterization of the bulk chemical composition of slag is essential to understanding its nature and environmental behavior. Analytes of interest include, but are not limited to major, minor, and trace elements, loss on ignition (LOI), C and S species, and, occasionally, stable isotopes. Solid slag material may be leached with different solutions to investigate the mobility of various elements (i.e., standardized leaching tests, sequential extractions). These partial digestion methods can also provide information on the solid-phase partitioning of metals. Instrumental methods used for analysis of either the solid material, sometimes after the solid is completely digested, or partial digestion solutions each have advantages and disadvantages and are generally used in some combination (see Crock et al., 1999 for detailed descriptions of methods and their advantages). For total sample analysis, some of the most commonly used techniques are X-ray fluorescence (XRF), inductively coupled plasma-mass spectroscopy (ICP-MS), inductively coupled plasma-atomic emission spectroscopy (ICP-AES), atomic absorption spectroscopy (AAS), and automated elemental analysis (EA) by combustion for C, N, S, and/or H (Fig. 5). Other methods reported include infrared analysis (IR) for C and S, neutron activation (NA), hydride generation (HG) for Hg, and gravimetric and volumetric analysis and photometry (GVP). The most commonly used methods to analyze slag chemistry based on over 70 studies are consistent with common methods of analysis for environmental samples reported by Crock et al. (1999).

3.1.2. Mineralogy

Many slag studies also report information on slag mineralogy. Although synthetically produced phases such as those found in slag samples are not minerals by definition, mineralogical terminology is used in this manuscript for the sake of clarity in their description. The majority of slag characterization studies included mineralogical analysis, with the most common mineralogical method being X-ray diffraction (XRD) (Fig. 5). X-ray diffraction is a relatively quick method used to identify crystalline phases present in solid samples. In addition to XRD, scanning electron microscopy (SEM) and electron microprobe analysis (EMPA) are also commonly used to characterize slag. Both SEM and EMPA can be used to determine the chemical composition of the various phases, including glass, which is not easily identified or quantified using XRD. The host phases for environmentally significant trace elements can also be determined. Also, Raman spectroscopy has also proved useful in identifying secondary weathering products on slag (Seignez et al., 2007; Kierczak et al., 2013).

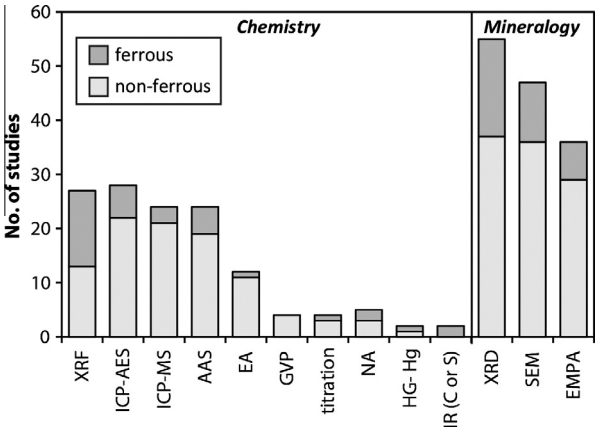

Fig. 5. Number of times methods were used to characterize the chemistry and mineralogy of slag from over 70 published studies. See text for abbreviations and Appendix A for references.

There are numerous challenges associated with characterizing the mineralogy of slag. First, quantifying the relative amounts of crystalline and amorphous phases in slag is a complex task. Quantification of phases can be estimated by petrographic methods such as point counting or by analyzing XRD patterns using single line, pattern summation, or Rietveld techniques, among others. Glass is generally ubiquitous in slag and only a few studies have attempted to quantify it (e.g., Parsons et al., 2001; Piatak et al., 2004; Piatak and Seal, 2010). Quantification of amorphous phases in samples can be challenging; Piatak and Seal (2014) discussed some of the challenges mentioned herein. For example, Rietveld XRD analysis requires a known amount of a crystalline internal standard to be added to the sample, homogenized, and analyzed. The addition of a standard can cause 'dilution' of phases or peak overlap issues. Examples of XRD patterns of pure glass, only crystalline phases, and a mixture of both crystalline and glass are shown in Fig. 6A for synthetic mixtures. The presence of glass raised the background in the approximately 20 to 40 degrees 2-theta interval in the pattern. Glasses with different compositions display different XRD signatures as illustrated in Fig. 6B for three glasses with three different silica contents. These results show that in order to confidently quantify crystalline phases and glass in slag, the accuracy of the method needs to be assessed using synthetic mixtures similar in composition to the slag phases.

Another challenge associated with characterizing the mineralogy of slag relates to EMPA analysis to determine the major and trace element composition of various phases. X-ray diffraction can provide insight into the major element composition of some phases, but is not definitive because of solid-solution effects. Neither SEM nor XRD can be used to quantify trace amounts of elements in phases. EMPA, the most commonly employed technique to determine the chemical composition of phases, can have unavoidable peak overlaps among elements within the mineral, which can result in erroneous measured concentrations. Overlaps may be minimized by changing the instrument and analysis settings but peaks for some elements will inevitably overlap. Examples of peak overlaps may include As and Mg in silicates and oxides and Co and Fe in all phases. In order to correct for peak overlaps, if the instrument configuration cannot be changed, users can determine an apparent amount or "phantom" concentration due solely to the overlap by analyzing standards with known compositions or by employing data-reduction algorithms that correct for peak overlaps. For example, trace amounts of phantom Co will be reported for phases with significant Fe. In Piatak et al. (2004), the concentrations of Co in sulfides with greater than approximately 7 wt.% Fe were adjusted for the peak overlap; phantom Co concentrations were approximately 0.2% of the Fe concentration. Also, overlap corrections will need to be determined each time data are collected because the instrument settings vary for each analysis package and settings may change over time as parts age and users adjust the instrument.

In addition to EMPA peak overlaps, recent investigations suggest that some of the standard micro-analytical mineralogical methods, such as EMPA and SEM, may need to be supplemented by techniques that can determine mineralogical and chemical variations on the nano-scale to accurately characterize a slag material. For example, Seignez et al. (2007) found discrete submicrometer-size Pb-rich and Fe-rich entities within Pb-slag glass using Raman spectroscopy and transmission electron microscopy (TEM). Using focused ion beam TEM, Ettler et al. (2012) revealed that K-rich pyroxenes reported in Cu slag from Zambia (Vítková et al., 2010) were actually an admixture of the nanometer-size leucite

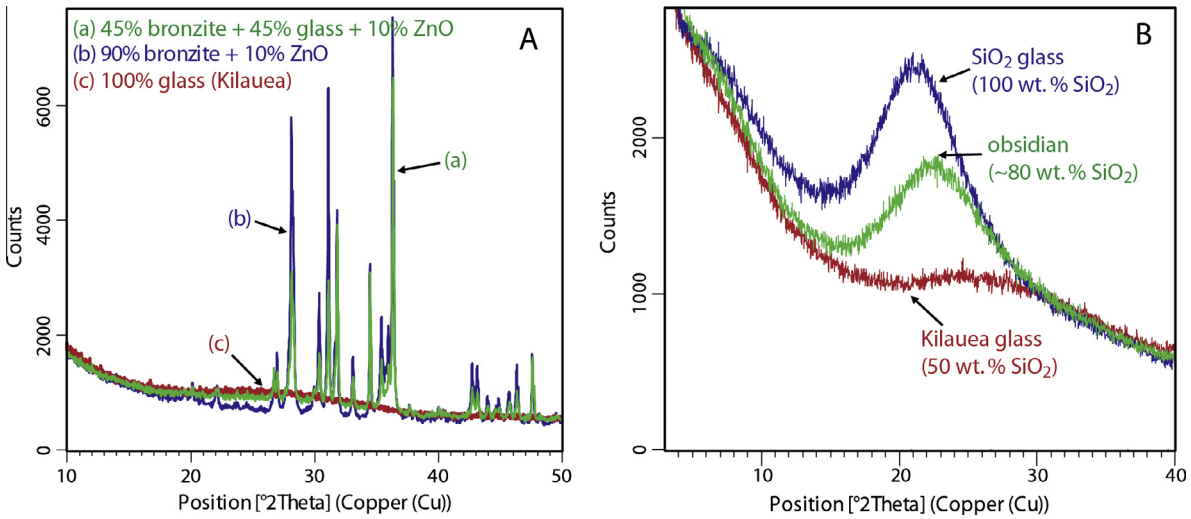

Fig. 6. X-ray diffraction patterns of (A) synthetic mixtures of crystalline and glass phases and (B) glass of varying SiO_2 compositions.

($KAlSi_2O_6$) inclusions within the pyroxene((Na,Ca)(Mg,Fe,Al)$(Al,Si)_2O_6$); the inclusions were not detected during SEM and EMPA work. These studies suggest that some caution is required when interpreting and reporting EMPA data for phases in slag that may be a mixture of phases on a nanometer-scale. Glass analyses, in particular, may be suspect due to the immiscibility between silicate and sulfide liquids (Ettler et al., 2012).

Yet another challenge associated with determining the composition of phases in slag is deciphering the speciation of elements that occur in multiple valence states. Sulfur speciation is particularly important because of its relationship to the acid-generating potential of slag. For example, Piatak and Seal (2012a) reported S concentrations in glass and melilite ($(Ca,Na)_2(Mg, Fe^{2+}, Al, Si)_3O_7$) in historical Fe slag from Pennsylvania, USA. In order to verify that the S was in the reduced (S^{2-}) state versus the oxidized state (S^{6+}), the wavelength of S$K\alpha$ in the glass and melilite were compared to that of sulfate and sulfide standards using EMPA. This method is based on determining S speciation in experimental glasses by Carroll and Rutherford (1988). One limitation of the method is that a significant amount of S needs to be present (>~1 wt.% S) in the phase in order to accurately measure the peak position used to determine valence. For the Pennsylvania Fe slag, sulfur was determined to be in the reduced state, which is in agreement with the reducing furnace conditions in this smelter. In contrast, determining S speciation using X-ray absorption near edge structure (XANES) spectroscopy has been achieved on samples containing as little as 450 mg/kg S for synthetic and natural glasses by Paris et al. (2001). XANES spectroscopy is an element-specific X-ray absorption technique that provides information about the local bonding of elements, which can be related to their valence state. Roy (2009) applied the XANES technique to steel slag and was able to estimate the relative amounts of more than one species of S. His results indicated that S was present as SO_4^{2-} in air-cooled Fe slag and mostly as S^{2-} in granulated Fe slag.

3.1.3. Leaching tests

Leaching tests are used to investigate the mobility of trace elements in solid wastes and to help predict their long-term environmental behavior. There are many types of leach test procedures that vary based on the sample preparation, leachant composition, method of contact, solid-to-solution ratio, leachant renewal, temperature, contact time, and ultimately purpose, among others. The most commonly employed leaching tests can be divided into several types. First, single batch tests are agitated to maintain a homogenous mixture to aid in achieving steady state conditions. Usually crushed or sieved, samples are mixed with a leachant solution at a specific ratio, with no leachant renewal. Single batch tests developed by the United States Environmental Protection Agency (USEPA) for regulatory compliance include the toxicity characteristic leaching procedure (TCLP), which replaced the extraction procedure toxicity test (EP-tox) in 1990, and the synthetic precipitation leaching procedure (SPLP) (USEPA, 2008). These two standard procedures use dilute acidic leachant solutions (acetic acid or acetate buffer for TCLP and EP-tox and sulfuric/nitric acid solution for SPLP) with a contact time of 18 h. The liquid-to-solid ratio is 20:1 (volume to mass) for material that is less than 9.5 mm in diameter (crushed if necessary). Fig. 7 summarizes the number of times various types of leaching tests have been conducted on slag based on the references listed in Appendix A. As shown, the USEPA tests are some of the most commonly used based on this survey. Another single batch test frequently applied to non-ferrous slag is the EN 12457-2 (Fig. 7), which was established by the European Committee for Standardization (European Committee for Standardization, 2002). This procedure uses distilled/deionized water as the leachant with a contact time of 24 h. The liquid-to-solid ratio is 10:1 using material with a particle size of less than 4 mm in diameter. Several studies have also reported reacting the surface of thin sections (i.e., a thin polished slice) of slag with various solutions to study the effect on the dissolution of specific crystalline or glass phases. Less

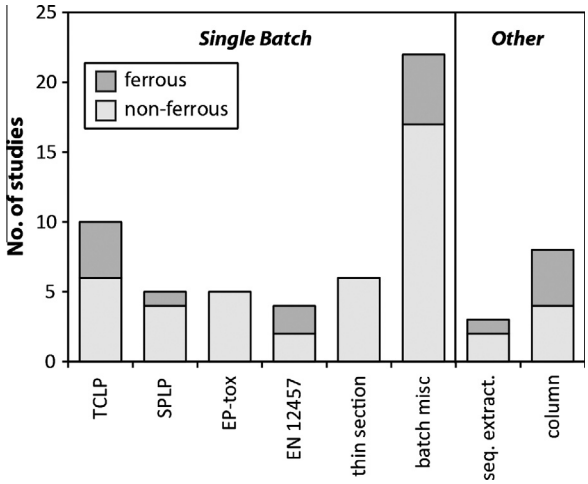

Fig. 7. Number of studies that used various leaching test procedures on slag. This chart is a summary of over 50 studies. See text for abbreviation and Appendix A for references.

commonly used or unique unstandardized procedures for single batch extraction tests were grouped together in Fig. 7. It is apparent from this figure that single batch extraction tests are the most common type of leaching tests used on slag. Sequential chemical extraction tests (seq. extract.) are reported far less commonly (Fig. 7). These tests use increasingly aggressive leachants to gain insight into the partitioning of contaminants among various operationally defined solid phases. In addition to these batch tests, dynamic tests such as flow-through or column tests have been conducted on slag to better understand the kinetic processes controlling metal release (Fig. 7). The leachant continuously or intermittently flows through the material to measure leaching under advective conditions.

Successful application of the results of leaching tests depends on the objective of the study. Many leaching tests are performed to simulate natural weathering of the slag or conditions in a landfill environment. These tests characterize and evaluate the release of potentially harmful trace elements from slag, and are often considered to represent 'worst-case' leaching scenarios because of the crushing of the material and constant agitation throughout the leaching test. For example, regulatory compliance tests such as TCLP, EP-tox, and EN 12457 were developed to classify material as hazardous or nonhazardous to determine if material is acceptable for disposal in a landfill without special treatment or handling. The results impact how slag waste is disposed, how slag waste piles are treated, and if and how slag is used as a resource for construction or environmental applications. In contrast, the SPLP test was developed to assess the impact of a material on groundwater and surface water by simulating interaction with atmospheric precipitation (i.e., rain, snow). Also, studies that examine the leaching behavior of the surface of thin sections give insight into which trace-element bearing phases may be the most reactive (Kucha et al., 1996; Seignez et al., 2007, 2008; Ettler et al., 2001b, 2002). Other studies have assessed the bioaccessibility of Pb from slag using simulated human gastric fluid as the extraction solution (Morrison and Gulson, 2007; Bosso and Enzweiler, 2008). Sequential extractions have also been applied to gain insight into element speciation and partitioning into various phases to determine trace element mobility and bioavailability and the related environmental impact of slag dumps (Álvarez-Valero et al., 2009; Pérez-López et al., 2008). In addition, toxicity tests have been performed on Fe and steel leachate to determine ecological risk with respect to reuse (Wendling et al., 2012, 2013). Dynamic tests represent far-from-equilibrium conditions that may more closely mimic slag dump weathering conditions. These tests may emulate field conditions in which secondary minerals containing trace elements precipitate directly from waters during dry periods and subsequently dissolve and release the trace elements into the environment during rainy periods (Navarro et al., 2008; Seignez et al., 2008). In addition to these environmentally-focused tests, some leaching tests are performed to determine an effective means for extracting valuable metals from slag (Gbor et al., 2000). Regardless of the details of the various leaching test procedures, leaching tests on slag can provide useful insight into the character and environmental aspects of slag.

3.2. Theoretical

3.2.1. Geochemical modeling

Geochemical modeling is a powerful tool that can be used to evaluate the major processes controlling the release, transport, and fate of metals from ferrous and non-ferrous slags during weathering, and to predict the long-term stability of slags under changing environmental conditions (Parsons et al., 2001). There are two main approaches to geochemical modeling: (1) inverse (mass-balance) modeling, which uses observed water compositions to deduce geochemical reactions, and (2) forward (mass-transfer) modeling, which uses hypothesized geochemical reactions to predict water compositions (Alpers and Nordstrom, 1999). In general, inverse modeling is used to calculate the moles of solid phases and gases that must enter or leave solution to account for differences in the composition of water samples along a known flow path, or from a reaction vessel (Parkhurst and Plummer, 1993). Mass-balance models are based solely on the compositions of water and of possible reactant and product phases, but can be further constrained by knowledge of thermodynamic and kinetic constraints (e.g., Garrels and Mackenzie, 1967; Glynn and Brown, 1996). Calculated mole transfers from inverse modeling serve as a useful guide for forward modeling, which predicts the results of hypothetical, irreversible water–rock-gas reactions applied to an initial solution of known composition (Helgeson, 1968). Forward models can be used to simulate solid phase dissolution and precipitation, fluid mixing, sorption, and other geochemical reactions as a function of time or reaction progress, and are particularly useful for developing remediation strategies for contaminated sites (e.g. Strömberg and Banwart, 1994; Alpers and Nordstrom, 1999; Parsons et al., 2001; Bethke, 2008). A wide range of computer programs are available to carry out geochemical modeling calculations, some of which are described by Alpers and Nordstrom (1999) and Bethke (2008).

The first step in using geochemical models to evaluate the environmental reactivity of smelter slags is to calculate the aqueous speciation of constituents of waters collected from the field (e.g. drainage from slag dumps), or of leachates from slag-leaching experiments. It is important to ensure that water chemistry data used for modeling purposes are of high quality, and include analytical results for all major and minor ions such that electrical charge imbalances are minimized. The output from a speciation calculation shows the distribution of dissolved constituents among various aqueous complexes and free ions for a given set of environmental conditions (temperature, pH, fugacities of $CO_2(g)$ and $O_2(g)$, etc.) (Alpers and Nordstrom, 1999). These results can then be used to determine the degree of saturation of the aqueous solution with respect to various phases according to the following equation:

$$SI = \log(Q/K) \quad (1)$$

where SI is the saturation index of an aqueous solution with respect to a solid phase, Q is the ion activity product and K the equilibrium constant for the dissolution reaction. If the SI is zero the solution composition reflects solubility equilibrium, a negative value indicates undersaturation, and a positive value indicates supersaturation. Once the saturation indices of various phases are known, the user can then determine what dissolution and precipitation reactions are thermodynamically possible in the absence of kinetic barriers (Parkhurst and Plummer, 1993).

Over the last two decades, many researchers have used aqueous speciation modeling to better understand the reactivity of slags in the field and in the lab. Most of these studies have focused on calculating the saturation indices of various solid phases in leachates from batch and flow-through leaching tests to evaluate possible solubility controls on metal concentrations (Bäverman et al., 1997; Mandin et al., 1997; Piatak et al., 2004; Seignez et al., 2008; De Windt et al., 2011). Some authors have also applied speciation modeling to waters draining slag dumps in the field to assess the main controls on dissolved metal concentrations (Parsons et al., 2001; Lottermoser, 2002; Roadcap et al., 2005; Navarro et al., 2008). In general, solid phases with saturation indices relatively close to zero (-1.0 SI $+1.0$) may control the solubility of elements in solution, provided these phases are kinetically likely to form within the timeframe of a leaching test, or during the transit of water through a slag dump (Nordstrom and Alpers, 1999). Observations of reacted slags in the lab or field can provide

direct evidence of secondary minerals that are most likely to control the mobility of elements during leaching tests or weathering reactions (e.g., Parsons et al., 2001; Lottermoser, 2002; Piatak et al., 2004; Roadcap et al. 2005; Navarro et al., 2008). The formation of secondary minerals can significantly reduce the mobility of elements released from both ferrous and non-ferrous slags during leaching or natural weathering reactions, although not necessarily rendering them environmentally benign; secondary minerals must be carefully chosen in geochemical modeling calculations.

Inverse modeling has not been widely used in studies of slags, but it can provide insight into the relative importance of solid phase dissolution and precipitation reactions (Parsons, 2001; Piatak et al., 2004). For example, Piatak et al. (2004) used mass-balance calculations of slag test leachates to show that the leachate chemistry cannot be explained strictly through dissolution of the primary crystalline and glass phases identified in the slag. Instead, precipitation of secondary phases such as $Al(OH)_3$ and ferrihydrite ($5Fe_2O_3{\cdot}9H_2O$) was required to fully account for the observed leachate chemistry. The calculated mass balances can be used to evaluate the relative reactivity of various slag phases, and to identify the key processes that control the aqueous concentrations of specific trace elements in slag test leachates and drainage from slag dumps (Parsons, 2001).

Forward modeling can be used to predict the long-term (i.e., tens to hundreds of years) leaching behavior of slags when properly constrained through careful field and laboratory studies. Early applications of forward modeling of smelter slags combined the results of laboratory leaching tests with reactive transport models to simulate the flow of surface water through a slag dump or the migration of metals into underlying soils (Tack et al., 1993; Bäverman et al., 1997; Mandin et al., 1997). However, the predictive capability and reliability of these models were limited by incomplete characterization of slag mineralogy and reactive surface area, uncertain equilibrium assumptions, insufficient field data with which to compare model results, and a lack of thermodynamic data for key phases and their solid solutions. In some cases, the leachate concentrations predicted from these models did not match the measured concentrations in relatively simple laboratory column tests, casting doubt on their ability to model long-term slag leaching in the natural environment (Bäverman et al., 1997). To improve the accuracy of forward models for slags, it is particularly important to include kinetic rate laws for dissolution of all crystalline and glass phases, given their relatively slow reaction rates at low temperatures (Wilson, 1994; Alpers and Nordstrom, 1999; De Windt et al., 2011).

Parsons et al. (2001) used forward modeling to simulate irreversible mass-transfer reactions between base-metal slag deposits and lake water at the Penn Mine in California. These models included kinetic rate laws for abiotic sulfide oxidation and surface-controlled dissolution of silicate, oxide, and glass phases in the slag. The surface area of slag in contact with 1 kg of lake water (the default fluid mass in these models) was estimated by measuring the grain-size distribution of the finer-grained material in the slag dump and calculating the specific geometric surface area. The reactive surface area of each crystalline or glass phase was then estimated by multiplying the total physical surface area by the average volume percentages of each phase in the slag. Reaction rates for dissolution and oxidation of phases in the slag were selected from the published literature based on their applicability over the range of pH values measured at the Penn Mine field site. The reaction rate for a metal-rich, interstitial glass phase in the slag was calculated from TCLP and SPLP leach test results (Parsons et al., 2001). The results of these modeling calculations suggested that the dissolved concentrations of Ba, Cu, Fe, SiO_2 and SO_4 in the slag dump pore waters were primarily controlled by the solubilities of various secondary minerals (Fig. 8), whereas Pb concentrations

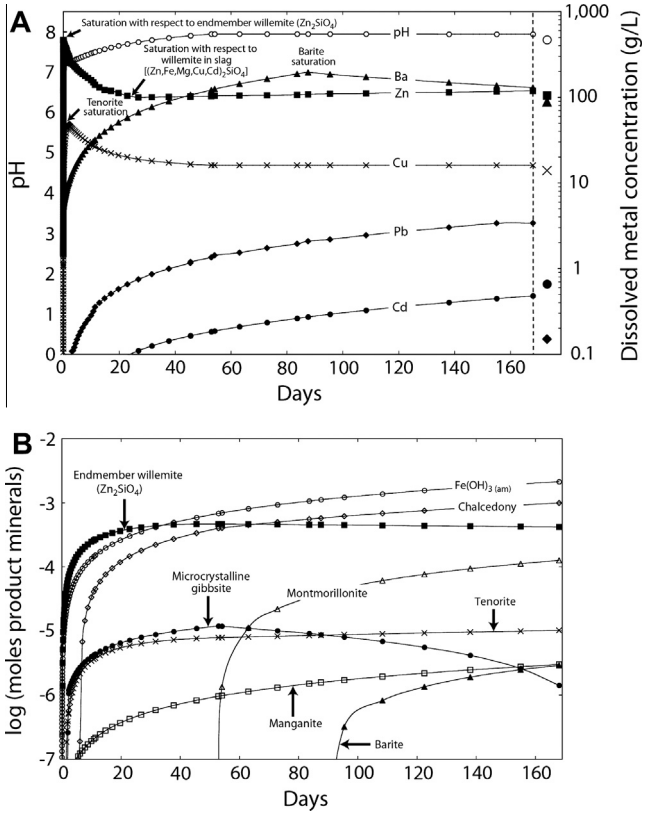

Fig. 8. (a) Dissolved metal concentrations and pH during forward modeling of reactions between Cu slag and lake water, Penn Mine, California. Field data for the slag dump pore waters are represented by the larger symbols to the right of the dashed vertical line. (b) Secondary minerals produced during forward modeling simulation of irreversible mass-transfer between the Penn Mine slag dump and lake waters. (From Parsons et al., 2001).

were most likely controlled by sorption and/or co-precipitation reactions (Parsons et al., 2001). The modeling results provide important insights into the main geochemical processes that control the release of elements from this slag dump, and how these may change over time in response to various remediation strategies. More recently, De Windt et al. (2011) have applied a similar forward modeling approach to basic oxygen furnace steel slags.

4. Chemical and mineralogical characteristics

4.1. Ferrous slag

4.1.1. Bulk chemistry and primary mineralogy

Ferrous slag composition is dominated by Ca and Si with variable amounts of Al, Fe, and Mg. Table 1 contains a summary of ferrous slag chemistry from nearly 40 sources; ferrous slag references containing bulk chemical compositions included in the table are listed in Appendix A. Major element concentrations are reported as oxides, which is the common convention for expressing major-element bulk chemical concentrations as well as the chemical composition of crystalline oxides and silicates. This enables slag compositions to be plotted on ternary phase diagrams. However, some major elements have been shown to exist in other than oxide forms. For example, Fe is commonly reported as FeO or Fe_2O_3 but in some slag it is present as minor or trace FeS or Fe metal. For each slag type, Table 1 lists the minimum, maximum, and average values, as well as the number of samples or analyses (n1) and the number of studies (n2) that reported the chemistry; values below the detection limit were not included in the compilation. Analyses include tables from reports that have published a summary of

Table 1
Summary of major, minor, and trace element chemistry of slag by slag type from almost 70 studies. All concentrations were included for samples identified as slag by the article's authors. Values below the detection limit were not included.

	Fe					Pre-1900 Fe					Steel					Ni laterite					Sn (historical)				
	Min	Max	Average	n1	n2	Min	Max	Average	n1	n2	Min	Max	Average	n1	n2	Min	Max	Average	n1	n2	Min	Max	Average	n1	n2
wt.%																									
Al_2O_3	5.86	41.2	14.3	41	13	3.42	22.3	10.6	42	4	0.02	44.3	7.49	60	25	2.79	18.0	12.9	8	1	3.37	22.1	10.5	25	1
CaO	0.15	93.4	36.1	38	12	1.34	40.1	15.2	42	4	1.63	70.1	34.9	62	25	9.92	57.6	22.8	8	1	1.66	16.8	6.24	25	1
FeO total	0.02	13.6	1.60	37	11	0.08	61.8	16.1	42	4	1.07	50.9	22.9	61	25	5.40	33.7	15.2	8	1	4.52	31.0	13.3	25	1
K_2O	0.08	5.06	0.99	33	10	0.19	3.67	1.41	37	4	0.01	3.89	0.24	29	13	0.6	2.31	1.25	7	1	0.67	4.89	2.11	25	1
MgO	1.66	19.6	8.78	41	13	0.14	24.7	8.87	42	4	0.43	19.9	7.22	58	25	2.04	10.1	5.05	8	1	1.17	5.82	2.80	25	1
MnO	0.01	26	1.90	34	10	0.04	11.6	0.95	42	4	0.2	21.5	4.32	55	25	0.22	1.72	0.71	8	1	0.06	0.29	0.12	25	1
Na_2O	0.09	2.65	0.49	33	12	0.06	0.76	0.36	37	3	0.02	0.57	0.16	31	16	0.19	2.24	0.85	7	1	0.33	1.47	0.70	25	1
S	0.38	3.15	1.27	26	6	0.02	0.96	0.19	20	1	0.03	1.06	0.22	30	8	–	–	–	–	–	–	–	–	–	–
SiO_2	26.6	46.1	35.3	41	13	27.2	61.3	45.2	42	4	0.03	61.1	16.9	56	23	18.2	44.6	38.5	8	1	20.9	70.4	40.0	25	1
TiO_2	0.02	3.7	0.63	36	9	0.02	1.1	0.79	37	3	0.12	1.98	0.66	37	20	0.09	0.73	0.52	8	1	0.89	10.9	3.16	25	1
LOI	0.1	4.52	1.86	5	3	0.03	2.26	0.65	9	1	0.2	11.2	3.55	16	7	–	–	–	–	–	0.42	6.62	3.01	25	1
mg/kg																									
As	0.5	25	6.5	7	2	2	12	4.5	6	1	0.5	244	24.6	16	8	–	–	–	–	–	6.53	26.4	14.7	14	1
Ba	180	1,110	557	9	4	120	2,030	806	30	2	24	1,800	366	32	10	–	–	–	–	–	99	2,299	480	20	1
Cd	–	–	–	–	–	0.3	0.3	0.3	1	1	0.1	128	14.7	21	7	–	–	–	–	–	–	–	–	–	–
Co	0.03	33	9.447	10	4	1	210	58.6	30	2	0.8	36	7.88	27	8	5	700	220	6	1	0.97	14.8	8.11	14	1
Cr	0.1	9,580	1,032	17	6	2	39	9.1	20	1	4	32,700	4,798	44	13	330	13,400	4,484	8	1	60.7	411	202	25	1
Cu	0.13	54	15.9	17	6	2.7	300	65.5	30	2	3	540	114	33	9	29	2,200	1,157	5	1	5	96.3	14.3	19	1
Ni	0.3	68	14.4	11	6	1.1	17.1	7.24	14	1	0.9	3,180	153	31	9	74	6,907	2,154	8	1	5	26.1	13.6	20	1
Pb	0.2	150	21.7	13	4	0.6	250	73.9	29	2	2	1,040	126	31	9	8	501	246	3	1	5.04	624	81.5	14	1
Zn	0.15	320	79.5	15	4	1	40	15.4	29	2	1	11,000	748	41	14	13	2,500	1,162	6	1	39.2	111	75.2	14	1

	Ni sulfide					Cu (± other base metals)					Pb–Ag, Ag–Pb, Pb, Pb–Zn					Zn, Zn–Pb				
	Min	Max	Average	n1	n2	Min	Max	Average	n1	n2	Min	Max	Average	n1	n2	Min	Max	Average	n1	n2
wt.%																				
Al_2O_3	6.72	7.00	6.87	6	1	0.01	18.9	6.17	97	13	1.74	11.1	4.94	27	12	0.9	21.9	14.3	19	3
CaO	2.74	3.96	3.03	7	2	0.15	21.9	7.06	97	13	0.45	23.1	9.41	30	13	0.18	23.6	11.1	19	3
FeO total	42.8	47.7	45.2	7	2	0.67	62.0	33.1	107	14	3.16	59.6	26.1	40	14	0.88	33.7	15.5	19	3
K_2O	–	–	–	–	–	0.01	4.83	1.35	95	12	0.23	2.58	1.21	25	10	0.04	3.91	1.22	18	2
MgO	1.56	3.20	2.88	7	2	0.09	6.45	1.79	96	12	0.37	5.44	1.67	25	10	0.61	10.7	4.02	17	2
MnO	0.06	0.06	0.06	6	1	0.03	6.55	0.54	94	11	0.09	8.95	2.45	29	12	0.01	1.21	0.30	18	2
Na_2O	–	–	–	–	–	0.01	4.31	0.45	95	12	0.02	1.4	0.36	34	10	0.05	3.93	0.89	16	2
S	0.99	1.03	1.01	6	1	0.01	6.51	1.40	91	11	0.12	3.4	0.85	25	11	0.08	2.68	1.08	19	3
SiO_2	29	39.3	36.9	7	2	9.82	70.7	35.9	93	12	17.6	54.6	36.7	29	12	2.04	57.1	35.2	19	3
TiO_2	0.23	0.24	0.24	6	1	0.1	1.66	0.39	88	11	0.01	5	0.58	22	8	0.07	1.14	0.66	18	2
LOI	–	–	–	–	–	0.1	11.8	1.73	25	4	–	–	–	–	–	0.36	29.6	6.45	14	2
mg/kg																				
As	–	–	–	–	–	0.8	75,865	3315	74	9	87	2900	491	32	10	1	10,710	1271	19	3
Ba	–	–	–	–	–	28	29,000	2226	66	8	169	190,000	20,630	33	9	76	2555	1104	18	2
Cd	–	–	–	–	–	0.43	14,000	1055	41	11	0.3	700	99.2	9	8	0.8	191	27.0	18	2
Co	1210	1400	1293	6	1	15	24,104	3317	53	7	6.1	185	41.1	26	5	8.5	242	40.23	10	1
Cr	–	–	–	–	–	13	7510	455	61	6	19	700	82.3	27	6	4	103	78.4	10	1
Cu	110	180	140	6	1	1400	353,580	25,088	97	11	88.5	7550	2502	26	10	16	6360	727	10	1
Ni	2600	2960	2762	6	1	2	935	70.9	65	8	5.6	240	97.1	19	5	24.3	107	46.8	10	1
Pb	–	–	–	–	–	6.2	183,800	14,205	92	10	5000	319,190	90,657	32	15	1.9	62,290	7302	17	3
Zn	180	190	187	6	1	44	280,000	36,314	95	10	701	120,000	31,162	40	14	212	379,694	56,569	19	3

Abbreviations: min = minimum value, max = maximum value, n1 = number of samples, n2 = number of studies that have values, – = data not available.
Note: All iron is reported as FeO.

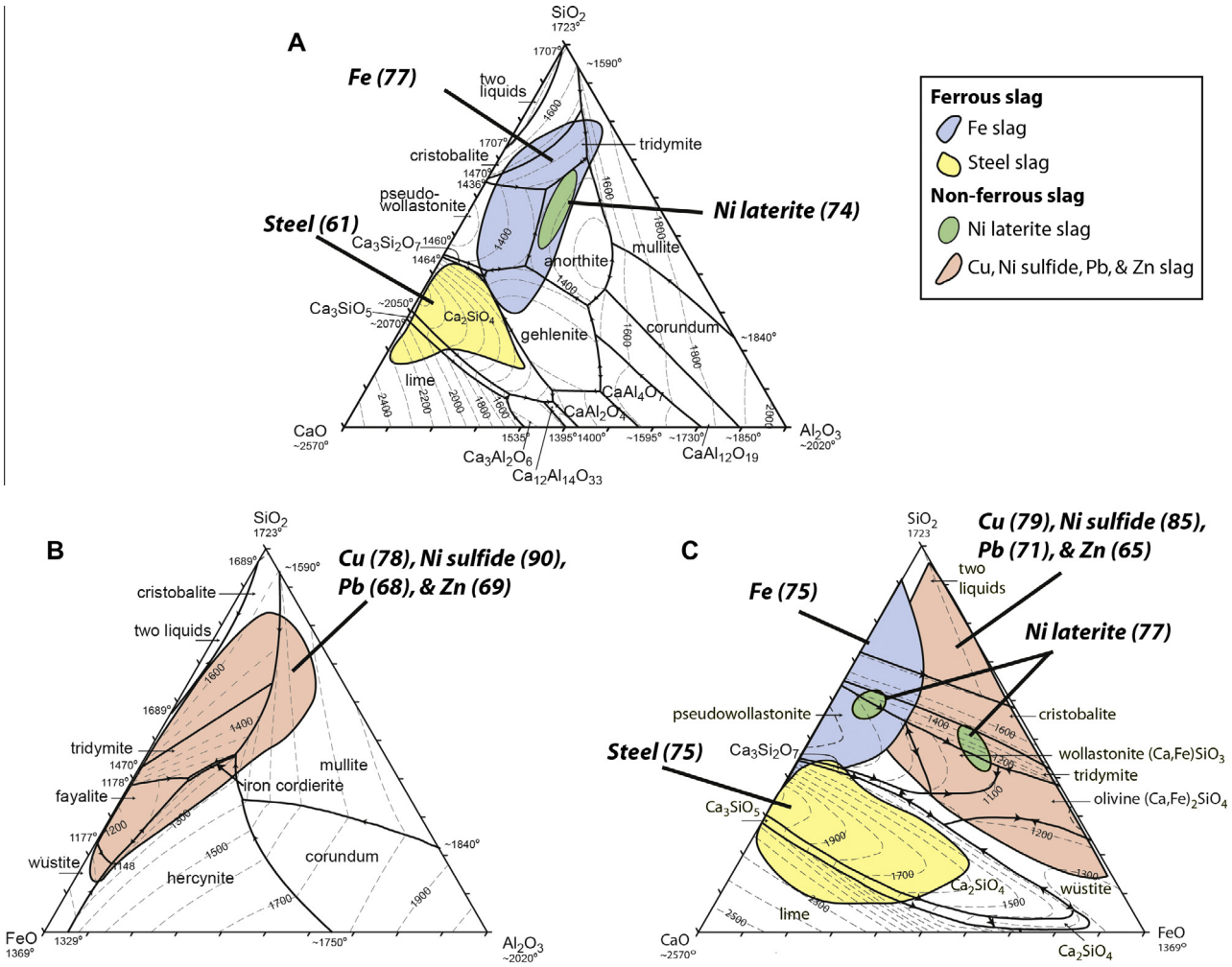

Fig. 9. Bulk chemical compositions of slag in weight percent on Al_2O_3-SiO_2-CaO (A), Al_2O_3-SiO_2-FeO (B), and FeO-SiO_2-CaO (C) ternary diagrams. Based on slag chemistry, one or two ternaries were chosen to represent the bulk composition of each slag type. The shaded fields on each diagram represent the majority of samples for each slag type (some outlying points were not included in the composition fields). Similar slag compositions were grouped. The average total weight percent represented by the fields or symbols are given in parentheses after the slag type. Phase boundaries and isotherms, in Celsius, from Levin et al. (1964). See Appendix A for references.

individual samples or compiled data from other sources. For example, the chemistry of ferrous slag from 58 active steel mills in the United States was summarized by Proctor et al. (2000). Their published data incorporated into Table 1 include only minimum, maximum, and mean values for Fe slag and two types of steel slag (not individual analyses). Nonetheless, it is obvious from Table 1 that CaO and SiO_2 generally dominate Fe slag with lesser amounts of Al_2O_3 and MgO. The compositions are shown as shaded fields on the Al_2O_3–SiO_2–CaO and FeO–SiO_2–CaO ternary diagrams in Fig. 9; these ternary systems represent an average of 77% and 75% of the total mass of the samples, respectively. The pre-1900 Fe slags dominate the SiO_2-rich end of the field, whereas modern Fe slag from steel-making plants is clustered closer to the CaO-rich end of the field. In comparison to Fe slag, steel slags are represented on the Al_2O_3–SiO_2–CaO and the FeO–SiO_2–CaO ternaries in Fig. 9; the latter ternary is more representative because more of the total bulk composition is encompassed such that the field represents an average of 75% of the total mass of the samples, compared to 61% for the Al_2O_3–SiO_2–CaO system. Both diagrams illustrate that most steel slag is dominated by CaO. Variations in the major-element chemistries among types of steel slag (i.e., BOF, EAF, and ladle slag) are discussed in Yildirim and Prezzi (2011).

The average concentrations of Al, Ca, and Mg for steel and Fe slag are similar and range from 15 to 36 wt.% for CaO, from 7 to 14 wt.% for Al_2O_3, and from 7 to 9 wt.% for MgO (Table 1). In contrast, steel slag contains, on average, higher concentrations of Fe (average of 23 wt.% FeO) compared to Fe slag (averages of 1 and 16 wt.% FeO for modern and pre-1900 samples) (Table 1). Also, steel slag generally contains lower concentrations of Si (average 17 wt.% SiO_2) compared to Fe slag (35 and 45 wt.% SiO_2 for modern and pre-1900 slag, respectively). Manganese oxide (MnO) averages 4 wt.% in steel slag compared to 2 wt.% (modern) and 1 wt.% (pre-1900) in Fe slag. The other major elements expressed as oxides include K_2O, Na_2O, and TiO_2 and average less than 2 wt.% in ferrous slag (Table 1).

In Fig. 9A, the pre-1900 Fe slag that dominates the SiO_2-rich end of the Fe slag field plots within the cristobalite (SiO_2 above 1470 °C), tridymite (SiO_2 below 1470 °C), anorthite ($CaAl_2Si_2O_8$), and pseudowollastonite ($CaSiO_3$ above ~1125 °C) fields. The primary mineralogy reported for pre-1900 Fe slag in Costagliola et al. (2008), Piatak and Seal (2012a), Severin et al. (2011), and Vivenzio and Farthing (2005) include quartz, cristobalite, and plagioclase ($(Na,Ca)(Si,Al)_4O_8$), which are all consistent with this phase diagram. Other Ca-rich silicates and aluminosilicates identified were olivine ($(Ca,Fe)_2SiO_4$)-, melilite-, and pyroxene-group phases, mullite ($Al_6Si_2O_{13}$), garnet ($X_3Y_2(SiO_4)_3$), and glass (Fig. 10). In addition, Fe and Ti oxides and calcite ($CaCO_3$), among others, were mentioned. The primary mineralogy of the pre-1900 iron slag is generally consistent with that predicted by the bulk composition based on Fig. 9A.

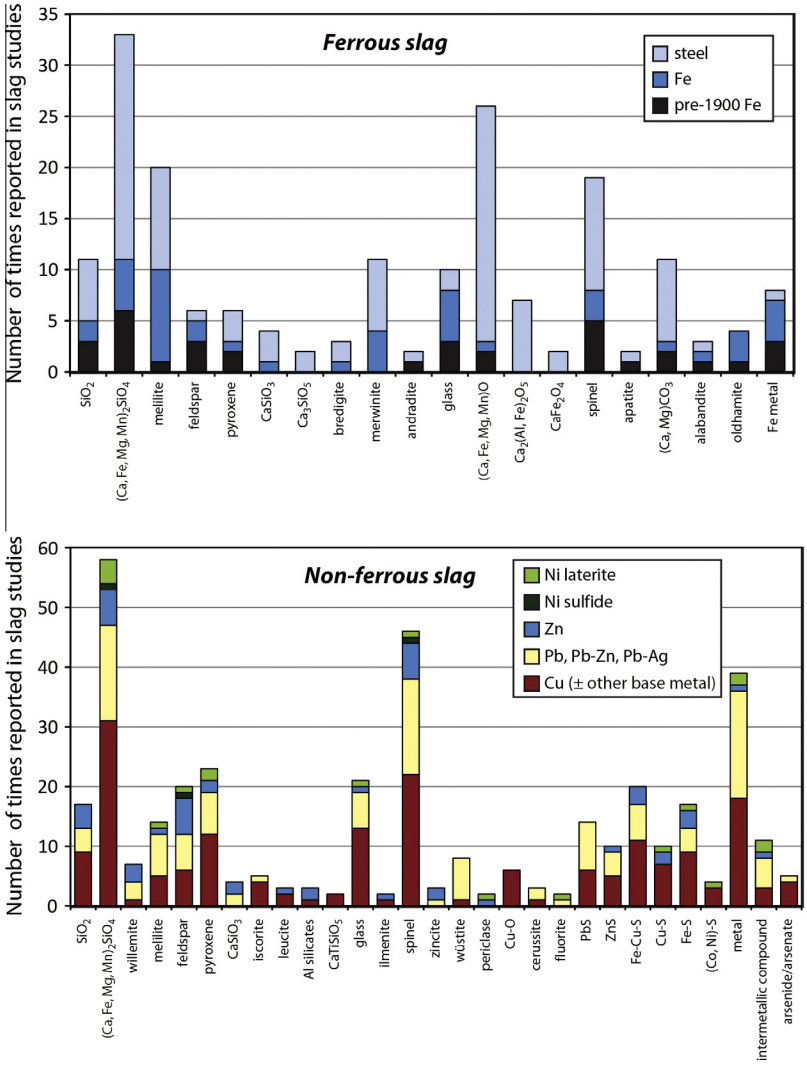

Fig. 10. Number of times primary minerals were identified in each ferrous and nonferrous slag type. Only phases that were identified repeatedly (at least twice) were included in the figure. See Appendix A for references.

The more Ca-rich steel-making Fe slag mostly plots within the pseudowollastonite and gehlenite ($Ca_2Al_2SiO_7$) fields (Fig. 9A). Melilites, in particular gehlenite, were the most commonly reported phase in Fe slag that was allowed to cool slowly enough for crystalline phases to form (Fig. 10). The next most commonly reported silicate phases include Ca and/or Mg silicates (olivine-group, merwinite ($Ca_3Mg(SiO_4)_2$), bredigite ($Ca_{14}Mg_2(SiO_4)_8$), wollastonite ($CaSiO_3$)) and glass (Fig. 10). Calcium sulfide (oldhamite) and Fe metal were identified in more than one study but are minor to trace in abundance. Like the pre-1900 Fe slag, the bulk composition of the more modern Fe slag in Fig. 9A may be used to gain insight into chemistry of the primary phases, if slowly cooled, or glass, if quenched.

Based on Fig. 9, steel slag samples will be composed mostly of Ca silicate (Ca_2SiO_4, larnite), tri-Ca silicate (Ca_3SiO_5, rankinite), and Ca oxide (CaO, lime) if slags are allowed to cool at a rate that crystalline phases form; if quenched, the slag will be a Ca silicate glass. The most commonly reported primary phase in steel slag studies (Fig. 10 and Appendix A) is larnite; tri-Ca silicate and Ca oxide were also reported in multiple samples. Aluminum, Fe, and Mg are less abundant and are generally present in Ca silicates that can accommodate these elements, e.g., monticellite ($CaMgSiO_4$), melilite, and merwinite (Fig. 10). In addition, Al, Fe, and Mg oxide phases including spinels and SiO_2 (quartz or cristobalite) are common in steel slags.

4.1.2. Mineral chemistry

As shown in Fig. 10, the most commonly reported primary phases in ferrous slag are olivine-group phases with the general formula $(Ca, Fe, Mg, Mn)_2SiO_4$. Larnite is the most common, followed by monticellite in this chemical group due to the Ca-rich nature of ferrous slag; forsterite (Mg_2SiO_4), fayalite (Fe_2SiO_4), and kirschsteinite–glaucochroite ($CaFeSiO_4$–$CaMnSiO_4$) have also documented by more than one study. Fig. 11 illustrates the composition of olivine-group phases based on electron microprobe analysis (EMPA) data (See Appendix A for references). Although larnite is the most commonly reported composition for ferrous slag olivines (typically based on X-ray diffraction (XRD), limited EMPA data exists for steel and modern Fe slags and therefore no data from these slags are shown in Fig. 11. Historical pre-1900 Fe slag is shown in Fig. 11 and compositions plot near forsterite in the ternary (Piatak and Seal, 2012a). This particular historical Fe slag contains less Ca than steel and modern Fe slags (Fig. 9). Therefore, the occurrence of Mg-rich olivines, rather than larnite, is consistent with the bulk chemistry.

The next most commonly reported phases in ferrous slags are oxides [(Ca, Fe, Mg, Mn)O] and melilites. Calcium oxide (CaO),

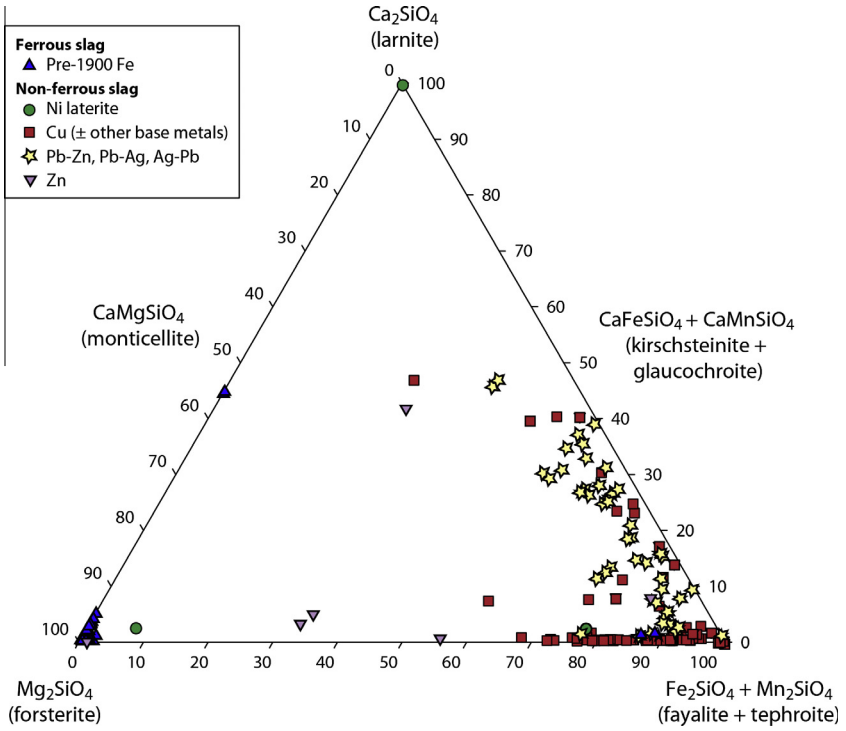

Fig. 11. Olivine compositions (in molar percentage) in the larnite-forsterite- (fayalite + tephroite) ternary diagram for various slag types based on EMPA data. See Appendix A for references.

MgO, and FeO are reported mostly in steel slag studies; these three oxides occur generally with the same frequency whereas MnO is reported less often. Compositions of melilite reported for Fe slag are between gehlenite and akermanite ($Ca_2MgSi_2O_7$). Sodium, Fe, and Mn are present in melilites in trace (0.5 wt.%) to undetectable amounts and the only trace element reported is Ni with a maximum of 0.63 wt.% NiO (Butler, 1977; Scott et al., 1986; Piatak and Seal, 2012a).

Glass is likely ubiquitous, even if present in only trace amounts, although not always mentioned as a phase in reports. Similar to the bulk chemical compositions of ferrous slag, glass in ferrous slag is usually dominated by the following major elements expressed as oxides: SiO_2, CaO, Al_2O_3, and MgO. The concentrations of these elements vary widely based on the few Fe slag studies that report weight percentages in glass (Table 2) (Butler, 1977; Scott et al., 1986; Severin et al., 2011; Piatak and Seal, 2012a) presumably due to a range in the melt compositions, variable cooling histories, and age range from ancient (3rd to 4th century A.D.) to modern. For instance, in slowly cooled slag, the glass will likely be enriched in elements that are not compatible with the crystallizing phases, whereas the glass in rapidly cooled slag will more likely resemble the original melt. In addition to the previously-mentioned major elements in glass, FeO, K_2O, MnO, Na_2O, S, and TiO_2 are commonly reported at a few weight percent or less in glass in Fe slag; trace elements were not reported or not detected (Table 2).

The few ferrous slag studies that identified pyroxenes are for Fe slag (Butler, 1977; Piatak and Seal, 2012a); the compositions of these pyroxenes are usually Al-rich (with maximum Al_2O_3 reaching over 20 wt.%) with Ca commonly greater than Mg with very little Fe (Fig. 12). Trace elements were not reported or were below detection in these pyroxenes. Wollastonite is also reported several times in Fe and steel slag. In addition to silicates and oxides, metal and sulfide phases such as Fe metal and Ca and Mn sulfides (alabandite–oldhamite) are more often or only found in Fe slag as compared to steel slag (Fig. 10).

4.2. Non-ferrous slag

4.2.1. Bulk chemistry and primary mineralogy

Table 1 includes a summary of non-ferrous slag chemistry from over 30 sources (see Appendix A). In Fig. 9, the bulk compositions of non-ferrous slags from base-metal sulfide ores are illustrated on the Al_2O_3–SiO_2–FeO and FeO–SiO_2–CaO ternary diagrams; Ni laterite slag is shown on Al_2O_3–SiO_2–CaO and FeO–SiO_2–CaO ternary diagrams. These ternaries generally represent greater than a third of the mass of the various slag samples (the average of the sum of the three components in weight percent for the individual analyses is given in parentheses after each slag type in Fig. 9). There is not one ternary that is representative of 100% of the mass of all samples in a slag type. As such, the ternaries may be used to gain insight into the likely crystalline phases but may not definitively depict all possible phases because of the presence of other components.

The major-element concentrations have similar ranges for non-ferrous slag from base-metal sulfide ores (e.g., Cu, Ni, Pb, and Zn (plus possibly Ag)) (Table 1). In Fig. 9B and C, the fields representing these types of base-metal slags are combined due to their similar compositions. In general, SiO_2 and FeO are more abundant than CaO and Al_2O_3 on these projections. Studies that discussed slags produced from the extraction of Cu, in addition to possibly Pb and Zn, were grouped together as Cu (± base metals) slag in Table 1. In general, non-ferrous slag is more Fe-rich than ferrous slag, in particular Fe slag, and the most Fe-rich non-ferrous samples in Fig. 9C are dominated by Cu and Ni sulfide slag. This observation is consistent with the fact that Fe is the commodity that is being removed from the ferrous material being smelted, whereas for base-metal slags, it is a contaminant that is removed by the slag. Although there is a wide-range in the Si and Ca concentrations for the base-metal slags, the averages expressed as oxides are similar among the various slag types within this group. For example, the averages for SiO_2 in Table 1 are between 35 and 40 wt.% and the averages for CaO are between 3 and 11 wt.% (excluding Ni

Table 2
Summary of electron microprobe analyses of glass for various slag types. See Appendix A for references that contain EMPA data. Several studies report minimum, maximum, and mean values only; these values were included. Concentrations below detection were not included.

	Fe (*n2* = 4)				Ni laterite (*n2* = 1)				Cu ± other base metals (*n2* = 6)				Pb–Ag, Pb–Zn, Ag–Pb (*n2* = 5)				Zn (*n2* = 1)				Sn (*n2* = 2)			
	Min	Max	Average	n1	Min	Max	Average	n1	Min	Max	Average	n1	Min	Max	Average	n1	Min	Max	Average	n1	Min	Max	Average	n1
wt.%																								
Al_2O_3	8.87	34.52	15.43	124	2.92	16.75	10.92	6	0.65	21.22	12.94	108	0.20	13.99	7.56	39	7.48	38.87	21.34	105	9.64	13.42	11.97	7
As_2O_3	–	–	–	–	–	–	–	–	0.07	2.99	1.02	8	0.03	0.42	0.18	13	–	–	–	–	–	–	–	–
BaO	0.06	0.66	0.18	109	–	–	–		1.30	2.11	1.77	5	0.13	6.52	2.10	14	0.01	0.71	0.12	102	–	–	–	–
CaO	0.31	43.58	15.58	124	9.75	22.70	16.06	6	0.80	32.06	6.91	108	1.01	33.08	10.60	39	0.15	19.68	6.04	105	–	–	–	–
CdO	–	–	–	–	–	–	–	–	0.03	3.36	0.66	10	–	–	–	–	–	–	–	–	–	–	–	–
CoO	–	–	–	–	0.004	0.05	0.02	6	0.005	0.91	0.09	56	–	–	–	–	–	–	–	–	–	–	–	–
Cr_2O_3	–	–	–	–	0.15	0.59	0.25	6	0.010	0.36	0.12	18	0.01	0.37	0.12	18	0.01	0.09	0.02	55	–	–	–	–
CuO	–	–	–	–	0.001	0.13	0.04	6	0.02	6.90	0.40	85	0.005	0.15	0.06	15	–	–	–	–	–	–	–	–
FeO	0.06	30.40	3.02	90	7.18	35.94	19.81	6	0.80	63.57	21.83	108	4.36	51.32	19.39	39	0.18	25.02	10.23	105	3.47	6.18	4.69	7
K_2O	0.33	10.28	2.01	115	0.77	1.77	1.10	6	0.01	10.39	2.54	107	0.03	6.45	2.20	39	0.18	5.48	2.70	105	–	–	–	–
MgO	0.61	26.47	9.51	117	0.17	17.31	4.92	6	0.01	6.51	1.24	99	0.01	2.97	0.74	35	0.22	3.80	1.08	105	0.34	0.34	0.34	1
MnO	0.03	2.08	0.55	110	0.15	1.48	0.60	6	0.01	1.32	0.20	27	0.05	6.31	2.37	32	0.01	0.43	0.12	101	0.02	0.02	0.02	1
Na_2O	0.07	1.53	0.38	118	0.14	2.17	0.85	6	0.01	15.18	3.04	106	0.10	2.27	0.83	39	0.01	3.54	1.43	104	–	–	–	–
NiO	–	–	–	–	0.004	0.17	0.11	6	–	–	–	–	0.01	0.01	0.01	1	–	–	–	–	–	–	–	–
P_2O_5	0.69	0.88	0.79	7	0.02	0.69	0.28	6	0.08	1.48	0.48	15	0.05	1.48	0.52	27	–	–	–	–	–	–	–	–
PbO	–	–	–	–	0.04	0.05	0.04	2	0.001	58.94	2.83	51	0.09	48.92	13.19	36	0.001	0.11	0.03	44	–	–	–	–
SiO_2	34.35	76.47	52.77	124	35.39	49.20	43.47	6	25.14	76.41	46.65	108	30.77	67.00	40.32	39	42.38	78.23	54.95	105	24.78	31.45	28.35	7
S	0.03	1.84	0.34	76	0.01	0.37	0.17	6	0.01	1.65	0.20	88	0.02	1.20	0.32	30	0.008	0.41	0.10	98	–	–	–	–
SnO_2	–	–	–	–	–	–	–	–	–	–	–	–	–	–	–	–	–	–	–	–	10.54	54.89	18.72	7
TiO_2	0.08	3.13	0.84	117	0.07	0.81	0.48	6	0.03	3.48	0.45	103	0.06	0.75	0.37	34	0.63	4.84	1.29	105	0.20	5.94	1.19	7
ZnO	–	–	–	–	0.01	0.27	0.10	6	0.07	16.21	2.16	94	0.71	9.8	3.79	36	0.003	2.13	0.36	69	–	–	–	–

Abbreviations: n1 = number of analyses, *n2* = number of studies for each slag type, each study within a slag type does not necessarily have data for all elements in the table, – = data not available.

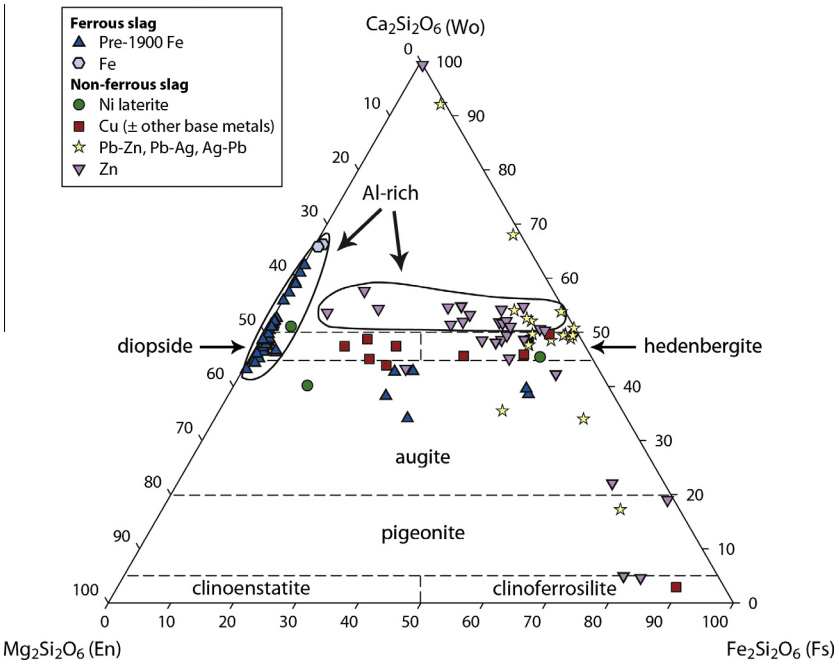

Fig. 12. Pyroxene compositions (in molar percentage) in the wollastonite (Wo)-clinoenstatite (En)-clinoferrosilite (Fs) ternary diagram for various slag types based on EMPA. See Appendix A for references.

laterite slag); Ca is significantly lower in non-ferrous slag compared to ferrous slag. The higher Ca concentrations in ferrous slag are a reflection of the common use of limestone as a flux in the smelting process. As for Al, averages range from 5 to 14 wt.% Al_2O_3 in Table 1 for base-metal slags. The concentrations of S in Cu slags reach almost 7 wt.%, whereas S only reaches about 3 wt.% in other non-ferrous slags. In general, the source of S is sulfide in the ore; for base metal production, roasting releases some or all of the S as SO_2 whereas matte smelting concentrates it in the matte (such as for Cu ores); however, some S ends up in slag. Most iron ores are dominated by magnetite (Fe_3O_4), hematite (Fe_2O_3), or goethite (FeO(OH)), with minimal pyrite (FeS_2) or pyrrhotite ($Fe_{1-x}S$), which explains the low S concentrations of ferrous slags. The other major elements expressed as oxides – K_2O, MgO, MnO, Na_2O, and TiO_2 – all average 4 wt.% or less in the non-ferrous base-metal sulfide slags (Table 1).

The bulk chemical composition gives insight into mineralogy. Base-metal slag fields fall within fields for high temperature SiO_2 (tridymite and cristobalite) and Fe–Ca silicates (olivine group, wollastonite, and pseudowollastonite). Some Fe-rich Cu slags overlap the wüstite (FeO) field and some Al-rich Zn slags fall within the mullite field (Fig. 9). The most commonly reported silicates are consistent with these ternary diagrams and include polymorphs of SiO_2 (most typically quartz), olivine group (most frequently fayalite or kirschsteinite), pyroxenes (most typically hedenbergite–$CaFeSi_2O_6$), melilite, and silicate glass (Fig. 10). Feldspars (typically plagioclase) and iron oxides are also commonly reported in base-metal slags and include wüstite and the spinel series (AB_2O_4, where A typically represents a divalent metal ion such as Mg, Fe, Ni, Mn, or Zn and B typically represents a trivalent metal ion such as Al, Fe, or Cr) (Fig. 10).

Slag produced from Ni laterite ore consists mostly of SiO_2, CaO, FeO, and Al_2O_3; the concentrations of these elements expressed as oxides vary widely because the slags were produced during different stages of smelting (Fig. 9A and C) (Kierczak et al., 2009). The ranges in concentrations for major elements such as Ca, Si, Fe, and Mg generally fall within those reported for other non-ferrous slags. The exception is Ca, which is higher in some of the Ni laterite slag when compared to most other non-ferrous slags. In Fig. 9, the compositions of the Ni laterite slag samples fall within the fields for Ca silicates, pseudowollastonite and wollastonite, those for the aluminosilicates anorthite, and within the tridymite field. The phases identified as abundant by Kierczak et al. (2009) include larnite, hatrurite (Ca_3SiO_5), Ca pyroxenes (diopside ($CaMgSi_2O_6$) – hedenbergite and melilite. Although the ternary diagram cannot be used to predict the phases that formed in this case, the major chemical components of the phases are in agreement, i.e., CaO and SiO_2, with some incorporation of the less abundant oxides of Al, Mg, and Fe.

Tin slag produced between 1650 and 1850 from South Africa consists of mostly Al, Fe, Si and Sn. The concentrations of Sn range from 1.5 to 54 wt.% and average 18 wt.%, which may be a reflection of the inefficiency of the extraction techniques at that time (Chirikure et al., 2010). The range for the other oxides and some trace elements are given in Table 1. The slags are predominantly glass and contain some crystalline phases such as cassiterite (SnO_2) and spinels; some Sn slag contains olivine and plagioclase (Heimann et al., 2010; Chirikure et al., 2010).

4.2.2. Mineral chemistry

Similar to ferrous slags, the most commonly reported primary phases in non-ferrous slag are olivine-group phases with the formula $(Ca, Fe, Mg, Mn)_2SiO_4$ (Fig. 10) (see Appendix A for references). In contrast to ferrous slag, which is Ca-rich, the most frequently reported phase with this formula in non-ferrous slag is fayalite due to the Fe-rich nature of these slags. EMPA data from various studies shown in Fig. 11 indicate that non-ferrous slags commonly contain olivine between kirschsteinite and fayalite in composition, or near the fayalite-end of the forsterite–fayalite join. Olivines in non-ferrous slags also may contain trace elements such as Zn, Ni, and Pb. The concentrations of Zn in olivines from base-metal slags may be a few weight percent Zn, reaching nearly 10 wt.% ZnO in Cu slag from California (Parsons et al., 2001); Zn substitutes for Fe in the crystal structure due their similar ionic radii. The Zn end-member, willemite ($ZnSiO_4$), is also occasionally reported. Nickel and Pb in olivines are less abundant than Zn and

reach almost 2 wt.% NiO in Ni laterite slag (Kierczak et al., 2009) and 0.3 wt.% PbO in Zn slag (Puziewicz et al., 2007). Nickel is a common trace element reported in naturally-occuring olivines with an average of about 0.4 wt.% NiO in upper mantle olivine but concentrations greater than 5 wt.% NiO for some Mg-rich olivines (Sato, 1977; Ishimaru and Arai, 2008).

The next most commonly reported phases in non-ferrous slags are of the spinel group, particularly magnetite. Other spinel-group phases identified include hercynite ($FeAl_2O_4$), franklinite ($ZnFe_2O_4$), gahnite ($ZnAl_2O_4$), and ulvöspinel (Fe_2TiO_4). Trace elements reported in spinels include Co and Cu (up to 5 wt.% CoO and 4 wt.% CuO in Cu–Co slag; Vítková et al., 2010), Pb (up to 1 wt.% PbO in Pb–Ag slag; Ettler et al., 2009a), and Sn (up to 36 wt.% Sn in Sn slag; Heimann et al., 2010).

The compositions of pyroxene in non-ferrous slags based on EMPA are illustrated in Fig. 12. Many analyses cluster near hedenbergite and diopside; those that fall just outside these fields towards wollastonite usually contain high concentrations of Al. End-member wollastonite is also reported, but less commonly than other compositions shown in Fig. 12. Similar to olivines, Zn is likely the most common trace element found in pyroxenes with concentrations reaching nearly 8 wt.% ZnO in Zn slag from Poland (Puziewicz et al., 2007). Other trace elements in pyroxenes include Co in Cu–Co slag from Zambia that contain approximately 1 wt.% CoO (Vítková et al., 2010) and Pb–Ag medieval slag from Czech Republic that contains up to 7 wt.% PbO (Ettler et al., 2009a).

The composition of melilite group phases varies considerably based on EMPA data and may be composed of mixed proportions of the end-members akermanite, Fe akermanite, gehlenite, and hardystonite ($Ca_2ZnSi_2O_7$). The predominant cation besides Si is Ca; some Na may be present, usually 3 wt.% Na_2O or less. Iron reaches approximately 20 wt.% FeO, whereas Mg only reaches approximately 10 wt.% MgO in non-ferrous slags. Manganese may be present, usually at 1 wt.% MnO or less. Navarro et al. (2008) reports Ba- and Fe-rich melilites with a little over 20 wt.% BaO and FeO in base-metal slag from Spain. End-member hardystonite has been reported in Zn slag in the United States and Poland (Puziewicz et al., 2007; Piatak and Seal, 2010). Besides Zn, Pb has been reported in melilites in numerous studies, at times in significant concentrations (over 50 wt.% PbO in Zn slag; Puziewicz et al., 2007). Sulfur has been reported in melilites at concentrations around 1 wt.% S in both non-ferrous (Navarro et al., 2008) and ferrous slag (Piatak and Seal, 2012a). Cadmium and Ni have also been found in trace amounts.

The range in concentrations of major oxides and trace elements in the glass for various non-ferrous slag types are given in Table 2. The composition of glass in non-ferrous slags, like the bulk composition, is dominated by Si (up to 78 wt.% SiO_2), Fe (up to 64 wt.% FeO), Al (up to 39 wt.% Al_2O_3), and Ca (up to 33 wt.% CaO) (Table 2). Other major elements expressed as oxides such as BaO, K_2O, MgO, MnO, Na_2O, when present, average a few weight percent oxide or less (Table 2). The average S content of glass in non-ferrous slag is between 0.1 and 0.3 wt.% S, with maximum values reaching 1.6 wt.% S (Table 2). In general, compared to glass in ferrous slag, glass in non-ferrous slag is Fe-rich and Mg-poor, and at times, Ca-poor. Glass can be the host for some trace elements such as Pb, Sn, and Zn, with concentrations that may exceed 10 wt.%, especially in late-stage interstitial glass. For example, Pb concentrations in glass reach over 50 wt.% PbO in base-metal slag from California (Parsons et al., 2001), Sn reaches an average value of 43 wt.% in Sn slag from South Africa (Heimann et al., 2010), and Zn reaches 16 wt.% ZnO in Cu slag from Namibia (Ettler et al., 2009b). Other trace elements such as As, Cd, and Cu are found in concentrations up to 3.0 wt.% As_2O_3, 3.4 wt.% CdO, and 6.9 wt.% CuO in Cu and base-metal slags (Table 2) (Parsons et al., 2001; Ettler et al., 2009b; Vítková et al., 2010).

Native metals and intermetallic compounds, especially Cu, Fe, and Pb, are commonly reported in non-ferrous slags as well as sulfides of Cu, Fe, Pb, and Zn (Fig. 10). These phases may also contain a suite of other trace elements such as Ag, As, Au, Co, Cd, Ni, Sn, and Sb.

5. Environmental aspects

5.1. Comparison with environmental guidelines

The concentrations of some elements in the various slag types exceed generic environmental guidelines based on multiple exposure pathways. Although slags are not directly comparable to soils, USEPA preliminary soil screening levels for contaminants at potentially hazardous waste sites (USEPA, 2010) were chosen for comparison for several reasons: (1) in the United States, the screening levels are used as a first-look guideline to compare element concentrations in waste materials found at the numerous hazardous waste sites that contain slag; (2) the guidelines are a useful screening tool such that if element concentrations in slag fall below the level, they are likely not an environmental issue, whereas, values that exceed guidelines warrant further study and may require remediation; and (3) guidelines can provide insight into options for slag reuse. Slags are surface materials that are present in both industrial and residential settings and reuse of land containing slag is commonplace. Therefore, the potential risk to human health from slag needs to be understood and comparison to generic screening guidelines is a useful first step in guiding management decisions.

For the major elements, guideline exceedances include Al and Fe. The concentrations of Al in some Zn and Fe slag samples are greater than the USEPA soil screening level for residential soils of 7.7 wt.% Al (equivalent to 14.5 wt.% Al_2O_3); only a few steel, Cu, Ni laterite, and historical Sn slag samples exceed the guideline (USEPA, 2010). The concentrations of Fe in most non-ferrous slag samples and many steel slag samples exceed the residential soil screening level of 5.5 wt.% Fe (equivalent to 7.1 wt.% FeO) (USEPA, 2010).

The concentrations of trace elements in the various slag types are illustrated in Fig. 13 with the ranges in concentrations and average values given in Table 1. In Fig. 13, the concentrations of the elements are compared to soil screening levels for residential use (shown as solid lines) and for industrial use (shown as dashed lines); criteria are from USEPA for all elements except Cr, which is a Canadian guideline (CCME, 2007; USEPA, 2010). The elements that are present in concentrations that exceed these environmental criteria in ferrous slags are As, Cr, and Mn, and locally Co and Pb (Table 3). As shown in Fig. 13, the concentrations of Cr in nearly all steel slag samples and a few Fe slag samples exceed both the residential and industrial soil screening guidelines. Steel slag concentrations reach 32,700 mg/kg Cr and Fe slag concentrations reach 9580 mg/kg Cr (not shown in Fig. 13 because Mn not reported for this sample) (Table 1). In Fig. 13, nearly all ferrous slag samples exceed the Mn residential guideline; some steel slag samples also exceed the industrial one. The average concentrations of Mn in steel, and pre-1900 and modern Fe slags are between 1 and 4 wt.% MnO in Table 1. The concentrations of Co and Pb in a few steel slag samples also exceed the guidelines (Fig. 13, Table 1). It is important to point out that all slag samples exceed the As residential soil guideline of 0.39 mg/kg and most exceed the industrial guideline of 1.6 mg/kg (USEPA, 2010); for comparison, the average concentration of As in soil in the United States is 7.2 mg/kg, which would also exceed the guidelines (Shacklette and Boerngen, 1984). Other elements such as Al and Cr also have environmental soil guidelines that are not significantly higher than the average for

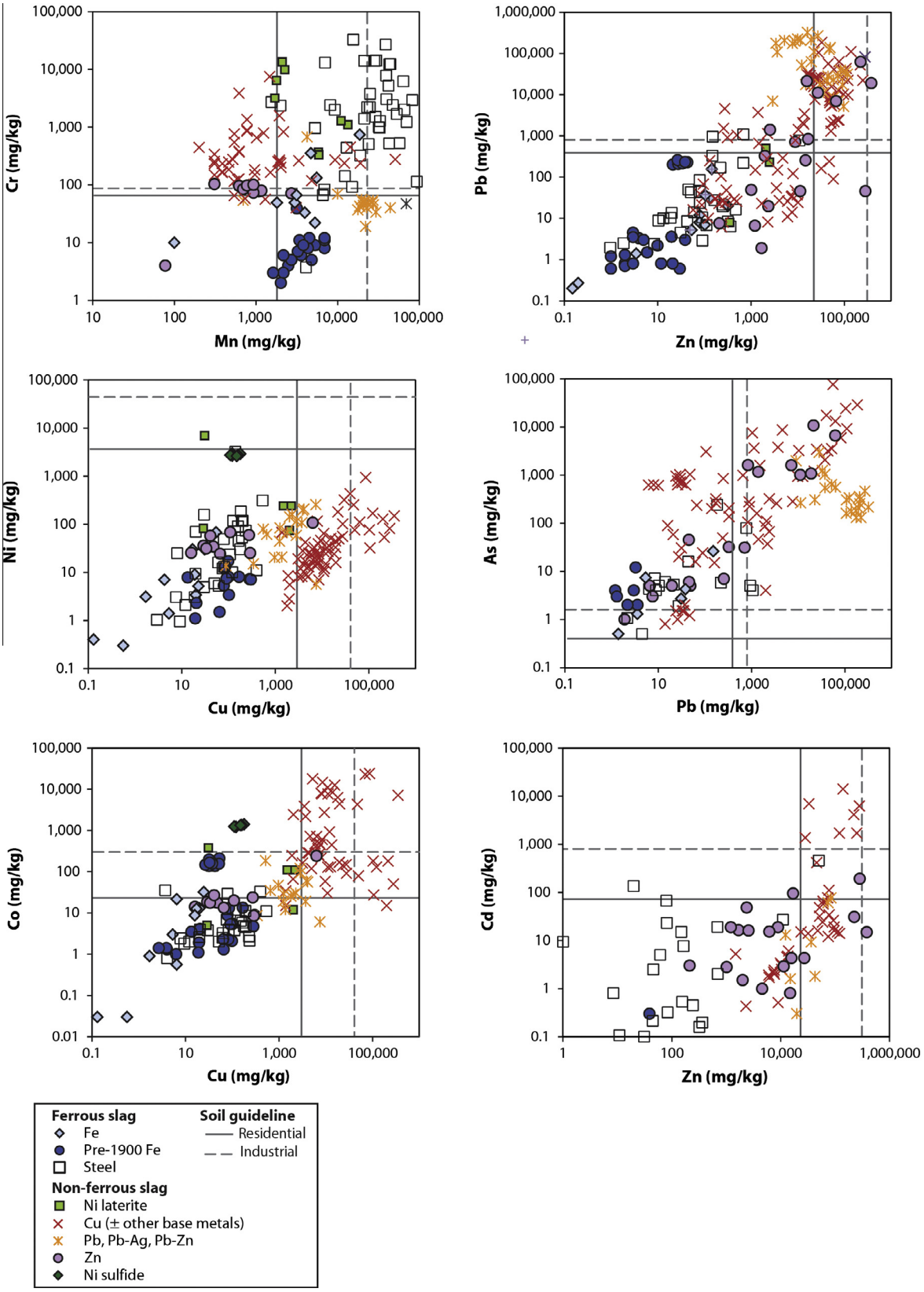

Fig. 13. Concentrations of elements in various slag types. Residential use (solid line) and industrial use (dashed line) soil screening levels are shown. Guidelines are from USEPA (2010) for all elements except Cr, which are Canadian guidelines (CCME, 2007). See Appendix A for references. Concentrations below the level of detection were not included.

soils in the United States. In addition for some elements, the maximum concentrations found in soils throughout the United States would exceed guidelines, in particular in mineralized areas.

For non-ferrous slag samples, trace element concentrations vary based on ore type. For example, slag from Cu sulfide and Ni laterite ores contain high Cr contents averaging 455 and 4484 mg/kg,

Table 3
Elements that may be of environmental concern based on bulk chemistry by slag type.

	Steel	Fe	Ni laterite	Ni sulfide	Cu	Pb	Zn
As	**	**			**	**	**
Ba						**	
Cd					*		
Co				**	**	**	
Cr	**	*	**		**		**
Cu					**		
Mn	**	**	**			**	
Ni			*	*			
Pb					**	**	**
Zn					**	**	**

Symbols: * = concentrations occasionally exceed criteria, ** = concentrations commonly exceed criteria, criteria are USEPA soil screening levels for all elements except for Cr, which was from CCME (USEPA, 2010; CCME, 2007).

respectively; the industrial soil screening level is 87 mg/kg (CCME, 2007). In addition to Cr, Ni laterite slag contains Mn (maximum of 1.72 wt.% MnO), and locally Ni (maximum of 6907 mg/kg Ni), in concentrations that exceed the residential environmental guidelines (Fig. 13, Tables 1 and 2). Copper slag commonly contains As, Co, Cu, Pb, and Zn, and locally Cd that exceeds one or both of the soil screening levels (Fig. 13). The concentrations of Ni and Zn in Pb slag samples are generally comparable to those found in Cu slag whereas the concentrations of As, Cd, Co, and Cu are usually lower (Fig. 13). In contrast, the concentrations of Mn in Pb slag generally exceed those in Cu slag (Fig. 13, Table 1). Elements that commonly exceed environmental soil screening levels in Pb slag include: As, Ba, Co, Mn, Pb, and Zn (Table 3). Zinc slag contains comparable amounts of Ni, Pb, and Zn to Cu slag but the As, Cd, Co, and Cu contents do not reach the maximum values found in Cu slag. Elements that commonly exceed environmental soil screening levels in Zn slag include As, Cr, Pb, and Zn (Table 3). Nickel sulfide slag contains Co in concentrations that exceed the industrial soil screening level. In summary, Pb and Zn (and As) can be found in significant concentrations as compared to environmental soil guidelines in Cu, Pb, and Zn slags, whereas Cd, Co, Cr, and Cu are anomalously high in Cu slag, Mn is anomalously high in Pb slag, and Ni is anomalously high in Ni sulfide slag compared to the other non-ferrous slag types (Fig. 13). The highest average concentration of Cu is found in Cu slag, Ni in Ni slags (both laterite and sulfide), Pb in Pb slag, and Zn in Zn slag (Table 1).

5.2. Secondary phases

Secondary weathering products formed from slag are an indication of the reactivity of the material and may be a means of releasing trace elements, acidity, or alkalinity into the environment. Secondary phases occur as surficial coatings or encrustations, infilled vesicles, and along grain or crystal edges. Published studies have characterized secondary phases formed by natural and simulated weathering and have used these as an indicator of the reactivity of various slags. The secondary phases that form from slag are the weathering products of the primary phases after interaction with air or water. Dissolution of the Ca oxides, carbonates, and silicates in ferrous slags produce an alkaline leachate, which then either evaporates or interacts with the slag to produce secondary phases. Examples of these acid-buffering reactions for Ca carbonate (calcite) and Ca silicate (larnite), phases commonly found in ferrous slag, are as follows:

$$CaCO_3(s) + 2H^+ \leftrightarrow Ca^{2+} + H_2O + CO_2 \quad (2)$$

$$Ca_2SiO_4(s) + 4H^+ \leftrightarrow 2Ca^{2+} + 2H_2O + SiO_2(aq) \quad (3)$$

Secondary carbonates, phosphates, and hydroxides of Ca, Fe, and Mg, among others, were reported on steel slag in a study by Svirenko et al. (2003). In addition, Fe oxides (goethite, hematite) and Ca sulfate (gypsum) have been reported in numerous studies as secondary phases on steel and Fe slag (Svirenko et al., 2003; Cravotta, 2005; Costagliola et al., 2008; Navarro et al., 2010; Piatak and Seal, 2012a).

In contrast, the list of secondary phases associated with non-ferrous slag is much more extensive and does not include Ca or Mg carbonates due to the generally near neutral to slightly acidic condition of the waters (i.e., surface water, groundwater, or precipitation) that result from interaction with non-ferrous slags. Acidity can be generated by the dissolution of certain sulfides in the slag such as pyrite according to the following reaction:

$$FeS_2 + 3.75O_2 + 3.5H_2O \leftrightarrow 2SO_4^{2-} + 4H^+ + Fe(OH)_3(s) \quad (4)$$

The most commonly reported phases include Fe oxides and sulfates of Ba, Ca, Cu, Fe, Mg, Pb, and Zn. For both ferrous and non-ferrous slag, secondary phases may host potentially toxic trace elements such as Cd, Cr, and Pb. During rainfall events, soluble secondary phases may dissolve and release trace elements, alkaline earth elements, and sulfate to surrounding waters. Also, the formation of some phases such as ferric hydroxide and Al hydroxide from the hydrolysis of Fe^{3+} and Al^{3+} may generate acid, thereby accelerating weathering reactions. An example of these types of hydrolysis reactions is shown by the following reaction:

$$Fe^{3+} + 3H_2O \leftrightarrow Fe(OH)_3(s) + 3H^+ \quad (5)$$

A study by Bril et al. (2008) found the Cu, Pb, and Zn sulfate phases brochantite ($Cu_4(SO_4)(OH)_6$), anglesite ($PbSO_4$), and bianchite ($(Zn,Fe)(SO_4)\cdot 6H_2O$), respectively, as secondary phases associated with Zn slag in Poland. Additionally, a recent study by Kierczak et al. (2013) reported langite ($Cu_4(SO_4)(OH)_6$) and malachite ($Cu_2(CO_3)(OH)_2$) as secondary phases associated with Cu slag in Poland. The occurrence of these phases indicates that trace element-bearing primary phases (e.g., zincite (ZnO), willemite, melilite, spinel, sulfides, metals, glass) are releasing metals at sufficient concentrations during weathering to result in the precipitation of secondary phases.

5.3. Acid–base accounting

Acid–base accounting is a means to quantify the amount of acid or alkalinity that may be released into the environment from a material. Mineralogical differences among the various slag types may result in very different acid-generating and acid-neutralizing potentials. Acid–base accounting evaluates the difference between the neutralization potential and acid-generating potential and is usually determined based on laboratory static tests. The acid-generating potential is commonly based on the S content and speciation to represent acid-generating Fe-sulfide minerals (e.g., reaction (4)) and the neutralization potential is based on the amount of acid-neutralizing minerals present (e.g., reactions (2) and (3)) determined by acid digestion of the sample and subsequent neutralization (Jambor, 2003). Although quantified using bulk geochemical laboratory methods, the acid-generating or neutralizing potential of a material is a function of its mineralogical composition.

Many of the crystalline phases found in ferrous slag samples such as Ca silicates (e.g. larnite), carbonates, and Ca oxide have positive acid neutralization potentials, which greatly outweigh the acid-generating potentials of any trace sulfides present. For example, Ziemkiewicz and Skousen (1999) found that steel slags from the eastern United States have neutralization potentials between 450 and 780 kg $CaCO_3$/t and when reacted with deionized

Table 4
Summary of slag types and leaching methods for references that were compared for this paper.

Slag type	Location	Leaching method[a]	Modification to method	References
Steel	Chicago area, Illinois	SPLP	2 mm size fraction	Piatak and Seal (unpublished)
Steel and Fe	Throughout United States	TCLP	None	Proctor et al. (2000)
Steel	Steelmaking companies, Sweden	EN 12457–2	None	Tossavainen et al. (2007)
Steel	Mingo Junction, Ohio	TCLP	3.2 mm size fraction	Ziemkiewicz and Skousen (1999)
Pre-1900 Fe	Hopewell Furnace, Pennsylvania	SPLP	2 mm size fraction	Piatak and Seal (2012a)
Cu	Vermont copper belt and Ducktown, Tennessee	SPLP	2 mm size fraction, 1-min. agitation, 24 h. contact	Piatak et al. (2004)
Cu	Penn Mine, California	TCLP SPLP	None	Parsons et al. (2001)
Cu and Pb–Cu	Tsumeb smelter, Namibia	TCLP EN 12457–2	0.1 mm size fraction	Ettler et al. (2009b)
Pb	Belledune smelter, New Brunswick	TCLP SPLP	None	Parsons (2001)
Pb–Zn	Clayton smelter, Idaho	SPLP	2 mm size fraction, 1-min. agitation, 24 h. contact	Piatak et al. (2004)
Zn	Hegeler smelter, Illinois	SPLP	2 mm size fraction	Piatak and Seal (2010

[a] See text for an explanation of the leaching methods.

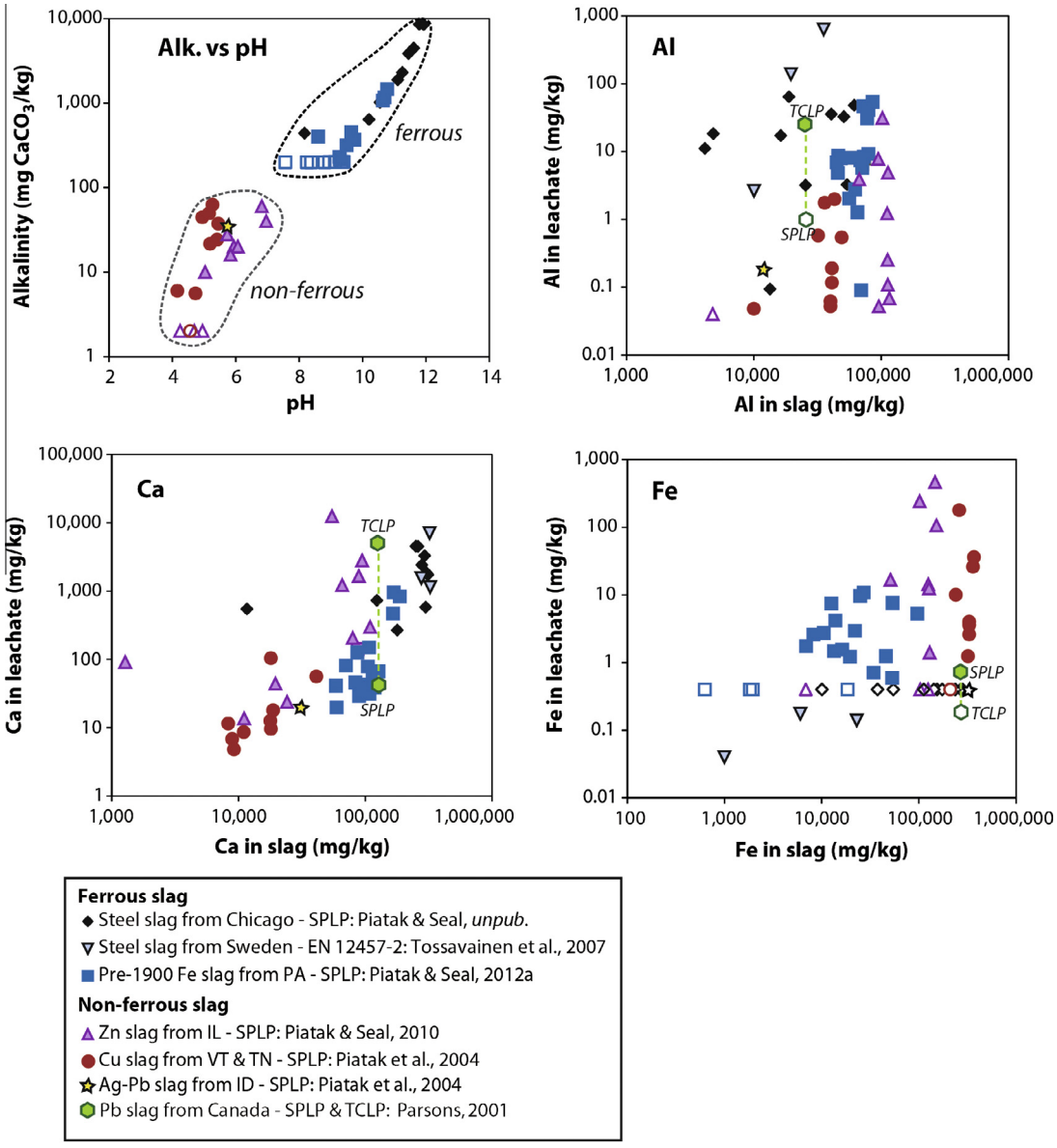

Fig. 14. Chemistry of slag leachates compared to leachate pH or the concentrations of elements in the slag based on bulk chemical analysis. Concentrations are in mg/kg for both leachate and bulk chemistry; leachate concentrations were multiplied by the liquid-to-solid ratio to convert mg/L to mg/kg. Open symbols indicate concentrations not detected at the detection limit of the method. Modifications to standardized leachate procedures include: SPLP performed on <2 mm size fractions and a 1-minute agitation and 24 h contact time used for the SPLP on the VT, TN, and ID slags.

water produced leachate with a pH of approximately 12. In addition, Wendling et al. (2010) reported an acid neutralization capacity of 130 kg $CaCO_3$/t (2.6 mol H+/kg) for steel slag. In contrast to ferrous slag, the sulfides, especially those that contain Fe, in non-ferrous base-metal slags from processing sulfide ores may generate acid upon weathering. These slags may also contain some acid-neutralizing phases such as olivines and pyroxenes; however, their relatively slow dissolution rates inhibit their neutralization contribution (Jambor, 2003). For example, base-metal slag in Spain from processing sulfide ores was found to generate acid with negative net neutralization potentials that average between approximately −90 and −170 kg $CaCO_3$/t (Álvarez-Valero et al., 2008) and acidic paste pH values between 3.1 and 5.0 (Lottermoser, 2005). In contrast to slags produced solely from sulfide ores, Zn slag produced in Belgium from smelting a combination of Zn-silicate, Zn-carbonate, and Zn-sulfide ores was found to neutralize acid with positive neutralization potentials of 30–56 kg $CaCO_3$/t (i.e., 594–1122 mmol/kg; Ganne et al., 2006).

5.4. Leachate chemistry

The constituents released from slag during weathering and interaction with surface and ground waters may have deleterious effects on the environment. The leaching behaviors of the various

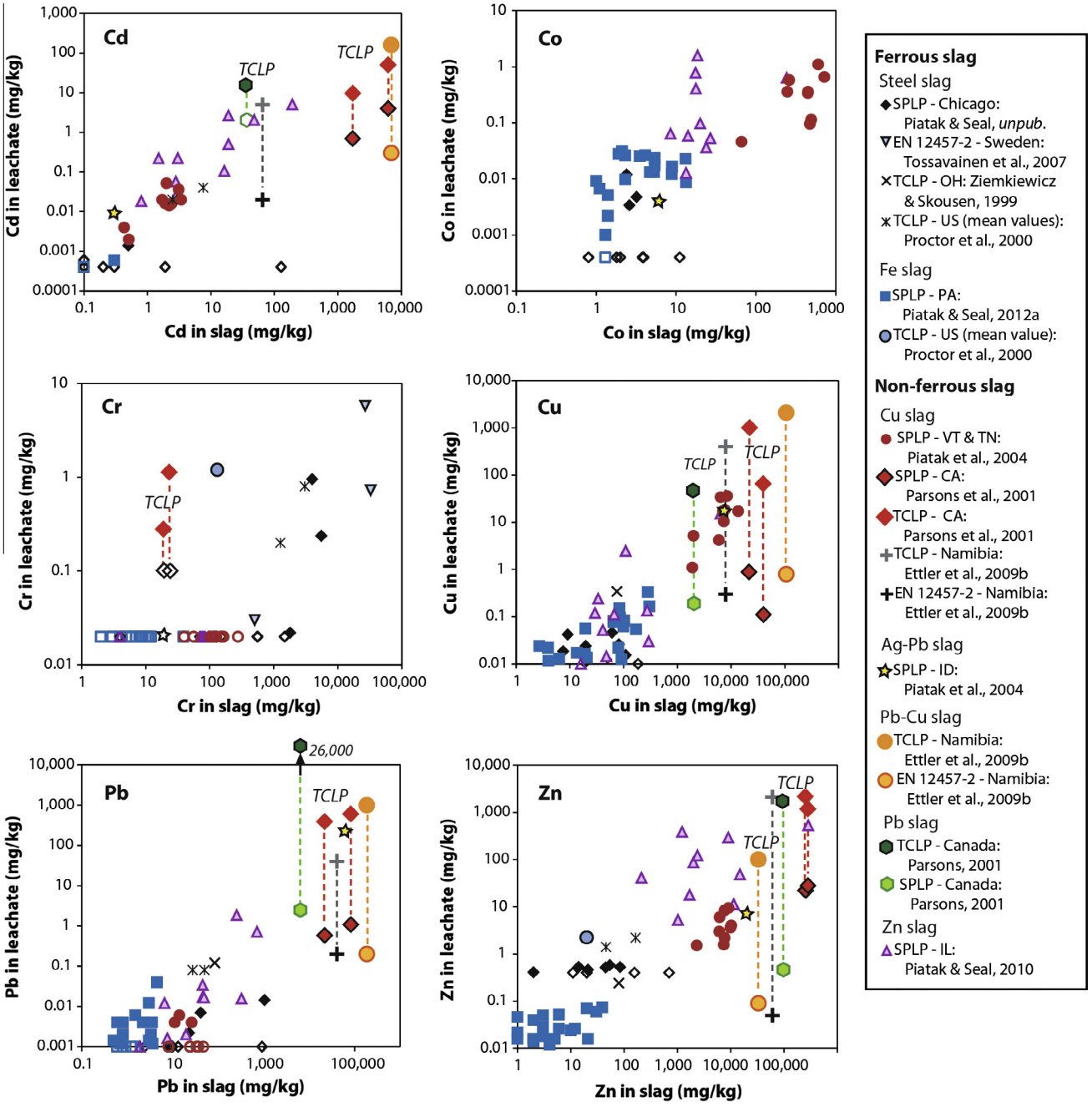

Fig. 15. Chemistry of slag leachates compared to concentrations of elements in the slag based on bulk chemical analysis. Concentrations are in mg/kg for both leachate and bulk chemistry; leachate concentrations were multiplied by the liquid-to-solid ratio to convert mg/L to mg/kg. Open symbols indicate concentrations below the detection limit of the method. Modifications to standardized leachate procedures include: SPLP performed on <2 mm size fractions for all samples except those from PA; a 1-minute agitation and 24 h contact time used for the SPLP on the ID, TN, and VT, slags; <0.1 mm in diameter material used for the slag from Namibia; < 3.2 mm in diameter material used for the slag from OH. The mean values are plotted for two types of steel slag (n = 17 & 45) and blast furnace iron slag (n = 11) collected from throughout the US (see Proctor et al., 2000 for details). Samples connected by dashed lines are the same material leached by two different methods.

slag types are unique and strongly controlled by their bulk chemistry and mineralogy. For this review, leachate results from several studies were examined to gain insight into the general leachate signatures of each slag type; Table 4 lists the references containing leachate chemistry. Results from three standardized single batch extraction test methods were compared: synthetic precipitation leaching procedure (SPLP), toxicity characteristic leaching procedure (TCLP), and EN-12457-2 (see Section 3.1.3 for an explanation of methods and references). The findings indicate that some slags release certain elements more than others and that the leachate concentrations of only some elements correlate to their bulk chemical concentrations in the slags. The results from these studies cannot all be compared directly to each other because each protocol has different leaching parameters. Despite this, general comparisons can be made and insight can be gained into how slags react in the various leachants and which elements are consistently released in the highest or lowest proportions. For comparison purposes, the element concentrations in the leachates were converted to an amount released from the solid by multiplying leachate concentrations (mg/L) by the liquid-to-solid ratio of the leachate method and are reported as milligrams per kilogram (mg/kg). Piatak and Seal (2012b) also summarized the leachate signatures by slag type from these studies and compared results to slag drainage chemistry.

Figs. 14 and 15 illustrate the composition of the leachates compared to the bulk compositions of the slags; some modifications to the standardized procedures are noted in the figure captions. Overall, the leachate signatures of the ferrous slags were very different from that of the non-ferrous slags. In Fig. 14, the pH and alkalinity from non-static pH leach tests were significantly higher for ferrous slag leachate than those for non-ferrous slag leachate from base metal extraction of mostly sulfidic ores. The alkaline leachate produced from ferrous slags is likely the consequence of the dissolution of Ca silicates, oxides, and/or carbonates (e.g., reactions (2) and (3)). The acidic pH of some leachates generated from non-ferrous slags may result from the oxidation of sulfide minerals (e.g., reaction (4)).

The dominant major cation released from the ferrous slag samples was Ca, followed by Si with lesser amounts of Al, Mg, and Fe (Fig. 14). Leaching of the abundant Ca silicates and oxides and glass found in these slags is the likely source of the Ca and Si (De Windt et al., 2011). Similar to ferrous slag, Ca and Si were the dominant cations released from non-ferrous slag. In contrast to ferrous slag, Fe was also a major constituent of the non-ferrous slag leachates due to its greater abundance in this slag type, and was commonly found in higher concentrations than either Al or Mg (Fig. 14). As for most minor and trace elements, ferrous slag commonly released low concentrations using all three types of leaching tests mostly due to the low abundance of many of these elements in the bulk slag samples (Fig. 15). Chromium, and occasionally Mn, is found in anomalously high concentrations in ferrous slag leachates when compared to most other slag types, which commonly released Cr below the level of detection (Fig. 15). The highest leachate concentrations of As, Cd, Co, Pb, and Zn are for the non-ferrous slags (Fig. 15). In general for equivalent leaching tests, the highest amounts of Cu are leached from Cu slags, the highest amounts of Pb are leached from Pb slag, and the highest amounts of Co, Cd, and Zn are leached from Cu and Zn slags.

For many of the minor and trace elements, the concentrations in the leachate generally correlate with the concentrations in the bulk slag sample when comparing the various slag types (Fig. 15). For example, Cu slags contain and leach the greatest amounts of Cu compared to the other slag types. In contrast, for some samples within a given study, the leachate concentrations and bulk chemical composition do not correlate or a correlation cannot be determined due to low concentrations. Low concentrations of some elements in the leachates may indicate that the elements are hosted by phases that are relatively insoluble under the leaching conditions. For example, the concentrations of Zn in steel slag from Chicago vary from 2 to 100 mg/kg but the concentrations of Zn in the leachates are consistently near or below the detection limit of 0.4 mg/kg (Fig. 15). In another example, leachate composition and bulk chemistry for the Zn slag from Hegeler, Illinois, do not correlate for many trace elements, which may reflect the varying leachate pH in the non-static pH leaching tests and the partitioning of elements in phases with wide-ranging solubilities including sulfides, oxides, and silicates (Fig. 15).

The general correlation between bulk chemical composition and leachate chemistry is also shown for the major element Ca. In contrast to Ca, Al and Fe concentrations in leachates do not correlate well with the bulk concentration of these elements in the slag (Fig. 14). These elements may be hosted by phases that react differently to the leaching conditions and the dissolved concentrations of these elements are likely controlled by the precipitation of secondary Al- or Fe-oxyhydroxides (Parsons, 2001; Ettler et al., 2002; Navarro et al., 2008; De Windt et al., 2011).

Overall, there are many types of leaching tests and the protocols may influence the concentrations and relative proportions of the elements that are released. For example, the TCLP method uses acetic acid or acetate buffer as the leaching solution, which has been shown to leach higher amounts of some trace elements compared to tests run side-by-side that used a leaching solution that did not include acetic acid (Fig. 15) (Parsons et al., 2001; Ettler et al., 2009b). This was likely due to the lower pH of the buffered TCLP solution and enhanced extraction by acetic acid (Parsons et al. 2001; Ettler et al. 2009b). The maximum amounts of Cd, Cr, Cu, Pb, and Zn for both ferrous and non-ferrous slag types were released when acetic acid was used in the extraction solution (Fig. 15, TCLP protocol). Other factors that influence the release of metals are particle sizes, the proportion of amorphous versus crystalline phases in the slag sample, among many others (Johnson et al., 1982; Robbins et al. 1983; Tossavainen et al., 2007; Vítková et al., 2011).

6. Case studies

6.1. Ferrous slag

With respect to the environmental aspects of slag, there are more published studies on non-ferrous slag than on ferrous slag. Most ferrous slag studies focus on physical characterization and applications of slag as a by-product (See Section 6). Due to the presence of Ca silicates, carbonates, and oxides, ferrous slag is commonly alkaline and has significant acid-neutralizing capacity (see reactions (2) and (3)), which in some applications is a favorable attribute (Cravotta, 2005). Ferrous slag also generally contains lower concentrations of many trace elements as compared to non-ferrous slag. As discussed previously, the elements most likely to be of environmental concern in ferrous slag include As, Cr, Mn, and rarely Co (Fig. 13). The release of these trace elements from the slag can be assessed under natural and simulated conditions. Trace elements are potentially leached into nearby waters and are found in residential soils where slags are used for construction purposes or from windblown smelter dust. In the United States, extensive deposits of Fe and steel slag do exist in some areas, especially in steel manufacturing locations where Fe smelting has occurred on a large scale since the Industrial Revolution. Also, hundreds of smaller historical iron furnaces left slag dumps across the United States. Although environmental effect studies on ferrous slag have been conducted in other countries (i.e., Svirenko et al., 2003; Navarro et al., 2010), only case studies in the United States on historical Fe slag and modern steel-making slag are highlighted here.

6.1.1. Historical iron slag

Very few studies have been conducted on the environmental aspects of historical Fe slag (e.g., Costagliola et al., 2008; Rizza and Farthing (abstract), 2007; Vivenzio and Farthing, 2005 (abstract), Piatak and Seal, 2012a). Studies on modern steel and blast-furnace Fe slags are more numerous but not directly applicable because of the influence of technological innovations on slag chemistry and mineralogy. Piatak and Seal (2012a) recently studied historical Fe slag at the Hopewell National Historical Site in Berks and Chester counties, Pennsylvania, USA. This work focused on characterizing the chemistry, mineralogy, and environmental behavior of the slag. In addition, the chemistry of groundwater, surface water, stream sediment, and soil at and near Hopewell was discussed in Sloto and Reif (2011). The Hopewell slag was produced from magnetite ores (skarn deposits) in 18th- and 19th-century iron smelters, mostly cold-blast charcoal-fired but also anthracite- and coke-fired. Overall, the slag is enriched in some trace elements but only a few of these exceed environmental guidelines (i.e., As, Fe, and Mn). These findings are consistent with those discussed previously on the bulk chemistry of ferrous slags (Table 3, Fig. 13). In addition, soils in the vicinity of the furnace contain higher concentrations of Cr, Cu, Fe, Pb, and Zn than unimpacted background soils likely due to air emissions from the furnace and/or contamination by slag; concentrations do not exceed local guidelines. The limited environmental impact of the slag is substantiated by SPLP leaching tests that found secondary drinking water guideline exceedances of Al, Fe, and Mn and ecosystem toxicity guideline exceedances of Al and Cu in some extract solutions (Figs. 14 and 15). In general, the compositions of the groundwater and surface water reported in Sloto and Reif (2011) were similar to leachate extract compositions validating the use of the leaching tests as a proxy for natural weathering.

6.1.2. Steel and iron slag

As stated earlier, studies on modern steel and Fe slag deposits are more numerous than on historical Fe slag but most focus on characterization and reuse. Some environmental characterization has been conducted on steel slags in the Chicago area near the border of Indiana and Illinois, USA. The geochemistry of waters and sediment in contact with some of these extensive steel slag deposits has been discussed in Bayless and Schulz (2003) and Bayless et al. (1998, 2004). These studies found that drainage from slag deposits along the shore of Lake Michigan contains elevated levels of trace elements and has affected the mineralogy of underlying sediments. Bayless et al. (1998) noted that Cr, Pb, and Zn are highest in groundwater from immediately below the slag deposits. Bayless and Schulz (2003) reported enhanced chemical weathering of silicate minerals in sediment as well as secondary precipitation of calcite, gypsum, and other minerals as a result of interaction with the hyperalkaline slag drainage; both of these may impact ground-water flow patterns. Bayless et al. (2004) used Sr and B isotopes to identify and delineate slag-affected sediments that have been transported into Lake Michigan. These studies indicate that drainage from slag deposits in the Chicago area is having an effect on nearby sediment and waters but the environmental consequence is not clear. Leaching tests recently conducted by Piatak and Seal (*unpublished*) on slag from this area revealed that only Al repeatedly exceeded environmental guidelines in SPLP extract solutions; Al commonly exceeded secondary drinking water guidelines and often exceeded aquatic ecosystem guidelines (Fig. 14). Roadcap and Kelly (1994) investigated shallow aquifer ground water beneath fill that is mostly steel slag in the Chicago area. The authors documented extremely alkaline pH (>12) and high concentrations of Fe and ammonia, as well as high levels of Ba, Cr, Mn, and moderate levels of other elements including As, Hg, and Pb that may or may not have originated in the slag. A follow-up study examined ground water associated with slag and secondary weathering products (Roadcap et al., 2005). The authors again found extremely alkaline pH (>12) waters as well as secondary Fe and Mn oxides and Fe, Mn, and Zn sulfides in the ground water system. Also, where ground water reached the surface, calcite precipitated that contained significant concentrations of some trace elements including Cd, Cr, Cu, Pb, Ni, and Zn indicating the mobility of these trace elements in the system (Roadcap et al., 2005). These studies show that ferrous slag deposits can have a deleterious impact on surface- and ground-water through the release of trace elements and hyperalkaline drainage.

6.2. Non-ferrous slag

Studies of the environmental characterization of non-ferrous slags are more numerous than for ferrous slags, partially because these slags generally contain significant concentrations of trace elements. Also, the ore from which base metals are extracted is commonly sulfide-rich; therefore, the slag also may contain residual sulfide phases, which can generate acid and release trace elements upon weathering. The trace elements that may be of concern include: As, Cd, Co, Cu, Cr, Mn, Ni, Pb, and Zn, and less commonly Ba (Fig. 13). Leaching tests and the weathering behavior of slags discussed below for each slag type can be used to understand the release of these potentially toxic metals into the environment. Also, slag or slag-containing soils or sediments can be transported by water or wind, extending the area of contamination. Case studies highlighted in this section focus on the most common types of non-ferrous slag, those produced mostly from the extraction of base metals from sulfide ores, with the last study focusing on Ni slag produced from non-sulfidic ores.

6.2.1. Copper slag

Parsons et al. (2001) used field and laboratory studies to characterize the composition, mineralogy, and reactivity of various Cu slag types found at the abandoned Penn Mine in California. Historical Cu smelting at the Penn Mine (1865–1919) generated approximately 200,000 m^3 of slag, which was dumped along the banks of the Mokelumne River. The slag deposits are now flooded for 6–8 months each year by a reservoir used for drinking water and irrigation. Slags are glassy to crystalline, and range in size from coarse sand to large ($0.6 \times 0.7 \times 1.5$ m), tub-shaped casts. The ranges in total metal and metalloid concentrations of the slag samples are as follows: 0.0004–0.92 wt.% As; 0.0014–1.4 wt.% Cd; 0.18–6.4 wt.% Cu; 0.02–11 wt.% Pb; and 3.2–28 wt.% Zn. On the basis of mineralogy, slags are characterized by four main types: fayalite-rich, glassy, willemite-rich, and sulfide-rich. X-ray diffraction and SEM analyses identified weathering-related secondary minerals on the slag, including hydrous ferric oxides, barite ($BaSO_4$), cerussite ($PbCO_3$), chalcanthite ($CuSO_4{\cdot}5H_2O$), hydrozincite ($Zn_5(CO_3)_2(OH)_6$), and malachite ($Cu_2CO_3(OH)_2$). The results of TCLP and SPLP leach tests on two willemite-rich samples showed that both Cd and Pb exceeded the regulatory guidelines in the TCLP leachates, but that the SPLP leached much lower metal concentrations (Fig. 15). Analyses of water samples collected within the flooded slag dump and adjacent reservoir revealed elevated metal concentrations near the slag deposits during reservoir drawdown, reflecting the influence of slag dump pore waters on the lake water chemistry.

Field and laboratory data were used to develop geochemical models with the program EQ3/6 to simulate irreversible mass-transfer between the Penn Mine slags and reservoir waters (Wolery, 1992; Wolery and Daveler, 1992). These models included kinetic rate laws for sulfide oxidation and dissolution of silicates, oxides, and glass. Calculations demonstrated that the main processes controlling dissolved metal concentrations in the slag dump pore

waters are (1) dissolution of fayalite, willemite, and glass; (2) sulfide oxidation; and (3) secondary mineral precipitation. The results of this study show that base-metal slags, especially those from historical smelters, are not chemically inert wastes, and can result in environmental contamination through leaching of potentially toxic elements. When properly constrained through careful field and laboratory studies, the geochemical modeling techniques demonstrated in Parsons et al. (2001) can be used to develop remediation strategies for slags at both historical and modern smelting sites.

The release of trace elements from slag resulting from the extraction of Cu from sulfide ores (volcanic-associated massive sulfide deposits) in the Vermont Copper Belt was reported by Piatak et al. (2004). Granulated Cu slag from the Ducktown mining district in Tennessee and Pb–Ag slag from the Clayton smelter in Idaho were also examined in the study. The smelters in Vermont were in operation from the mid-1800s to the early 1900s, similar to the Clayton smelter operations, but earlier than the operation that produced the granulated slag from Ducktown. The Cu slags from Vermont may pose an environmental risk based on results of simulated weathering leaching tests that produced leachates containing concentrations of Cu and Zn in excess of aquatic life guidelines (Fig. 15). Also, secondary minerals, including copper sulfates, on the slag deposits provide evidence that the material is reactive and weathering naturally. The study also highlighted that most potentially toxic trace elements (i.e., As, Co, Cu, Pb) are hosted in relatively reactive glass, sulfides, and intermetallic compounds. In contrast, some trace elements such as Zn are hosted in the relatively less reactive crystalline silicates and oxides. These findings are generally consistent with an aquatic ecosystem assessment of one of the mine sites, the Ely Copper Mine, from which Cu slag was collected. The assessment by Seal et al. (2010) indicated Cu as the main stressor in the aquatic environment downstream of the slag dump. Albeit, the weathering of other mine wastes at the site also releases significant amounts of Cu and, likely, in higher amounts than that released from the slag.

6.2.2. Zinc slag

Similar to the Cu slag in Vermont, Zn slag from the Hegeler smelter in Illinois may pose an environmental risk (Piatak and Seal, 2010). This slag was produced from the processing of sulfide ore (likely Mississippi Valley type Pb–Zn deposits) in the early- to mid-1900s. Leachate concentrations from all samples exceeded aquatic life guidelines for Zn and Cd, whereas guidelines for Cu and Pb are only locally exceeded. The surface and ground water compositions at the site are consistent with the leachate results in that natural site waters exceeded the drinking water and acute and chronic aquatic life guidelines for both Zn and Cd. Also, natural weathering is reflected in secondary phases including a Zn sulfate on the surface of slags. According to this case study, elements of potential concern in the Zn slag are Cd, Cu, Zn, and Pb. The results of leaching tests are not completely consistent with findings based on bulk chemical composition for Zn slag (Table 3 and Fig. 15), which suggest that bulk chemistry is not the only aspect of the slag that needs to be examined. The partitioning of potentially toxic trace elements among various phases and their relative reactivity and leachability is essential to understanding the environmental behavior of the slag. In these samples, the partitioning of Zn among the phases in the slag was dependent on the overall bulk concentration of Zn: Zn was hosted mainly in spinel and silicate glass in Zn-rich samples, whereas Zn was hosted mainly in sulfides in samples with lower bulk Zn concentrations. The host phase of the Zn affected the leaching of this trace element with spinel being less reactive than the sulfides.

In addition to the release of potentially deleterious trace elements into nearby waters, soils in the vicinity of smelters can contain high concentrations of some trace elements. Residential soils in towns neighboring the Hegeler zinc smelter site occasionally contained concentrations of Co, Cu, Fe, and Pb that exceeded USEPA soils screening levels for human contact; the highest concentration of some trace elements were routinely found in residential roadway soil (Weston Solutions, Inc., 2007). Slag used as fill material for private drives, roadways, and railways presumably contaminated the soils. The human health risk from exposure to the trace elements present in the residential soils was found to be low when considering incidental ingestions, dermal absorption, and inhalation of dusts (Weston Solutions, Inc., 2007). This is in contrast to a site in La Oroya, Peru, where the same exposure and dose–response modeling conducted for contaminated soils in the vicinity of a smelter, which recovers Cu, Pb, Zn, and other byproducts, indicated that Pb in soil was a serious health problem (Reuer et al., 2012). At the smelter site in Peru, and many other smelter sites throughout the world, the contamination of soils is likely predominantly from point-source stack and fugitive emissions from the smelter. However, Reuer et al. (2012) did suggest at least one of the soils containing high concentrations of trace elements was impacted by the advection of fine-grained material from nearby slag heaps.

6.2.3. Lead–zinc slag

There have been numerous environmental studies on Pb–Zn slag from smelting sulfide ores (mostly from polymetallic vein deposits) in the Příbram mining district, Czech Republic (Ettler et al., 2000, 2001a, 2001b, 2002, 2003, 2004, 2005, 2009a). The smelting operations occurred from the Middle Ages to modern times. Studies have focused on mineralogical and chemical characterization and numerous leaching tests. Extraction solutions including organic-rich acidic solutions, deionized water, and hyperalkaline buffer solutions were used in leaching tests to gain insight into the behavior of slag under various conditions. Studies found that significant amounts of trace elements were released during the leaching with organic-rich solutions but they were subsequently bound to, or trapped within, newly precipitated phases (Ettler et al., 2004, 2005). These results have implications with respect to covering slag waste piles with soil and encouraging vegetation to grow. Also, oxidizing near-neutral conditions helped to limit the mobility of some elements such as Pb and As through precipitation and absorption processes (Ettler et al., 2003). In contrast, alkaline solutions that simulate slag use in concrete resulted in the release of Pb (Ettler et al., 2001b). In Ettler et al. (2002), the partitioning of trace elements among various phases and the relative stabilities of these phases in various solutions were also examined. Overall, the release of trace elements during leaching tests suggested that some environmental risk is associated with these slag deposits, but understanding their behavior under field conditions may help to inform decisions concerning slag reuse and remediation.

6.2.4. Nickel slag

The mineralogy and weathering of Ni slag produced from smelting of lateritic ores in southwestern Poland were summarized by Kierczak et al. (2009). Overall, the phases and textures of these slags are similar to those produced during the smelting of sulfide-rich ore, but with lower amounts of sulfides present in the laterite slags. Because gypsum was added as a flux during the smelting of the lateritic ores, the reducing conditions of the furnace produced sulfides of Fe, Ni, and Cu. According to Kierczak et al. (2009), sulfides and intermetallic compounds are the most important hosts of Cu, Ni, and Sn. In addition, Cr occurs as chromite and in diopside, Ni is found in olivine, and Zn in melilite. Despite being exposed to atmospheric conditions for 30–80 years, the slag remains mostly unaltered, but does contain some indications of weathering including vesicles with corrosion embayments, weathering-induced margins on slag surfaces, and the dissolution of sulfides. The authors noted the relative reactability of sulfides, glass,

and crystalline silicates and oxides. They concluded that the potential environmental risk of the slag is limited due to the immobility of Cr, Ni, and Zn in relatively stable silicates and oxides, and the entrapment of small inclusions of more reactive sulfide and metallic alloys that contain Cu, Ni, and Sn within the stable silicates and oxides and slightly less stable silicate glass.

7. Slag as a resource

The majority of slag used for construction and environmental applications is from Fe and steel production. Iron and steel slag is considered a commodity and its supply and demand is summarized yearly by the United States Geological Survey (USGS). Also, several associations focus on promoting the use of slag, predominantly ferrous, such as the National Slag Association (NSA), the European Slag Association (EUROSLAG), and the Australiasian Slag Association (ASA). Slag production and reuse is a global business. In 2011, an estimated 260 to 330 million tonnes (Mt) of Fe slag and an estimated 150–220 Mt of steel slag were produced in the world; the United States produced approximately 8–9 Mt of Fe slag and approximately 9–13 Mt of steel slag in 2009 (Van Oss, 2013). By comparison, there are relatively limited data on the quantities of non-ferrous slag produced each year. According to the NSA (2009), non-ferrous slags constitute approximately 12% of total slag production. Based on ferrous slag estimates from Van Oss (2013), this would imply that approximately 50–66 Mt of non-ferrous slag were produced worldwide that year. According to Gorai et al. (2003), approximately 24.6 Mt of slag is generated each year from world production of Cu. When it comes to reuse, ferrous slag is generally considered for use in construction and environmental applications, whereas non-ferrous slag is the focus of research on reprocessing, especially historical dump material, for secondary metal recovery.

7.1. Construction materials

The majority of ferrous slag, and some non-ferrous slag, is used for construction purposes. As briefly discussed previously, the method used to cool the slag affects the physical properties of the material and influences how it is used. Although commonly vesicular, the hard and dense nature of air-cooled Fe and steel slags make them suitable for construction aggregate. Table 5, detailing ferrous slag use in the United States in 2011, indicates that most air-cooled Fe slag is used in ready-mixed concrete, asphaltic concrete, road bases and surfaces, and fills; air-cooled steel slag has similar uses which the exception of ready-mixed concrete (Van Oss, 2013). A study by Maslehuddin et al. (2003) suggested that using steel slag aggregate in concrete produces a more durable product compared to using limestone aggregate. Most steel slag and about one-half of the Fe slag is air-cooled in the United States (Van Oss, 2013). Air-cooled slag also is used for roofing, mineral wool, as well some environmental applications discussed below.

The glassy nature of granulated Fe slag gives the material hydraulic cementitious properties, which increase in strength if combined with free lime during hydration. Hadjsadok et al. (2012) found improved durability as well as less deterioration in sulfate-rich solutions for concrete and mortar containing granulated Fe slag. In 2010, approximately one-half of Fe slag was granulated and 95% of that material was used as cementitious material (Table 5) (Van Oss, 2013). In contrast to the United States, the majority (over two-thirds) of slag produced in Europe in 2004 was granulated; similar to the United States, the most common use of the material is in cement production (EUROSLAG, 2006). The average price per tonne for granulated Fe slag is significantly higher than for the other types of ferrous slag. In Table 5, the average price per tonne of granulated Fe slag in 2011 is $74, compared to $7 for air-cooled Fe slag; approximately 70% of the value of total slag sales is from granulated material (Van Oss, 2013). Pelletized slag usually contains abundant vesicles making it an ideal lightweight aggregate. If pelletized slag is finely ground, it may also be used as a cementitious material. This type of slag is the least abundant type, usually accounting for less than one percent of the Fe slag produced in the United States (Van Oss, 2013).

Table 5
Use of iron and steel slag in the United States in 2011 (from Van Oss, 2013).

	Blast furnace iron[a]		Steel furnace
	Air cooled	Granulated	
Percentage			
Ready-mixed concrete	11.1	–	–
Concrete products	5.1	–	–
Asphaltic concrete	19.3	–	12.1
Road bases and surfaces	38.7	4.5	46.8
Fill	13.3		19.3
Cementitious material	–	95.0	–
Clinker raw material	0.8	–	4.7
Misc.[b]	6.6	0.5	–
Other	5.1	–	17.1
Average price per tonne	$7.14	$74.25	$5.18
Million tonnes sold or used	5.5	2.5	7.3

[a] Pelletized slag quantities are very small and not included.
[b] Includes railroad ballast, roofing, mineral wool, or soil conditioner.

Non-ferrous slag also has construction reuse applications but according to the United States Department of Transportation (FHWA, 1997), most non-ferrous slag produced is disposed of in waste dumps. These slags are commonly air cooled but can also be quenched influencing how the material can be reused. Zinc slag has been used to manufacture ceramic tile and used as an aggregate in asphalt. Copper and Ni slags have been used as aggregate in asphalt, as fill, in railway ballast materials, in roofing material, and as cementitious material (granulated) (FHWA, 1997). Recent research has revealed that the addition of small amounts of Cu slag to cement actually improved its burnabilty (Ali et al., 2013). Gorai et al. (2003) gave a brief review of the use of Cu slag and also listed the following uses: as an abrasive for cutting tools, in pavement and concrete, as flooring tiles, and in colored glass, among others.

The use of some slag types, in particular from non-ferrous smelters, in construction materials has been shown to release trace elements into the environment. As previously discussed, Zn slag from the Hegeler smelter in Illinois that was used as fill for private drives, roadways and railways has contaminated residential soils with some trace elements (Weston Solutions, Inc., 2007). Laboratory and pilot scale leaching tests on road materials, mostly cements, containing Zn and Pb slag indicated that Zn and Pb are released during simulated environmental conditions and only a limited amount of some slag types can be incorporated into these materials (Barna et al., 2004; De Angelis and Medici, 2012). In contrast, laboratory leaching tests on asphalt mixes containing EAF steel slag did not release environmental significant amounts of Cr or other trace elements suggesting these materials are appropriate substitutes (Milačič et al., 2011).

7.2. Environmental applications

The use of ferrous slag in environmental applications has been increasing with recent studies on the removal of phosphorus, nitrogen, or trace elements from solution and controlling unwanted industrial emissions. Numerous studies discuss the effectiveness of using steel slag to remove P from wastewater or agricultural runoff (Baker et al., 1998; Drizo et al., 2002, 2006; Weber et al., 2007; Bowden et al., 2009; Barca et al., 2012); another study highlighted the removal of nitrogen in constructed wetlands using steel slag (Sun et al., 2009). In addition, emission of nitrogen

oxides, which may increase levels of ozone, form acid rain, and acidify aquatic ecosystems, can be reduced by the addition of steel slag into cement kilns used to produce clinker by lowering the firing temperature (Srivastava et al., 2005).

Ferrous slag is also used as an acid-neutralizing agent (Gahan et al., 2009) for treating acid-mine drainage resulting from coal and base-metal operations (Cravotta, 2005; Simmons et al., 2002; Ziemkiewicz and Skousen, 1999). Ferrous slags have high neutralization potentials from the dissolution of Ca silicates, oxides, and carbonates (see reactions (2) and (3)), which increases alkalinity and pH. In Ziemkiewicz and Skousen (1999), the authors suggested allowing rainfall or runoff to interact with steel slag, producing an alkaline drainage that is then allowed to infiltrate directly into an acidic waste piles or is mixed with acid-mine drainage. Another study by Simmons et al. (2002) revealed that a leach bed constructed of steel slag was effectively neutralizing acidic drainage at a coal mine site. Cravotta (2005) conducted laboratory experiments allowing acid-mine drainage to interact with steel slag and reported that the slag effectively neutralized the acidic waters. Additionally, laboratory studies indicated that steel slag effectively neutralized and adsorbed Cu from synthetic acidic drainage water (Wendling et al., 2010).

Research has also focused on the use of steel slag to remove trace elements from water. A few studies investigated the removal of As or U from wastewaters, mine effluent, and synthetic solutions (Blowes et al., 2005; Kwon et al., 2008; Hanski et al., 2007; Oh et al., 2012). Another application is using steel slag to reduce carcinogenic Cr(VI) to less soluble and less toxic Cr (III) in contaminated groundwater or in synthetic solutions (Ochola and Moo-Young, 2004; Hanski and Kankaala, 2009). In addition, Dimitrova (2002) experimented with using granulated Fe slag to remove Pb from solution, which is applicable to decontaminating Pb-bearing industrial wastewaters.

Ferrous slag has also been used as a soil conditioner, fertilizer, or soil liming material. Some applications of this type are included in the "other" category in Table 5. Calcium, Fe, and Mg in ferrous slag can be plant nutrients, although their availability may be influenced by the simultaneous uptake of Si (Anderson, 1991). Slag may also help stabilize the soil and the basicity may increase soil pH. In addition, some trace elements (i.e., Cu, Mn, Zn) in the slag can provide micronutrients to plants and animals. Lopez Gomez et al. (1999) discussed the preparation of fertilizers from steel slag and its influence on the composition of soil and grass and the economic benefits. Anderson (1991) examined the benefits of Ca silicate slag applications to soil and leaf nutrients in sugarcane. Ali et al. (2008) found that silicate Fe slag from steelmaking increased rice productivity when applied to a wetland paddy field; the amount of methane emitted from the field was also reduced. Negim et al. (2010) experimented with using steel slag as an additive to Cu-contaminated soils and the effect on bean plant growth. Chang et al. (2013) reported a decrease in bioaccessible Cd in acidic industrial-contaminated soils amended with iron (BFS) slag. Another study conducted by Qiu et al. (2012) reported successful metal attenuation and a reduction in metal bioavailability after adding steel slag to acidic metal-rich (Cd, Cu, Pb, and Zn) soils from a mining-influenced area. Toxicity testing on leachate from Fe and steel slag using algae and bacteria suggested that the material is potentially suitable for soil amendments, but may require mixing with other media to reduce the leachate pH prior to use (Wendling et al., 2012, 2013).

7.3. Secondary metal recovery

The reprocessing of slag for secondary metal recovery at both ferrous and non-ferrous smelters is common practice. The production of steel usually involves the reprocessing of furnace slag to recover additional iron compounds; the recovered material is used within the steel plant as blast furnace feed or for the production of Fe metal (Fig. 2) (FHWA, 1997). Non-ferrous slag may also be reprocessed at the smelter to enhance metal recovery (Fig. 4). In addition to immediate reprocessing, an increase in the demand and value of some metals has led to research on determining the most effective means to recover metals from historical non-ferrous slag dumps that commonly contain significant concentrations of some metals. For example, Sn slag from northern South Africa (Rooiberg Valley, Limpopo) produced between 1650 and 1850 contains up to 54 wt.% Sn (Chirikure et al., 2010). Also, Pb–Ag slag from a 14th century smelter in the Příbram district, Czech Republic, contains up to 32 wt.% Pb (Ettler et al., 2009a). In some areas, the metal targeted for secondary recovery in the slag may be different than the metal targeted during the initial processing of the ore. For example in the Zambian Copperbelt, historical Cu slag produced beginning in 1931 has been reprocessed for recovery of Co at a modern smelter (Vítková et al., 2010).

The optimal reprocessing techniques for recovering metals from slags are the subject of numerous studies. Reprocessing of slag may involve crushing, grinding, magnetic separation, flotation, roasting, and leaching in various combinations. Secondary metal recovery from base-metal slags has been researched using various extraction solutions including the following: ferric chloride (Anand et al., 1980), acidic ferric sulfate or ammonia–ammonium carbonate solutions (Shelley, 1975), sulfuric acid (Shibayama et al., 2010), subsequent leaches with sulfuric acid and sodium chlorate (Yang et al., 2010), high pressure oxidative acid leaching (Li et al., 2009), nitric acid or ammonia solutions (Tshiongo et al., 2010), and aqueous sulfur dioxide (Gbor et al., 2000, 2006). In addition to leaching, Rao and Nayak (1992) experimented with using flotation processing to recover Cu (and lesser amounts of Co and Ni) from Cu slag. These studies all focus on recovery of trace elements such as As, Cu, Co, Ni, Pb, and Zn. Ferrous slag studies are less numerous and involve recovering Cr and V from steel slag by additional smelting (Park et al., 1994). Another study used magnetic separation and gravity methods to recovery Cr and Ni from stainless steel slag (Lopez et al., 1997). Sánchez and Sudbury (2013) discussed recovering Mo and Cu in Cu slag and V in steel slag as well as utilizing Fe separated from slag to use in the iron and steel industry and SiO_2 in ceramics and glass wool fabrication. The recovery of metal from non-ferrous and ferrous slag may be a means of not only generating revenue, but also reducing the environmental impacts of slag by removing potentially hazardous elements and diminishing the overall volume of smelter waste.

8. Conclusions

Interest in slag has been increasing steadily and because large volumes, on the order of 400 Mt or more, are produced worldwide annually, there is a need to understand the potential environmental impacts of this material and its role as a valuable resource. This chapter reviewed over 150 published studies on slag. Because of variable melt compositions and furnace conditions, slags have a range in bulk chemistry, mineralogy, chemical composition of phases, and leachate chemistry. Summarizing these characteristics by slag type from a variety of locations allowed us to make generalizations that are useful when considering the environmental aspects of slag. For instance, ferrous slag commonly has acid-neutralizing capacity and does not readily release environmentally significant amounts of most trace elements making it an attractive resource for construction purposes and in treating acid-mine drainage, among other uses. In contrast, non-ferrous slag may generate acid and release slag-type-specific trace elements when weathered and therefore is more commonly dumped in waste piles, but also has the potential to be reprocessed for secondary metal recovery. As the global population grows and technology advances, it is likely

that slag will continue to be a valuable resource for reuse and recycling and a source of contamination: understanding its nature will only become increasingly more important.

Acknowledgements

The authors would like to thank Natalia Ainsfield of the USGS for her assistance in compiling the data and references used in this report. The manuscript benefited from reviews by Dr. Havey Belkin (USGS), Dr. Alexandre Desbarats (Geological Survey of Canada), Dr. Vojtěch Ettler (Charles University), and Dr. Heather Jamieson (Queen's University). This is Contribution Number 20120177 of the Earth Sciences Sector, Natural Resources Canada. The use of trade, product, industry, or firm names in this paper is for descriptive purposes only and does not constitute endorsement by the United States Government.

Appendix A. Summary of slag characterization references and type of data from each that was used in this paper

References	Slag type	Chemistry	Leachate	Methods	Mineralogy	Sec. min.	EMPA
Ali et al. (2013)	Cu	x		x	x		
Altepeter and James (1992)	Zn		x				
Álvarez-Valero et al. (2008)	Base metals (Cu, Pb, Zn)	x		x	x	x	
Álvarez-Valero et al. (2009)	Base metals (Cu, Pb, Zn)		x	x	x		x
Barca et al. (2012)	Steel	x		x			
Barna et al. (2004)	Pb, Zn	x		x			
Bäverman et al. (1997)	Steel	x	x				
Bayless and Schulz (2003)	Fe, steel			x			
Bayless et al. (1998)	Fe, steel			x			
Bosso and Enzweiler (2008)	Pb	x		x	x		
Bril et al. (2008)	Zn		x	x	x	x	
Butler (1977)	Fe	x		x	x		x
CDM Fed Programs Corp. (1993)	Base metals		x				
Chaudhuri and Newesely (1993)	Pb–Zn	x		x	x		x
Chaurand et al. (2006)	Steel	x					
Chaurand et al. (2007)	Steel	x					
Chirikure et al. (2010)	Sn	x		x	x		x
Costagliola et al. (2008)	Base metals (pyrite, Cu–Pb–Zn, Ag), Fe			x	x		
Cravotta (2005)	Fe	x			x		
De Andrade Lima and Bernardez (2011)	Pb	x	x	x	x		
De Angelis and Medici (2012)	Pb–Zn	x					
De Windt et al. (2011)	Steel	x	x	x	x		
Douglas and Zerbino (1986)	Fe	x		x	x		
Douglas et al. (2012)	Steel	x		x	x		
Drizo et al. (2002)	Steel	x					
Drizo et al. (2006)	Steel	x					
Ettler et al. (2000)	Pb–Zn			x	x		x
Ettler et al. (2001a)	Pb–Zn			x	x		x
Ettler et al. (2001b)	Pb–Zn		x	x			
Ettler et al. (2002)	Pb–Zn		x	x	x		x
Ettler et al. (2003)	Pb–Ag, Ag–Pb, Pb, Pb–Zn	x	x	x			
Ettler et al. (2004)	Pb–Ag, Ag–Pb, Pb, Pb–Zn	x	x	x			
Ettler et al. (2005)	Pb–Zn		x	x			
Ettler et al. (2009a)	Pb–Ag–Zn	x		x	x		x
Ettler et al. (2009b)	Cu–Pb, Cu	x	x	x	x		x
Ettler et al. (2012)	Cu			x			
EUROSLAG (2003)	Fe	x					
Fällman and Hartlén (1994)	Steel	x	x	x			
FHWA (1997)	Steel, Cu, P, Ni, Pb	x					
Gahan et al. (2009)	Steel	x		x	x		
Ganne et al. (2006)	Zn		x	x	x		
Gbor et al. (2000)	Ni	x	x	x	x		
Gee et al. (1997)	Pb			x	x	x	
Heimann et al. (2010)	Sn			x			x
Ivanov (2000)	Fe, steel, Cu, Pb				x		

(*continued on next page*)

Appendix A (*continued*)

References	Slag type	Chemistry	Leachate	Methods	Mineralogy	Sec. min.	EMPA
Johnson et al. (1982)	Cu		x	x			
Kierczak et al. (2009)	Ni	x		x	x		x
Kierczak and Pietranik (2011)	Cu	x		x	x		
Kierczak et al. (2013)	Cu			x	x	x	
Kourounis et al. (2007)	Steel	x					
Kucha et al. (1996)	Zn–Pb	x	x	x	x		x
Lagos and Luraschi (1997)	Cu		x	x			
Leonard et al. (1977)	Cu, Pb		x				
Lewis (1982)	Fe	x			x		
Lottermoser (2002)	Base metals (Cu, Cu–Zn, Ag–Pb)	x		x	x	x	x
Lottermoser (2005)	Pyrite, base metals	x		x	x	x	
Mahé-Le Carlier et al. (2000)	Fe, base metals (Ag, Pb, Cu)	x		x			
Manasse et al. (2001)	Cu	x		x	x		x
Manz and Castro (1997)	Ag, Pb, Zn, Cu		x	x			
Matthes (1980)	Cu			x			
May and Peterson (1991)	Pb		x				
Milačič et al. (2011)	Steel	x		x	x		
Morrison and Gulson (2007)	Pb–Zn		x	x			
Morrison Knudsen Corp. (1992)	Pb		x				
Muhmood et al. (2009)	Fe, steel	x					
Narayan (1995)	Fe			x			
Navarro et al. (2008)	Ag–Pb	x	x	x	x	x	x
Navarro et al. (2010)	Steel	x		x	x		
Nelson (1993)	Base metal		x				
Oh et al. (2012)	Steel	x		x			
Parsons et al. (2001)	Cu–Zn	x	x	x	x		x
Partymiller (1992)	Pb		x				
Pérez-López et al. (2008)	Base metals (Cu, Pb, Zn)		x	x			
Pérez-López et al. (2010)	Base metals (Cu, Pb, Zn)	x		x			
Piatak et al. (2004)	Cu, Pb–Ag	x	x	x	x	x	x
Piatak and Seal (2010)	Zn	x	x	x	x	x	x
Piatak and Seal (2012a)	Pre-1900 Fe	x	x	x	x		x
Piatak and Seal (2014)	Steel	x	x	x	x		
Proctor et al. (2000)	Fe, steel	x	x	x			
Puziewicz et al. (2007)	Zn	x		x	x		x
Rai et al. (2002)	Ferro-Mn	x		x	x		
Rizza and Farthing (2007)	Fe			x			
Roadcap et al. (2005)	Steel	x					
Robbins et al. (1983)	Pb, Cu		x	x			
Rosado et al. (2008)	Base metals (Cu, Pb, Zn)			x	x		
Sáez et al. (2003)	Cu	x		x	x		x
Scheinert et al. (2009)	Ag–Pb–Zn–Cu			x			
Scott et al. (1986)	Fe	x		x	x		x
Seignez et al. (2007)	Pb		x	x	x	x	
Seignez et al. (2008)	Pb		x	x			
Severin et al. (2011)	Fe	x		x	x		x
Shen et al. (2009)	Steel	x					
Sidenko et al. (2001)	Zn			x	x		
Singh et al. (2008)	Fe	x					
Sobanska et al. (2000)	Pb	x		x	x		
Suer et al. (2009)	Steel	x					
Svirenko et al. (2003)	Fe	x		x	x	x	
Tack et al. (1993)	Non-ferrous		x				
Tatarinov (2002)	Cu	x		x	x		
Tetra Tech Inc (1985)	Cu		x				
Tossavainen et al. (2007)	Steel	x	x	x			
Tsakiridis et al. (2008)	Steel	x					
Twidwell (1983)	Cu, Pb		x				
Twidwell and Mehta (1985)	Cu, Pb		x				
Vdović et al. (2006)	Pb–Zn			x			

Appendix A (*continued*)

References	Slag type	Chemistry	Leachate	Methods	Mineralogy	Sec. min.	EMPA
Vítková et al. (2010)	Cu–Co	x		x	x		x
Vítková et al. (2011)	Cu–Co	x	x	x	x		
Vivenzio and Farthing (2005)	Fe			x	x		
Wendling et al. (2010)	Steel	x		x	x		
Wendling et al. (2012)	Steel		x				
Wendling et al. (2013)	Fe, steel	x	x	x	x		
West (1902)	Fe	x					
Wilson (1994)	Many			x			
Woodley and Walters (1986)	Pb BFS		x	x			
Yildirim and Prezzi (2011)	Steel	x		x	x		
Ziemkiewicz and Skousen (1999)	Steel	x	x	x			

Abbreviations: Sec. min.= secondary minerals, EMPA = electron microprobe analysis, x = indicates type of data reported in article, Fe = blast furance iron.

Appendix B. Summary of slag application and reuse references for this paper (not including references listed above)

References	Slag type
Ali et al. (2008)	Steel
Anand et al. (1980)	Cu
Anderson (1991)	Ferrous
Baker et al. (1998)	Steel
Blowes et al. (2005)	Steel
Bowden et al. (2009)	Steel
Chang et al. (2013)	Fe
Cravotta (2005)	Fe
Dimitrova (2002)	Fe
Drizo et al. (2002)	Steel
Drizo et al. (2006)	Steel
EUROSLAG (2006)	Ferrous
FHWA (1997)	Steel, Cu, P, Ni, Pb
Gahan et al. (2009)	Steel
Gbor et al. (2006)	Ni
Gbor et al. (2000)	Ni
Gorai et al. (2003)	Cu
Hadjsadok et al. (2012)	Fe
Hanski et al. (2007)	Steel
Hanski and Kankaala (2009)	Steel
Kwon et al. (2008)	Steel
Li et al. (2009)	Cu–Ni
Lopez et al. (1997)	Steel
Lopez Gomez et al. (1999)	Steel
Maslehuddin et al. (2003)	Steel
Negim et al. (2010)	Steel
Ochola and Moo-Young (2004)	Steel
Park et al. (1994)	Steel
Qiu et al. (2012)	Steel
Rao and Nayak (1992)	Cu
Sánchez and Sudbury (2013)	Cu
Shelley (1975)	Non-ferrous
Shibayama et al. (2010)	Non-ferrous
Simmons et al. (2002)	Steel
Srivastava et al. (2005)	Steel
Sun et al. (2009)	Steel
Tshiongo et al. (2010)	Cu
Van Oss (2013)	Ferrous
Weber et al. (2007)	Steel
Yang et al. (2010)	Cu
Ziemkiewicz and Skousen (1999)	Steel

References

Ali, M.A., Oh, J.H., Kim, P.J., 2008. Evaluation of silicate iron slag amendment on reducing methane emission from flood water rice farming. Agric. Ecosyst. Environ. 128, 21–26.

Ali, M.M., Agarwal, S.K., Pahuja, A., 2013. Potentials of copper slag utilization in the manufacture of ordinary Portland cement. Adv. Cem. Res. 25 (4), 208–216.

Alpers, C.N., Nordstrom, D.K., 1999. Geochemical modeling of water–rock interactions in mining environments. In: Plumlee, G.S., Logsdon, M.J. (Eds.), The Environmental Geochemistry of Mineral Deposits, Part A: Processes, Techniques, and Health Issues: Reviews in Economic Geology, vol. 6A. Society of Economic Geologists, Littleton, CO, pp. 289–323.

Altepeter, M., James, S., 1992. Proposed treatment of neutral Leach residue at Big River Zinc. In: Reddy, R.J., Imrie, W.P., Queneau, P.B. (Eds.), Residues Effluents: Processing Environmental Considerations. Minerals, Metals, and Materials Society, pp. 449–459.

Álvarez-Valero, A.M., Pérez-López, R., Matos, J., Capitán, M.A., Nieto, J.M., Sáez, R., Delgado, J., Caraballo, M., 2008. Potential environmental impact at São Domingos mining district (Iberian Pyrite Belt, SW Iberian Peninsula): evidence from a chemical and mineralogical characterization. Environ. Geol. 55, 1797–1809.

Álvarez-Valero, A.M., Pérez-López, R.M., Nieto, J.M., 2009. Prediction of the environmental impact of modern slags: a petrological and chemical comparative study with Roman age slags. Am. Mineral. 94, 1417–1427.

Anand, S., Rao, P., Jena, P., 1980. Recovery of metal values from copper converter and smelter slags by ferric chloride leaching. Hydrometallurgy 5, 355–365.

Anderson, D.L., 1991. Soil and leaf nutrient interactions following application of calcium silicate slag to sugarcane. Nutr. Cycl. Agroecosyst. 30, 9–18.

Baker, M.J., Blowes, D.W., Ptacek, C.J., 1998. Laboratory development of permeable reactive mixtures for the removal of phosphorus from onsite wastewater disposal systems. Environ. Sci. Technol. 32, 2308–2316.

Barca, C., Gérente, C., Meyer, D., Chazarenc, F., Andrès, 2012. Phosphate removal from synthetic and real wastewater using steel slags produced in Europe. Water Res. 46, 2376–2384.

Barna, R., Moszkowicz, P., Gervais, C., 2004. Leaching assessment of road materials containing primary lead and zinc slags. Waste Manage. (Oxford) 24, 945–955.

Bäverman, C., Sapiej, A., Moreno, L., Neretnieks, I., 1997. Serial batch tests performed on municipal solid waste incineration bottom ash and electric arc furnace slag, in combination with computer modeling. Waste Manage. Res. 15, 55–71.

Bayless, E.R., Schulz, M.S., 2003. Mineral precipitation and dissolution at two slag-disposal sites in northwestern Indiana, USA. Environ. Geol. 45, 252–261.

Bayless, E.R., Greeman, T.K., Harvey, C.C., 1998, Hydrology and Geochemistry of a Slag-affected Aquifer and Chemical Characteristics of Slag-Affected Ground Water, Northwestern Indiana and Northeastern Illinois: U.S. Geological Survey, Water-Resources Investigations, Report 97-4198, 67p.

Bayless, E.R., Bullen, T.D., Fitzpatrick, J.A., 2004. Use of $^{87}Sr/^{86}Sr$ and $\delta^{11}B$ to identify slag-affected sediment in southern Lake Michigan. Environ. Sci. Technol. 38, 1330–1337.

Bethke, C.M., 2008. Geochemical and Biogeochemical Reaction Modeling, second ed. Cambridge University Press, New York, 543p.

Blowes, D.W., Bain, J.G., Smyth, D., McGregor, R., Ludwig, P., Wilkens, J.A., Ptacek, C.J., Spink, L., 2005, Treatment of Arsenic Using Permeable Reactive Barriers: Geological Society of America Annual Meeting Program with Abstracts, vol. 37, no. 7, p. 102.

Bosso, S.T., Enzweiler, J., 2008. Bioaccessible lead in soils, slag, and mine wastes from an abandoned mining district in Brazil. Environ. Geochem. Health 30, 219–229.

Bowden, L.I., Jarvis, A.P., Younger, P.L., Johnson, K.L., 2009. Phosphorus removal from waste waters using basic oxygen steel slag. Environ. Sci. Technol. 43 (7), 2476–2481.

Brandt, D.A., Warner, J.C., 2009. Metallurgy Fundamentals, fifth ed. Goodheart-Wilcox Company Inc., Tinley Park, Illinois, 301p.
Bril, H., Zainoun, K., Puziewicz, J., Courtin-Nomade, A., Vanaecker, M., Bollinger, J.-C., 2008. Secondary phases from the alteration of a pile of zinc-smelting slag as indicators of environmental conditions: An example from Świętochłowice, Upper Silesia, Poland. Can. Mineral. 46, 125–1248.
Butler, B.C.M., 1977. Al-rich pyroxene and melilite in a blast-furnace slag and a comparison with the Allende meteorite. Mineral. Mag. 41, 439–493.
Carroll, M.R., Rutherford, M.J., 1988. Sulfur speciation in hydrous experimental glasses of varying oxidation states: results from measured wavelength shifts of sulfur X-rays. Am. Mineral. 73, 845–849.
Canadian Council of Ministers of the Environment (CCME), 2007. Canadian Soil Quality Guidelines for the Protection of Environmental and Human Health: Summary Tables. Updated September, 2007. In: Canadian Environmental Quality Guidelines, 1999, Canadian Council of Ministers of the Environment, Winnipeg.
CDM Fed Programs Corporation, 1993. Draft Work Plan for Waste Compatibility Evaluation Study – Sharon Steel Tailings Site/Midvale Slag Site. USEPA, Midvale, Utah. Contract No. 68-W9-0021.
Chang, Y.-T., His, H.-C., Hseu, Z.-Y., Jheng, S.-L., 2013. Chemical stabilization of cadmium in acidic soil using alkaline argronomic and industrial by-products. J. Environ. Sci. Health, Part A 48, 1748–1756.
Chaudhuri, J.N.B., Newesely, H., 1993. Mineralogical characterization of old Harz Mountain slags. Can. Metall. Q. 32 (1), 1–12.
Chaurand, P., Rose, J., Domas, J., Botter, J.-Y., 2006. Speciation of Cr and V within BOF steel slag reused in road constructions. J. Geochem. Explor. 88, 10–14.
Chaurand, P., Rose, J., Briois, V., Olivi, L., Hazemann, J.-L., Proux, O., Domas, J., Bottero, J.-Y., 2007. Environmental impacts of steel slag reused in road construction: a crystallographic and molecular (XANES) approach. J. Hazard. Mater. B139, 537–542.
Chirikure, S., Heimann, R.B., Killick, D., 2010. The technology of tin smelting in the Rooiberg Valley, Limpopo Province, South Africa, ca. 1650–1850 CE. J. Archaeol. Sci. 37, 1656–1669.
Costagliola, P., Benvenuti, M., Chiarantini, L., Bianchi, S., Di Benedetto, F., Paolieri, M., Rossato, L., 2008. Impact of ancient metal smelting on arsenic pollution in the Pecora River Valley, Southern Tuscany, Italy. Appl. Geochem. 23, 1241–1259.
Cottrell, A., 1995. An Introduction to Metallurgy, second ed. Hodder Arnold Publishers Ltd., 548p.
Cravotta III, C.A., 2005. Assessment of Characteristics and Remedial Alternatives for Abandoned Mine Drainage: Case Study at Staple Bend Tunnel Unit of Allegheny Portage Railroad National Historic Site, Cambria Country, Pennsylvania, 2004: U.S. Geological Survey Open-File, Report 2005-1283, 52p.
Crock, J.G., Arbogast, B.F., Lamothe, P.J., 1999. Laboratory methods for the analysis of environmental samples. In: Plumlee, G.S., Logsdon, M.J. (Eds.), The Environmental Geochemistry of Mineral Deposits, Part A: Processes, Techniques, and Health Issues: Reviews in Economic Geology, vol. 6A, pp. 265–287 (Chapter 13).
De Andrade Lima, L.R.P., Bernardez, L.A., 2011. Characterization of the lead smelter slag in Santo Amaro, Bahia, Brazil. J. Hazard. Mater. 189, 692–699.
De Angelis, G., Medici, F., 2012. Reuse of slags containing lead and zinc as aggregate in a portland cement matrix. J. Solid Waste Technol. Manage. 38, 117–123.
De Windt, L., Chaurand, P., Rose, J., 2011. Kinetics of steel slag leaching: batch tests and modeling. Waste Manage. (Oxford) 31, 225–235.
Dimitrova, S.V., 2002. Use of granular slag columns for lead removal. Water Res. 36, 4001–4008.
Douglas, E., Zerbino, R., 1986. Characterization of granulated and pelletized blast furnace slag. Cem. Concr. Res. 16, 662–670.
Douglas, G.B., Wendling, L.A., Coleman, S., 2012. Productive use of steelmaking by-product in environmental applications (I): mineralogy and major and trace element geochemistry. Miner. Eng. 35, 49–56.
Drizo, A., Comeau, Y., Forget, C., Chapuis, R.P., 2002. Phosphorus saturation potential: a parameter for estimating the longevity of constructed wetland systems. Environ. Sci. Technol. 36, 4642–4648.
Drizo, A., Forget, C., Chapuis, R.P., Comeau, Y., 2006. Phosphorus removal by electric arc furnace steel slag and serpentinite. Water Res. 40, 1547–1554.
Ettler, V., Johan, Z., Touray, J.-C., Jelínek, E., 2000. Zinc partitioning between glass and silicate phases in historical and modern lead–zinc metallurgical slags from the Příbram district, Czech Republic. Comptes Rendus de l'Académie des Sciences, Sciences de la Terre et des Planètes 331, 245–250.
Ettler, V., Legendre, O., Bodénan, F., Touray, J., 2001a. Primary phases and natural weathering of old lead–zinc pyrometallurgical slag from Příbram, Czech Republic. Can. Mineral. 39, 873–888.
Ettler, V., Mihaljevič, M., Touray, J.-C., 2001b. Metallurgical slag behaviour in extreme conditions: surface leaching and metal mobility. Ecole Nationale Superieure des Mines de Paris Mémoire des Sciences de la Terre 40, 81–83.
Ettler, V., Mihaljevič, M., Touray, J.-C., Piantone, P., 2002. Leaching of polished sections: an integrated approach for studying the liberation of heavy metals from lead–zinc metallurgical slags. Bull. Soc. Geol. Fr. 173, 161–169.
Ettler, V., Piantone, P., Touray, J.-C., 2003. Mineralogical control on inorganic contaminant mobility in leachate from lead–zinc metallurgical slag: experimental approach and long-term assessment. Mineral. Mag. 67 (6), 1269–1283.
Ettler, V., Komárková, M., Jehlička, J., Coufal, P., Hradil, D., Machovič, V., Delorme, F., 2004. Leaching of lead metallurgical slag in citric solutions: Implications for disposal and weathering in soil environments. Chemosphere 57, 567–577.
Ettler, V., Jehlička, J., Mašek, V., Hruška, J., 2005. The leaching behaviour of lead metallurgical slag in high-molecular-weight (HMW) organic solutions. Mineral. Mag. 69 (5), 737–747.
Ettler, V., Červinka, R., Johan, Z., 2009a. Mineralogy of medieval slag from lead and silver smelting (Bohutín, Příbram District, Czech Republic): towards estimates of historical smelting conditions. Archaeometry 51, 987–1007.
Ettler, V., Johan, Z., Kříbek, B., Šebek, O., Mihaljevič, M., 2009b. Mineralogy and environmental stability of slags from the Tsumeb smelter, Namibia. Appl. Geochem. 24, 1–15.
Ettler, V., Johan, Z., Vítkova, M., Skála, R., Kotrlý, M., Habler, G., Klementová, M., 2012. Reliability of chemical microanalyses for solid waste materials. J. Hazard. Mater. 221–222, 298–302.
European Committee for Standardization, 2002. Final Draft prEN 12457–2. Characterization of Waste Leaching-compliance Test of Leaching of Granular Waste Material and Sludges – Part 2: One-stage Batch Test at a Liquid to Solid Ration of 10 l/kg for Materials With Particle Size Below 4 mm (With or Without Particle Reduction), Czech Standard Institute, Prague.
European Slag Association (EUROSLAG), 2003. Granulated Blastfurnace Slag, Technical Leaflet No. 1, 4p. http://www.euroslag.org/fileadmin/_media/images/Research/FACT_SHEETS/LeafletGBS.pdf> (accessed May 2013).
European Slag Association (EUROSLAG), 2006. Legal Status of Slags, Position Paper, January 2006, 15p. http://www.euroslag.org/fileadmin/_media/images/Status_of_slag/Position_paper_Jan_2006.pdf> (accessed May 2013).
Fällman, A.-M., Hartlén, J., 1994. Leaching of slags and ashes – controlling factors in field experiments versus laboratory tests. In: Goumans, J.J.J.M., van de Sloot, H.A., Aalbers, Th.G. (Eds.), Environmental Aspects of Construction with Waste Materials: Studies in Environmental Science, vol. 60, pp. 39–54.
Federal Highway Administration (FHWA), U.S. Department of Transportation, 1997.User Guidelines for Waste and Byproduct Materials in Pavement Construction: FHWA-RD-97-148, McLean, VA, USA. http://www.fhwa.dot.gov/publications/research/infrastructure/structures/97148/> (accessed February 2012).
Gahan, C.S., Cunha, M.L., Sandström, Å., 2009. Comparative study on different steel slags as neutralising agent in bioleaching. Hydrometallurgy 95, 190–197.
Ganne, P., Cappuyns, V., Vervoort, A., Buvé, L., Swennen, R., 2006. Leachablity of heavy metals and arsenic from slags of metal extraction industry at Angleur (eastern Belgium). Sci. Total Environ. 356, 69–85.
Garrels, R.M., Mackenzie, F.T., 1967, Origin of the chemical compositions of some springs and lakes. In: Equilibrium Concepts in Natural Waters, Advances in Chemistry Series 67: American Chemical Society, Washington, DC, pp. 222–242 (Chapter 10).
Gbor, P.K., Ahmed, I.B., Jia, C.Q., 2000. Behaviour of Co and Ni during aqueous sulphur dioxide leaching of nickel smelter slag. Hydrometallurgy 57, 13–22.
Gbor, P.K., Hoque, S., Jia, C.Q., 2006. Dissolution behavior of Fe Co, and Ni from non-ferrous smelter slag in aqueous sulphur dioxide. Hydrometallurgy 81, 130–141.
Gee, C., Ramsey, M.H., Maskall, J., Thornton, I., 1997. Mineralogy and weathering processes in historical smelting slag and their effect on the mobilization of lead. J. Geochem. Explor. 58, 249–257.
Glynn, P., Brown, J., 1996. Reactive transport modeling of acidic metal-contaminated ground water at a site with sparse spatial information. In: Lichtner, P.C., Steefel, C.I., Oelkers, E.H. (Eds.), Reactive Transport in Porous Media: Mineralogical Society of America, Reviews in Mineralogy, vol. 34, pp. 377–438 (Chapter 9).
Gorai, B., Jana, R.K., Premchand, 2003. Characteristics and utilization of copper slag – a review. Resour. Conserv. Recycl. 39 (4), 299–313.
Hadjsadok, A., Kenai, S., Courard, L., Michel, F., Khatib, J., 2012. Durability of mortar and concretes containing slag with low hydraulic activity. Cement Concr. Compos. 34, 671–677.
Hanski, E., Kankaala, A., 2009. Reduction of aqueous hexavalent chromium by steel slag: abstracts of the 19th annual V. M. Goldschmidt conference. Geochim. Cosmochim. Acta 73 (13S), A492.
Hanski, E.J., Mäkela, K., Manninen, M., Kujala, K., Perämäki, 2007. Removal of uranium, arsenic and phosphorus from aqueous solutions using steel slag: Goldschmidt conference abstracts. Geochim. Cosmochim. Acta 71 (15S), A379.
Heimann, R.B., Chirikure, S., Killick, D., 2010. Mineralogical study of precolonial (1650–1850 CE) tin smelting slags from Rooiberg, Limpopo Province, South Africa. Eur. J. Mineral. 22, 751–761.
Helgeson, H.C., 1968. Evaluation of irreversible reactions in geochemical processes involving minerals and aqueous solutions—I. Thermodynamic relations. Geochim. Cosmochim. Acta 32, 853–877.
Ishimaru, S., Arai, S., 2008. Nickel enrichment in mantle olivine beneath a volcanic front. Contrib. Miner. Petrol. 156, 119–131.
Ivanov, I.T., 2000. Phase composition of metallurgical slags in Bulgaria. In: Rammlmair, D., Mederer, J., Oberthür, Th., Heimann, R.B., Pentinghaus, H. (Eds.), Proceedings of the Sixth International Congress on Applied Mineralogy ICAM 2000, Göttingen, Germany, July 17–19, 2000.
Jambor, J.L., 2003. Mine-waste mineralogy and mineralogical perspectives of acid–base accounting. In: Jambor, J.L., Blowes, D.W., Ritchie, A.I.M. (Eds.), Environmental Aspects of Mine Wastes, Short Course Series, Mineralogical Association of Canada, vol. 31, pp. 117–145.
Johnson, E.A., Oden, L.L., Sanker, P.E., 1982. Results of E.P.A. Extraction Procedure Toxicity Test Applied to Copper Reverberatory Slags: U.S. Bureau of Mines Report of Investigation 8648, 16p.
Kierczak, J., Pietranik, A., 2011. Mineralogy and composition of historical Cu slags from the Rudawy Janowickie Mountains, Southwestern Poland. Can. Mineral. 49, 1281–1296.

Kierczak, J., Néel, C., Puziewicz, J., Bril, H., 2009. The mineralogy and weathering of slag produced by the smelting of the lateritic Ni ores, Szklary, Southwestern Poland. Can. Mineral. 47, 557–572.
Kierczak, J., Potysz, A., Pietranik, A., Tyszka, R., Modelska, M., Néel, C., Ettler, V., Mihaljevič, M., 2013. Environmental impact of the historical Cu smelting in the Rudawy Janowickie Mountains (south-western Poland). J. Geochem. Explor. 124, 183–194.
Kourounis, S., Tsivilis, S., Tsakiridis, P.E., Papadimitriou, G.D., Tsibouki, Z., 2007. Properties and hydration of blended cements with steelmaking slag. Cem. Concr. Res. 37, 815–822.
Kucha, H., Martens, A., Ottenburgs, R., De Vos, W., Viaene, W., 1996. Primary minerals of Zn–Pb mining and metallurgical dumps and their environmental behavior at Plombiéres, Belgium. Environ. Geol. 27, 1–15.
Kwon, J.-S., Yun, Seong-Taek, Jo, H.-Y., Jung, S.-H., 2008. Geochemical Processes Including Sorption and Incorporation of Heavy Metals and Arsenic by Scoria and Steel Slag: Abstracts of the 18th Annual V. M. Goldschmidt Conference, Geochimica et Cosmochimica Acta, vol. 72, no. 12S, p. A507.
Lagos, G.E., Luraschi, A., 1997. Toxicity Characteristic Leaching Procedure (TCLP) Applied to Chilean Primary Copper Slags: Transactions of the Institution of Mining and Metallurgy Section C—Mineral Processing and Extractive Metallurgy, vol. 106, pp. C95–C97.
Leonard, R.P., Ziegler, R.C., Brown, W.R., Yang, J.Y., Reif, H.C., 1977. Assessment of Industrial Hazardous Waste Practices in the Metal Smelting and Refining Industry, vol. IV, Appendices: U.S. Environmental Protection Agency, EPA/530/SW-145c.4, pp. 31–39.
Levin, E.M., Robbins, C.R., McMurdie, H.F., 1964. Phase Diagrams for Ceramists: The American Ceramic Society. Columbus, Ohio.
Lewis, D.W., 1982. Properties and Uses of Iron and Steel Slags: National Slag Association (NSA) MF 182-6, Presented at the Symposium on Slag national Institute for Transport and Road Research South Africa, February, 1982. http://www.nationalslag.org/archive/legacy/nsa_182-6_properties_and_uses_slag.pdf> (updated 1992) (accessed February 2012).
Li, Y., Papangelakis, V.G., Perederiy, I., 2009. High pressure oxidative acid leaching of nickel smelter slag, characterization of feed and residue. Hydrometallurgy 97 (3–4), 185–193.
Lopez, F.A., Lopez-Delgado, A., Belcazar, N., 1997. Physico-chemical and mineralogical properties of EAF and AOD slags: associazione Italiana de. Metallurgia, 417–426.
LopezGomez, F.A., Aldecoa, R., Fernandez Prieto, M.A., Rodrigues, J.M., 1999. Preparation of NPK Fertilizers from Ferrous-Metallurgy. Simoes C Eur Commun [Rep] 18616, pp. 1–57.
Lottermoser, B.G., 2002. Mobilization of heavy metals from historical smelting slag dumps, north Queensland, Australia. Mineral. Mag. 66 (4), 475–490.
Lottermoser, B.G., 2005. Evaporative mineral precipitates from the historical smelting slag dump, Río Tinto, Spain. Neues Jahrbuch für Mineralogie-Abhandlungen 181, 183–190.
Mahé-Le Carlier, C., Le Carlier de Veslud, C., Ploquin, A., Royer, J.-J., 2000. Natural weathering of archaeo-metallurgical slags: an analog for present day vitrified wastes. Earth Planet. Sci. 330, 179–184.
Manasse, A., Mellini, M., Viti, C., 2001. The copper slags of the Capattoli Valley, Campiglia Marittima, Italy. Eur. J. Mineral. 13, 949–960.
Mandin, D., van der Sloot, H.A., Gervais, C., Barna, R., Mehu, J., 1997. Valorization of lead–zinc primary smelters slags. In: Goumans, J.J.J., Senden, G.J., van der Sloot, H.A. (Eds.), Waste Materials in Construction: Putting Theory into Practice. Studies in Environmental Science, vol. 71, pp. 617–630.
Manz, M., Castro, L.J., 1997. The environmental hazard caused by smelter slags from the Sta. Maria de la Paz mining district in Mexico: Environmental Pollution 98, 7–13.
Maslehuddin, M., Sharif, A.M., Shameem, M., Ibrahim, M., Barry, M.S., 2003. Comparison of properties of steel slag and crushed limestone aggregate concretes. Constr. Build. Mater. 17, 105–112.
Matthes, S.A., 1980. Rapid Low-cost Analysis of a Copper Slag for 13 Elements by Flame Atomic Absorption Spectroscopy: U.S. Bureau of Mines Report of Investigations 8484, 8p.
May, A., Peterson, J.B., 1991. Assessment of lead slag landfill site and the use of a computational program for chemical species. In: Proceedings of the Symposium on Environmental Management for the 1990's, Denver, Colorado, February 25–28, pp. 217–223.
Milačič, R., Zuliani, T., Oblak, T., Mladenovič, A., Ščančar, J., 2011. Environmental impacts of asphalt mixes with electric arc furnace steel slag. J. Environ. Qual. 40, 1153–1161.
Morrison, A., Gulson, B., 2007. Preliminary findings of chemistry and bioaccessibility in base metal smelter slags. Sci. Total Environ. 382, 30–42.
Morrison Knudsen Corporation, 1992. Final Report for Lead Slag Pile Remedial Investigation at the California Gulch Site, Leadville, Colorado. Denver Rio Grande Western Railroad Company.
Muhmood, L., Vitta, S., Venkateswaran, D., 2009. Cementitious and pozzolanic behavior of electric arc furnace steel slags. Cem. Concr. Res. 39, 102–109.
Narayan, C., 1995. Report on the Analysis of Iron Slag Samples from Saugus Iron Works, MA Using Rutherford Backscattering Spectroscopy (RBS) and Proton Induced X-ray Emission (PIXE) Techniques. University of Massachusetts Lowell Radiation Laboratory, 15p.
Navarro, A., Cardellach, E., Mendoza, J.L., Corbella, M., Domènech, L.M., 2008. Metal mobilization from base-metal smelting slag dumps in Sierra Almagrera (Almería, Spain). Appl. Geochem. 23, 895–913.
Navarro, C., Díaz, M., Villa-García, M.A., 2010. Physico-chemical characterization of steel slag. Study of Its Behavior Under Simulated Environmental Conditions: Environmental Science and Technology 44, 5383–5388.
Negim, O., Eloifi, B., Mench, M., Bes, C., Gaste, H., Montelica-Heino, M., Le Coustumer, P., 2010. Effect of basic slag addition on soil properties, growth and leaf mineral composition of bean sin a Cu-contaminated soil. Soil Sediment Contam. 19, 174–187.
Nelson, T., 1993. Data on Slag Samples Collected from the Midvale Slag Site, Midvale, Utah: Sverdup Corporation Memorandum No. 10865R00(1.1)-91 to M. Strieby, U.S. Environmental Protection Agency Region VIII.
Nordstrom, D.K., Alpers, C.N., 1999. Geochemistry of acid mine waters. In: Plumlee, G.S., Logsdon, M.J. (Eds.), The Environmental Geochemistry of Mineral Deposits, Part A: Processes, Techniques, and Health Issues. Reviews in Economic Geology, vol. 6A. Society of Economic Geologists, Littleton, CO, pp. 133–160 (Chapter 6).
National Slag Association (NSA), 2009. Slag's Ain't Slag's. http://www.nationalslag.org/appmatrix.htm> (accessed February 2012).
Ochola, C.E., Moo-Young, H.K., 2004. Establishing and elucidating reduction as the removal mechanism of Cr(VI) by reclaimed limestone residual RLR (modified steel slag). Environ. Sci. Technol. 38, 6161–6165.
Oh, C., Rhee, S., Oh, M., Park, J., 2012. Removal characteristics of As(III) and As(V) from acidic aqueous solution by steel making slag. J. Hazard. Mater. 213–214, 147–155.
Paris, E., Giuli, G., Carroll, M., Davoli, I., 2001. The valence and speciation of sulfur in glasses by X-ray absorption spectroscopy. Can. Mineral. 39, 331–339.
Park, H.S., Ban, B.C., Cho, K.S., 1994. Smelting reduction for vanadium-recovery from LD-slag (I). Kor. J. Met. Mater. 32 (8), 982–988.
Parkhurst, D.L., Plummer, L.N., 1993. Geochemical models. In: Alley, W.M. (Ed.), Regional Ground-Water Quality. Van Nostrand Reinhold, New York, pp. 199–225.
Parsons, M.B., 2001. Geochemical and Mineralogical Controls on Trace Element Release from Base-metal Smelter Slags. Unpublished Ph.D. Thesis, Stanford University, Stanford, California, 307p.
Parsons, M.B., Bird, D.K., Einaudi, M.T., Alpers, C.N., 2001. Geochemical and mineralogical controls on trace element release from the Penn Mine base-metal slag dump, California. Appl. Geochem. 16, 1567–1593.
Partymiller, K., 1992. Horsehead Resource Development Company, Inc. Flame Reactor Technology: Applications Analysis Report. Environmental Protection Agency, EPA/540/A5-91/005.
Pérez-López, R., Álvarez-Valero, A.M., Nieto, J.M., Sáez, R., Matos, J.X., 2008. Use of sequential extraction procedure for assessing the environmental impact at regional scale of the São Domingos Mine (Iberian Pyrite Belt). Appl. Geochem. 23, 3452–3463.
Pérez-López, R., Delgado, J., Nieto, J.M., Márquez-Garciá, B., 2010. Rare earth element geochemistry of sulphide weathering in the São Domingos mine area (Iberian Pyrite Belt): a proxy for fluid–rock interaction and ancient mining pollution. Chem. Geol. 276, 29–40.
Piatak, N.M., Seal II, R.R., 2010. Mineralogy and the release of trace elements from slag from the Hegeler Zinc smelter, Illinois (USA). Appl. Geochem. 25, 302–320.
Piatak, N.M., Seal II, R.R., 2012a. Mineralogy and environmental geochemistry of historical iron slag, Hopewell Furnace National Historic Site, Pennsylvania, USA. Appl. Geochem. 27, 623–643.
Piatak, N.M., Seal II, R.R., 2012b. Leaching tests to characterize ferrous and nonferrous slag drainage chemistry. In: Price, W.A., Hogan, C., Tremblay, G. (Eds.), Proceedings from the Ninth International Conference on Acid Rock Drainage, Ottawa, Canada, 12p.
Piatak, N.M., Seal II, R.R., 2014. Challenges of quantifying the partitioning of metals within solid phases: an example of zinc in slag from the Hegeler Zinc smelter, Illinois. In: McLemore, V.T, Smith, K.S., Russell, C.C. (Eds.), Environmental Sampling and Monitoring for the Mine-Life Cycle, Appendix 5—Case Studies of Sampling and Monitoring: Eaglewood, CO, Society for Mining, Metallurgy, and Exploration, Inc.
Piatak, N.M., Seal II, R.R., Hammarstrom, J.M., 2004. Mineralogical and geochemical controls on the release of trace elements from slag produced by base- and precious-metal smelting at abandoned mine sites. Appl. Geochem. 19, 1039–1064.
Proctor, D.M., Fehling, K.A., Shay, E.C., Wittenborn, J.L., Green, J.J., Avent, C., Bigham, R.D., Connolly, M., Lee, B., Shepker, T.O., Zak, M.A., 2000. Physical and chemical characteristics of blast furnace, basic oxygen furnace, and electric arc furnace steel industry slags. Environ. Sci. Technol. 34, 1576–1582.
Puziewicz, J., Zainoun, K., Bril, H., 2007. Primary phases in pyrometallurgical slags from a zinc-smelting waste dump, Świętochłowice, Upper Silesia, Poland. Can. Mineral. 45, 1189–1200.
Qiu, H., Gu, H.-H., Wang, S.-Z., Qiu, R.-L., 2012. Attenuation of metal bioavailabilty in acidic multi-metal contaminated soil treated with fly ash and steel slag. Pedosphere 22 (4), 544–553.
Rai, A., Prabakar, J., Raju, C.B., Morchalle, R.K., 2002. Metallurgical slag as a component in blended cement. Constr. Build. Mater. 16, 489–494.
Rao, G.V., Nayak, B.D., 1992. Flotation of copper from converter slags. J. Mines Met. Fuels 40 (3–4), 131.
Reuer, M.K., Bower, N.W., Koball, J.H., Hinostroza, E., De la, Torre Marcas, M.E., Hurtado Surichaqui, A.H., Echevarria, S., 2012. Lead, Arsenic, and Cadmium Contamination and Its Impact on Children's Health in La Oroay, Peru. International Scholarly Research Network, Public Health, vol. 2012, 12p.
Rizza, I.L., Farthing, D.J., 2007. Catch the Rainbow: Geochemical Analysis of Colored Slag from Ironville, Adirondack State Park, New York: Geological Society of America, Abstracts with Programs, vol. 39, no. 6, p. 320.

Roadcap, G.S., Kelly, W.R., 1994. Shallow ground-water chemistry in the Lake Calumet Area, Chicago, Illinois. In: Pederson, G.L. (Ed.), National Symposium on Water Quality. American Water Resources Association, Herndon, Virginia, pp. 253–262.
Roadcap, G.S., Kelly, W.R., Bethke, C.M., 2005. Geochemistry of extremely alkaline (pH > 12) ground water in slag-fill aquifers. Ground Water 43 (6), 806–816.
Robbins, D.A., Bundy, S.D., Stanga, G.R., 1983. Availability of toxic metals from non-ferrous metallurgical slags using various procedures. In: Sohn, H.Y., George, D.B., Zunkel, A.D. (Eds.), Advances in Sulfide Smelting, vol. 2. The Metallurgical Society of AIME, pp. 923–934.
Rosado, L., Morais, C., Candeias, A.E., Pinto, A.P., Guimarães, F., Mirão, J., 2008. Weathering of S. Domingos (Iberian Pyritic Belt) abandoned mine slags. Mineral. Mag. 72, 489–494.
Rosenqvist, T., 2004. Principles of Extractive Metallurgy, second ed. Tapir Academic Press, Trondheim.
Roy, A., 2009. Sulfur speciation in granulated blast furnace slag: an X-ray absorption spectroscopic investigation. Cem. Concr. Res. 39, 659–663.
Sáez, R., Nocete, F., Nieto, J.M., Capitán, Á., Rovira, S., 2003. The extractive metallurgy of copper from Cabezo Juré, Huelva, Spain: chemical and mineralogical study of slags dated to the third millennium B.C. Can. Mineral. 41, 627–638.
Sánchez, M., Sudbury, M., 2013. Physiochemical characterization of copper slag and alternatives of friendly environmental management. J. Min. Metall., Sect. B – Metall. 49 (2), 161–168.
Sato, H., 1977. Nickel content of basaltic magmas: identification of primary magmas and a measure of the degree of olivine fractionation. Lithos 10 (2), 113–120.
Scheinert, M., Kupsch, H., Bletz, B., 2009. Geochemical investigations of slags from the historical smelting in Freiberg, Erzgebirge (Germany). Chem. Erde 69, 81–90.
Scott, P.W., Critchley, S.R., Wilkinson, F.C.F., 1986. The chemistry and mineralogy of some granulated and pelletized blast furnace slags. Mineral. Magaz. 50 (355), 141–147.
Seal II, R.R., Kiah, R.G., Piatak, N.M., Besser, J.M., Coles, J.F., Hammarstrom, J.M., Argue, D.M., Levitan, D.M., Deacon, J.R., Ingersoll, C.G., 2010. Aquatic Assessment of the Ely Copper Mine Superfund Site, Vershire, Vermont: U.S. Geological Survey Scientific Investigation, Report 2010-5084, 150p.
Seignez, N., Gauthier, A., Bulteel, D., Buatier, M., Recourt, P., Damidot, D., Potdevin, J.L., 2007. Effect of Pb-rich and Fe-rich entities during alteration of a partially vitrified metallurgical waste. J. Hazard. Mater. 149, 418–431.
Seignez, N., Gauthier, A., Bulteel, D., Damidot, D., Potdevin, J.-L., 2008. Leaching of lead metallurgical slags and pollutant mobility far from equilibrium conditions. Appl. Geochem. 23, 3699–3711.
Severin, T., Rehren, T., Schleicher, H., 2011. Early metal smelting in Aksum, Ethiopia: copper or iron? Eur. J. Mineral. 23, 981–992.
Shacklette, H.T., Boerngen, J.G., 1984. Element Concentrations in Soils and Other Surficial Materials of the Conterminous United States. U.S. Geological Survey Professional Paper 1270, 104p.
Shelley, T., 1975. Possible methods for recovering copper from waste smelter slags by leaching. Trans. Inst. Min. Metall. Sect. C—Mineral Process. Extract. Metall. 84, 1–4.
Shen, W., Zhou, M., Ma, W., Hu, J., Cai, Z., 2009. Investigation on the application of steel slag-fly ash–phosphogypsum solidified material as road base material. J. Hazard. Mater. 164, 99–104.
Shibayama, A., Takasaki, Y., William, T., Yamatodani, A., Higuchi, Y., Sunagawa, S., Ono, E., 2010. Treatment of smelting residues for arsenic removal and recovery of copper using pyro-hydrometallurgical process. J. Hazard. Mater. 181 (1–3), 1016–1023.
Sidenko, N.V., Gieré, R., Bortnikova, S.B., Cottard, F., Pal'chik, N.A., 2001. Mobility of heavy metals in self-burning waste heaps of the zinc smelting plant in Belovo (Kemerovo Region, Russia). J. Geochem. Explor. 74, 109–125.
Simmons, J., Ziemkiewicz, P., Black, D.C., 2002. Use of steel slag leach beds for the treatment of acid mine drainage. Mine Water Environ. 21, 91–99.
Singh, S.P., Tripathy, D.P., Ranjith, P.G., 2008. Performance evaluation of cement stabilized fly ash-GBFS mixes as a highway construction material. Waste Manage. (Oxford) 28, 1331–1337.
Sloto, R.A., Reif, A.G., 2011. Distribution of Trace Metals at Hopewell Furnace National Historic Site, Berks and Chester Counties, Pennsylvania: U.S. Geological Survey Scientific Investigations, Report 2011-5014, 90p.
Sobanska, S., Ledésert, B., Deneele, D., Laboudigue, A., 2000. Alteration in soils of slag particles resulting from lead smelting. Earth Planet. Sci. 331, 271–278.
Srivastava, R.K., Neuffer, W., Grano, D., Khan, S., Staudt, J.E., Jozewicz, W., 2005. Controlling NOx emission from industrial sources. Environ. Prog. 24 (2), 181–197.
Strömberg, B., Banwart, S., 1994. Kinetic modelling of geochemical processes at the Aitik mining waste rock site in northern Sweden. Appl. Geochem. 9, 583–595.
Suer, P., Lindqvist, J.-E., Arm, M., Frogner-Kockum, P., 2009. Reproducing ten years of road ageing – accelerated carbonization and leaching of EAF steel slag. Sci. Total Environ. 407, 5110–5118.
Sun, S.-M., Shan, B.-Q., Peng, W.-J., 2009. Transformation of inorganic nitrogen in slag-wetland during the start-up period. Environ. Sci. 30 (5), 1357–1361.
Svirenko, L., Vergeles, J., Spirin, O., 2003. Environmental effects of ferrous slags – comparative analysis and a systems approach in slag impact assessment for terrestrial and aquatic ecosystems. Approach. Handl. Environ. Probl. Min. Metall. Reg., 211–229.
Tack, F.M.G., Masscheleyn, P.H., Verloo, M.G., 1993. Leaching behavior of granulated non-ferrous metal slags. Stud. Environ. Sci. 55, 103–117.
Tatarinov, A.V., 2002. Metallurgical slags with spinifex textures. Geochem. Int. 40 (11), 1075–1082.
Tetra Tech Inc., 1985. Granulated Slag Pile: Draft Stage 1 Remedial Investigation Report. Anaconda Minerals Company.
Tossavainen, M., Engstrom, F., Yang, Q., Menad, N., Lidstrom Larsson, M., Bjorkman, B., 2007. Characteristics of steel slag under different cooling conditions. Waste Manage. (Oxford) 27, 1335–1344.
Tsakiridis, P.E., Papadimitriou, G.D., Tsivilis, S., Koroneos, C., 2008. Utilization of steel slag for Portland cement clinker production. J. Hazard. Mater. 152, 805–811.
Tshiongo, N., Mbaya, R.K.K., Maweja, K., Tshabalala, L.C., 2010. Effect of cooling rate on base metals recovery from copper matte smelting slags. World Acad. Sci. Eng. Technol. 70, 273–277.
Twidwell, L.G., 1983. Safe disposal of arsenic bearing flue dust by dissolution in smelter slags. J. Hazard. Mater. 8, 85–90.
Twidwell, L.G., Mehta, A.K., 1985. Disposal of arsenic bearing copper smelter flue dust. Nucl. Chem. Waste Manage. 5, 297–303.
U.S. Environmental Protection Agency (USEPA), 2008. Test Methods for Evaluating Solid Waste, Physical/Chemical Methods. SW-846 third ed. http://www.epa.gov/osw/hazard/testmethods/sw846/index.htm> (accessed February 2012).
U.S. Environmental Protection Agency (USEPA), 2010. Regional Screening Levels (Formerly PRGs). http://www.epa.gov/region9/superfund/prg/index.html> (accessed February 2012).
Van Oss, H.G., 2013. Slag, Iron and Steel: U.S. Geological Survey, 2011 Minerals Yearbook, vol. 1, pp. 69.1–69.9.
Vdović, N., Billon, G., Gabelle, C., Potdevin, J., 2006. Remobilization of metals from slag and polluted sediments (Case Study: the canal of the Deûle River, northern France). Environ. Pollut. 141, 359–369.
Vítková, M., Ettler, V., Johan, Z., Kříbek, B., Šebek, O., Mihaljevič, M., 2010. Primary and secondary phases in copper-cobalt smelting slags from the Copperbelt Province, Zambia. Mineral. Mag. 74 (4), 581–600.
Vítková, M., Ettler, V., Mihaljevič, M., Šebek, O., 2011. Effect of sample preparation on contaminant leaching from copper smelting slag. J. Hazard. Mater. 197, 417–423.
Vivenzio, R.M., Farthing, D.J., 2005. Tahawus: an insight to the geochemistry of an industrial waste site. Geol. Soc. Am. Program. Abst. 37 (7), 358.
Weber, D., Drizo, A., Twohig, E., Bird, S., Ross, D., 2007. Upgrading constructed wetlands phosphorus reduction from a dairy effluent using electric arc furnace steel slag filters. Water Sci. Technol. 56 (3), 135–143.
Wendling, L., Douglas, G., Coleman, S., Yuan, Z., 2010. Assessment of the Ability of Low-Cost Materials to Remove Metals and Attenuate Acidity in Contaminated Waters: CSIRO – Water for a Healthy Country National Research Flagship, 138p. http://www.water.wa.gov.au/PublicationStore/first/97303.pdf> (assessed September 2013).
Wendling, L.A., Douglas, G.B., Coleman, S., 2012. Productive use of steelmaking by-product in environmental radioactivity. Miner. Eng. 39, 219–227.
Wendling, L.A., Binet, M.T., Yuan, Z., Gissi, F., Koppel, D.J., Adams, M.S., 2013. Geochemical and ecotoxicological assessment of iron- and steel-making slags for potential use in environmental applications. Environ. Toxicol. Chem. 32 (11), 2602–2610.
West, T.D., 1902. Metallurgy of Cast Iron, seventh ed. The Cleveland Printing and Publishing Co., p. 656.
Weston Solutions, Inc., 2007. Final Remedial Investigation Report Hegeler Zinc Site, Danville, Vermilion County, Illinois. Document Control No. RFW250-2A-AWOO. Prepared for USEPA. http://www.epa.gov/region5/cleanup/hegelerzinc/pdfs/hegeler_ri_200704.pdf> (accessed 09.09.13).
Wilson, L.J., 1994. Literature Review on Slag Leaching: Canada Centre for Mineral and Energy Technology, Mineral Sciences Laboratories Division Report 94-3 (CR), Ottawa.
Wolery, T.J., 1992. EQ3NR, A Computer Program for Geochemical Aqueous Speciation Solubility Calculations: Theoretical Manual, User's Guide, and Related Documentation (Version 7.0): UCRL-MA-110662-PT-III, Lawrence Livermore National Laboratory, Livermore, California.
Wolery, T.J., Daveler, S.A., 1992. EQ6, A Computer Program for Reaction Path Modeling of Aqueous Geochemical Systems – Theoretical Manual, User's Guide, and Related Documentation (Version 7.0): UCRL-MA-110662-PT-IV. Lawrence Livermore National Laboratory, Livermore, California.
Woodley, N.K., Walters, J.V., 1986. Hazardous waste characterization extraction procedures for the analysis of blast-furnace slag from secondary lead smelters. Environ. Prog. 5 (1), 217–223.
Yang, Z., Rui-lin, M., Wang-dong, N., Hui, W., 2010. Selective leaching of base metals from copper smelter slag. Hydrometallurgy 103 (1–4), 25–29.
Yildirim, I.Z., Prezzi, M., 2011. Chemical, mineralogical, and morphological properties of steel slag. Adv. Civil Eng. 2011, 13.
Ziemkiewicz, P., Skousen, J., 1999. Steel slag in acid mine drainage treatment and control. In: Proceedings of the Annual National Meeting of the Society for Surface Mining and Reclamation, vol. 16, pp. 651–656.